Dual Hamiltonian Transformation and Magneto-electro-thermo-viscoelastic Contact Analysis

Lizichen Chen[a], C. W. Lim[a,b], and Weiqiu Chen[a,c,d,*]

[a]Key Laboratory of Soft Machines and Smart Devices of Zhejiang Province, Department of Engineering Mechanics, Soft Matter Research Center, Zhejiang University, Hangzhou 310027, P.R. China

[b]Department of Architecture and Civil Engineering, City University of Hong Kong, Tat Chee Avenue, Kowloon, Hong Kong SAR, P. R. China

[c]Center for Soft Machines and Smart Devices, Huanjiang Laboratory, Zhuji 311816, P.R. China

[d]Faculty of Mechanical Engineering and Mechanics, Ningbo University, Ningbo 315211, P.R. China

Abstract: The application of high-throughput testing methodologies and the involvement of functionally graded specimens for material characterization show immense potential and plays an indispensable role in the progressive advent of advanced materials. Nevertheless, the inherent material inhomogeneity and multi-field coupling pose great obstacles in the fundamental theory and analysis for the behavior of functionally graded specimens, thus necessitating the proposal of new and innovative analytical approaches. Here, the contact model and analysis of a finite-sized magneto-electro-thermo-viscoelastic plane with a horizontal exponential material gradient is established based on a new symplectic approach. With prior linearization via Laplace transform, the state equations are constructed in the matrix form, resulting in the dual Hamiltonian transformation under homogeneous displacement constraint. The dual adjoint

[*] Corresponding author. Tel./Fax: 85-571-87951866; E-mail: chenwq@zju.edu.cn.

symplectic orthogonality is introduced and proved, elucidating the implications of symmetry breaking. General and particular solutions are derived to constitute the complete solution in the symplectic expansion. The analytical solution is verified by comparing with highly precise finite element solutions in the entire domain. This current work not only paves the way for an efficient and robust analytical framework via the symplectic methodology, but also sets a foundation with benchmark exact solutions for future research endeavors.

Graphical abstract:

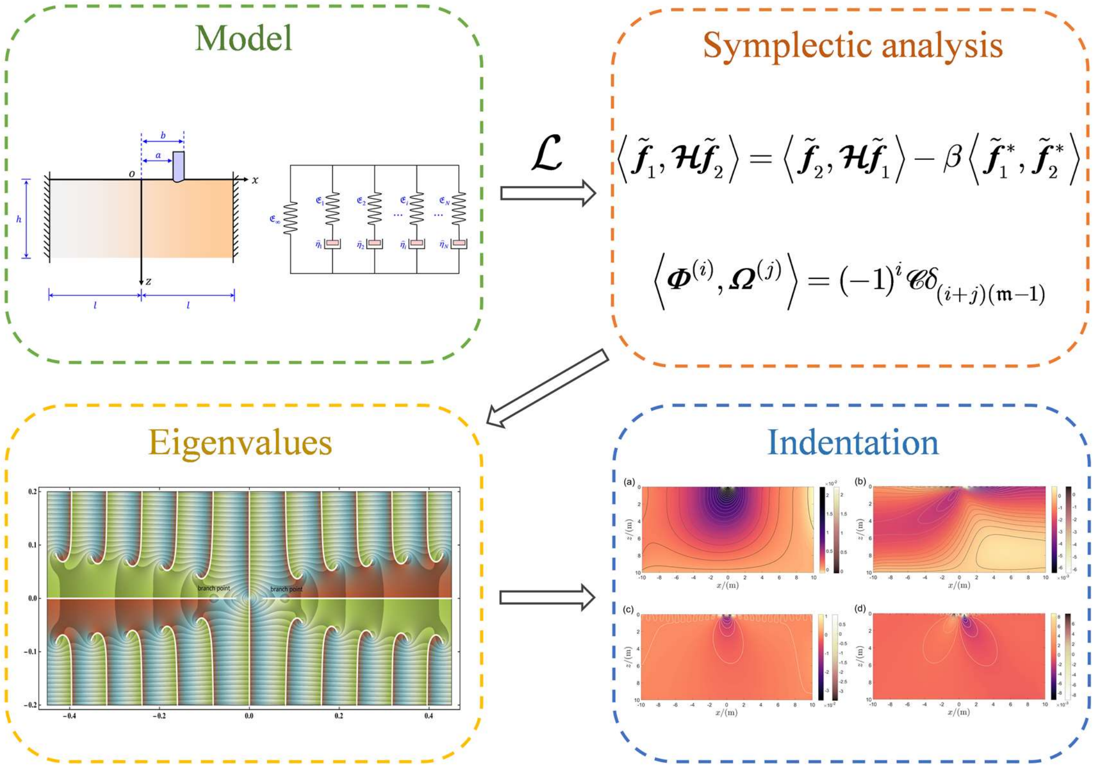

Keywords: symplectic; contact analysis; multi-physics coupling; dual Hamiltonian transformation; horizontal exponential gradient; dual adjoint symplectic orthogonality

1. Introduction

Numerous novel materials such as polymers, synthetic rubbers, and ceramics have found widespread applications in industry [1-5]. These materials share a common characteristic: they exhibit both elasticity and viscosity [6-12]. To show the intricate behaviors of viscoelastic materials endowed with complex rheological attributes accurately, sophisticated models were proposed, notably the generalized Maxwell model and the generalized Kelvin model [9,13-18]. The rheological properties of viscoelastic materials necessitate the inclusion of "time" into the governing equations, giving rise to phenomena as creep or stress relaxation [19-21]. In the light of these behavior, the loading conditions and service environments of materials significantly impact their performance, underscoring the need for investigating the viscoelastic properties to ensure the safety of engineering structures [22-25].

A significant advancement in modelling the viscoelastic materials lies in the application of Laplace transform that reduces the viscoelastic problems to the corresponding elastic representation [26-30]. Linearly viscoelastic problems can be efficiently solved by leveraging the theory of elasticity established before, which is adapted through the elastic-viscoelastic correspondence principle initially formulated analytically by Lee and Radok [31]. Meanwhile, material property testing also promoted the development of high-throughput characterization technologies such as contact analysis [32-37]. In this regard, Hunter [38] and Goriacheva [39] presented solutions of the rolling contact between a rigid indenter and a viscoelastic half-space. Fu [40] formulated analytical solutions specifically tailored for scenarios where the entire indenter surface is in contact with the viscoelastic half-space, elucidating the complicated relationship between load and indentation depth. Greenwood [41] introduced a theoretical model that addresses the contact problem between an axisymmetric indenter and a viscoelastic half-space. Argatov and Mishuris ventured into new territories beyond half-space, thus developing analytical solutions for elliptical [42] and rebound spherical [43] indentation contact problems between compressible, and incompressible layers composed of viscoelastic materials.

Many scholars have undertaken profound explorations into the frictionless or sliding friction contact problems by utilizing models [44,45] where material parameters vary exponentially [46-49] or in power-law [50-54]. Nevertheless, complexity of the theoretical underpinnings of inhomogeneous material contact analysis poses great challenges for the derivation of analytical solutions [55-58] that hindered its further development. Consequently, there is an urgent need to establish a novel analytical framework. The pioneering work of Zhong [59-61] that established the symplectic theory and solution methodology for elasticity illustrated remarkably the efficiency and impact of the approach [62-72], and it was applied to viscoelasticity by Xu and Zhang [73-75] subsequently. Chen and Chen [76] recently extended the symplectic approach to contact mechanics, addressing the problem of contact between a rigid punch and a finite-sized plane with horizontally exponential gradient.

This article proposes a theoretical model with symplectic solutions for a rigid punch with arbitrary profile applied over an identified region of a finite-sized magneto-electro-thermo-viscoelastic plane with a horizontal exponential material gradient. The state equations and dual Hamiltonian transformation are constructed analytically, and the dual adjoint symplectic orthogonality is proved in Section 2.1. The absence of special eigenvalue is elucidated in Section 2.2, while the general eigenvalues and the corresponding eigen-solutions are derived Section 2.3. General and particular solutions are obtained to constitute the complete solution in the symplectic expansion in Section 2.4. Numerical examples are presented in Section 3, with finite element simulations conducted for verification on the whole domain. The multi-indenter with multi-physical effects is also discussed. The concluding remarks are presented in Section 4.

2. Contact Analysis of a Finite-sized Viscoelastic Plane with Horizontal Gradient

A rigid punch of an arbitrary profile with predetermined contact region (i.e., $x \in [a,b]$) is applied on the surface of a finite-sized functionally graded magneto-electro-thermo-viscoelastic plane. Without loss of generality, the contact region is assumed to be two-dimensional while a more in-depth three-dimensional contact region will be reported in a future work. The material is assumed to have the poling direction along the z-axis as illustrated in Fig. 1. The plane is transversely isotropic, with $c_{ij}(x,t)$, $e_{ij}(x)$, $q_{ij}(x)$, $\varepsilon_{ij}(x)$, $\gamma_{ij}(x)$, $d_{ij}(x)$, $\mathfrak{a}_i(x)$, $\mathfrak{b}_3(x)$, and $\mathfrak{c}_3(x)$ being the elastic (i.e., relaxation modulus), piezoelectric, piezomagnetic, dielectric, magnetic, electromagnetic, thermal, pyroelectric, and pyromagnetic parameters, respectively. These parameters are assumed to vary exponentially along the x-direction, as

$$\begin{aligned}
&c_{ij}(x,t)=c_{ij}^0(t)\mathrm{e}^{\beta x}, \quad e_{ij}(x)=e_{ij}^0\mathrm{e}^{\beta x}, \quad q_{ij}(x)=q_{ij}^0\mathrm{e}^{\beta x}, \quad \varepsilon_{ij}(x)=\varepsilon_{ij}^0\mathrm{e}^{\beta x}, \\
&\gamma_{ij}(x)=\gamma_{ij}^0\mathrm{e}^{\beta x}, \qquad d_{ij}(x)=d_{ij}^0\mathrm{e}^{\beta x}, \quad \mathfrak{a}_i(x)=\mathfrak{a}_i^0\mathrm{e}^{\beta x}, \quad \mathfrak{b}_3(x)=\mathfrak{b}_3^0\mathrm{e}^{\beta x}, \\
&\mathfrak{c}_3(x)=\mathfrak{c}_3^0\mathrm{e}^{\beta x},
\end{aligned} \tag{1}$$

where β is the material gradient index. For $\beta>0$, the material is stiffened along the x-direction, while it softens for $\beta<0$.

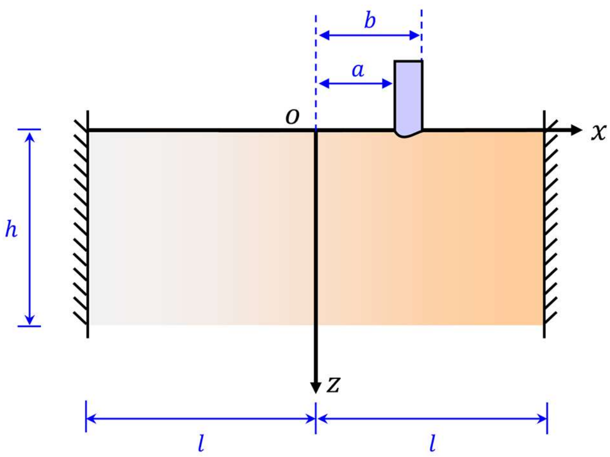

Fig. 1. Application of a rigid punch on the surface of a finite-sized horizontally graded magneto-electro-thermo-viscoelastic plane.

In the subsequent sections, we convert the basic formulas into symplectic form and construct the dual Hamiltonian transformation. The special and general eigenvalues corresponding to a quasi-Hamiltonian operator and the particular solution of the state equations are further analyzed, which are appropriately combined into complete solutions.

2.1. Basic formulations and dual Hamiltonian transformation

The two-dimensional constitutive relations for plane strain are established in the form of:

$$\begin{cases} \sigma_{xx} = c_{11} * \mathrm{d}\left(\dfrac{\partial u_x}{\partial x}\right) + c_{13} * \mathrm{d}\left(\dfrac{\partial u_z}{\partial z}\right) + e_{31}\dfrac{\partial \varphi}{\partial z} + q_{31}\dfrac{\partial \psi}{\partial z} - \mathfrak{a}_1 T, \\ \sigma_{zz} = c_{13} * \mathrm{d}\left(\dfrac{\partial u_x}{\partial x}\right) + c_{33} * \mathrm{d}\left(\dfrac{\partial u_z}{\partial z}\right) + e_{33}\dfrac{\partial \varphi}{\partial z} + q_{33}\dfrac{\partial \psi}{\partial z} - \mathfrak{a}_3 T, \\ \sigma_{xz} = c_{44} * \mathrm{d}\left(\dfrac{\partial u_x}{\partial z} + \dfrac{\partial u_z}{\partial x}\right) + e_{15}\dfrac{\partial \varphi}{\partial x} + q_{15}\dfrac{\partial \psi}{\partial x}, \\ D_x = e_{15}\left(\dfrac{\partial u_x}{\partial z} + \dfrac{\partial u_z}{\partial x}\right) - \varepsilon_{11}\dfrac{\partial \varphi}{\partial x} - d_{11}\dfrac{\partial \psi}{\partial x}, \\ D_z = e_{31}\dfrac{\partial u_x}{\partial x} + e_{33}\dfrac{\partial u_z}{\partial z} - \varepsilon_{33}\dfrac{\partial \varphi}{\partial z} - d_{33}\dfrac{\partial \psi}{\partial z} + \mathfrak{b}_3 T, \\ B_x = q_{15}\left(\dfrac{\partial u_x}{\partial z} + \dfrac{\partial u_z}{\partial x}\right) - d_{11}\dfrac{\partial \varphi}{\partial x} - \gamma_{11}\dfrac{\partial \psi}{\partial x}, \\ B_z = q_{31}\dfrac{\partial u_x}{\partial x} + q_{33}\dfrac{\partial u_z}{\partial z} - d_{33}\dfrac{\partial \varphi}{\partial z} - \gamma_{33}\dfrac{\partial \psi}{\partial z} + \mathfrak{c}_3 T, \end{cases} \tag{2}$$

where σ_{ij} are the stress components; u_x and u_z are the displacement components in the x- and z-directions, respectively; φ and ψ are the electric potential and magnetic potential, respectively; D_i and B_i are the components of the electric displacement and the magnetic induction, respectively; T represents the incremental temperature ($T=0$ corresponds to the state where stresses, electric displacements and magnetic inductions vanish). The symbol $*$ stands for convolution with respect to time variable. In the case of plane stress, the constitutive relations adopt alternative but similar formulations.

Applying Laplace transform defined in Eq. (3)

$$\mathcal{L}[f(t)] \equiv \tilde{f} = \int_0^\infty f(t)\mathrm{e}^{-\omega t}\mathrm{d}t, \tag{3}$$

on the constitutive relations and the equilibrium equations without body forces, we derive the following equations by separating different partial derivatives, as

$$
\begin{cases}
\dfrac{\partial \tilde{u}_x}{\partial z} = -\dfrac{\partial \tilde{u}_z}{\partial x} - \dfrac{e_{15}}{\tilde{c}'_{44}}\dfrac{\partial \tilde{\varphi}}{\partial x} - \dfrac{q_{15}}{\tilde{c}'_{44}}\dfrac{\partial \tilde{\psi}}{\partial x} + \dfrac{1}{\tilde{c}'_{44}}\tilde{\sigma}_{xz}, \\
\dfrac{\partial \tilde{u}_z}{\partial z} = -\dfrac{\tilde{c}'_{13}}{\tilde{c}'_{33}}\dfrac{\partial \tilde{u}_x}{\partial x} - \dfrac{e_{33}}{\tilde{c}'_{33}}\dfrac{\partial \tilde{\varphi}}{\partial z} - \dfrac{q_{33}}{\tilde{c}'_{33}}\dfrac{\partial \tilde{\psi}}{\partial z} + \dfrac{1}{\tilde{c}'_{33}}\tilde{\sigma}_{zz} + \dfrac{\mathfrak{a}_3}{\tilde{c}'_{33}}\tilde{T}, \\
\dfrac{\partial \tilde{\varphi}}{\partial z} = \dfrac{e_{31}}{\varepsilon_{33}}\dfrac{\partial \tilde{u}_x}{\partial x} + \dfrac{e_{33}}{\varepsilon_{33}}\dfrac{\partial \tilde{u}_z}{\partial z} - \dfrac{d_{33}}{\varepsilon_{33}}\dfrac{\partial \tilde{\psi}}{\partial z} - \dfrac{1}{\varepsilon_{33}}\tilde{D}_z + \dfrac{\mathfrak{b}_3}{\varepsilon_{33}}\tilde{T}, \\
\dfrac{\partial \tilde{\psi}}{\partial z} = \dfrac{q_{31}}{\gamma_{33}}\dfrac{\partial \tilde{u}_x}{\partial x} + \dfrac{q_{33}}{\gamma_{33}}\dfrac{\partial \tilde{u}_z}{\partial z} - \dfrac{d_{33}}{\gamma_{33}}\dfrac{\partial \tilde{\varphi}}{\partial z} - \dfrac{1}{\gamma_{33}}\tilde{B}_z + \dfrac{\mathfrak{c}_3}{\gamma_{33}}\tilde{T}, \\
\dfrac{\partial \tilde{\sigma}_{xz}}{\partial z} = -\dfrac{\partial \tilde{\sigma}_{xx}}{\partial x}, \\
\dfrac{\partial \tilde{\sigma}_{zz}}{\partial z} = -\dfrac{\partial \tilde{\sigma}_{xz}}{\partial x}, \\
\dfrac{\partial \tilde{D}_z}{\partial z} = -\dfrac{\partial \tilde{D}_x}{\partial x}, \\
\dfrac{\partial \tilde{B}_z}{\partial z} = -\dfrac{\partial \tilde{B}_x}{\partial x},
\end{cases}
\tag{4}
$$

where $\tilde{c}'_{ij} = \omega \tilde{c}_{ij}(x,\omega)$. By setting $\tilde{\tilde{\sigma}}_{ji} = \tilde{\sigma}_{ji}\mathrm{e}^{-\beta x}$, $\tilde{\tilde{D}}_i = \tilde{D}_i\mathrm{e}^{-\beta x}$, and $\tilde{\tilde{B}}_i = \tilde{B}_i\mathrm{e}^{-\beta x}$ $(i,j = z,x)$, the state equations are simplified further as

$$
\begin{cases}
\dfrac{\partial \tilde{u}_x}{\partial z} = -\dfrac{\partial \tilde{u}_z}{\partial x} - a_1\dfrac{\partial \tilde{\varphi}}{\partial x} - a_2\dfrac{\partial \tilde{\psi}}{\partial x} + a_3\tilde{\tilde{\sigma}}_{xz}, \\
\dfrac{\partial \tilde{u}_z}{\partial z} = -a_4\dfrac{\partial \tilde{u}_x}{\partial x} + a_5\tilde{\tilde{\sigma}}_{zz} + a_6\tilde{\tilde{D}}_z + a_7\tilde{\tilde{B}}_z + \iota_1\tilde{T}, \\
\dfrac{\partial \tilde{\varphi}}{\partial z} = a_8\dfrac{\partial \tilde{u}_x}{\partial x} + a_6\tilde{\tilde{\sigma}}_{zz} - a_9\tilde{\tilde{D}}_z + a_{10}\tilde{\tilde{B}}_z + \iota_2\tilde{T}, \\
\dfrac{\partial \tilde{\psi}}{\partial z} = a_{11}\dfrac{\partial \tilde{u}_x}{\partial x} + a_7\tilde{\tilde{\sigma}}_{zz} + a_{10}\tilde{\tilde{D}}_z - a_{12}\tilde{\tilde{B}}_z + \iota_3\tilde{T}, \\
\dfrac{\partial \tilde{\tilde{\sigma}}_{xz}}{\partial z} = a_{13}\dfrac{\partial^2 \tilde{u}_x}{\partial x^2} - a_4\dfrac{\partial \tilde{\tilde{\sigma}}_{zz}}{\partial x} + a_8\dfrac{\partial \tilde{\tilde{D}}_z}{\partial x} + a_{11}\dfrac{\partial \tilde{\tilde{B}}_z}{\partial x} + \iota_4\dfrac{\partial \tilde{T}}{\partial x} + \beta\left(a_{13}\dfrac{\partial \tilde{u}_x}{\partial x} - a_4\tilde{\tilde{\sigma}}_{zz} + a_8\tilde{\tilde{D}}_z + a_{11}\tilde{\tilde{B}}_z + \iota_4\tilde{T}\right), \\
\dfrac{\partial \tilde{\tilde{\sigma}}_{zz}}{\partial z} = -\dfrac{\partial \tilde{\tilde{\sigma}}_{xz}}{\partial x} - \beta\tilde{\tilde{\sigma}}_{xz}, \\
\dfrac{\partial \tilde{\tilde{D}}_z}{\partial z} = a_{14}\dfrac{\partial^2 \tilde{\varphi}}{\partial x^2} + a_{15}\dfrac{\partial^2 \tilde{\psi}}{\partial x^2} - a_1\dfrac{\partial \tilde{\tilde{\sigma}}_{xz}}{\partial x} + \beta\left(a_{14}\dfrac{\partial \tilde{\varphi}}{\partial x} + a_{15}\dfrac{\partial \tilde{\psi}}{\partial x} - a_1\tilde{\tilde{\sigma}}_{xz}\right), \\
\dfrac{\partial \tilde{\tilde{B}}_z}{\partial z} = a_{15}\dfrac{\partial^2 \tilde{\varphi}}{\partial x^2} + a_{16}\dfrac{\partial^2 \tilde{\psi}}{\partial x^2} - a_2\dfrac{\partial \tilde{\tilde{\sigma}}_{xz}}{\partial x} + \beta\left(a_{15}\dfrac{\partial \tilde{\varphi}}{\partial x} + a_{16}\dfrac{\partial \tilde{\psi}}{\partial x} - a_2\tilde{\tilde{\sigma}}_{xz}\right),
\end{cases}
\tag{5}
$$

and the supplementary equations yield

$$\begin{cases} \tilde{\hat{\sigma}}_{xx} = -a_{13}\dfrac{\partial \tilde{u}_x}{\partial x} + a_4\tilde{\hat{\sigma}}_{zz} - a_8\tilde{\hat{D}}_z - a_{11}\tilde{\hat{B}}_z - \iota_4\tilde{T}, \\ \tilde{\hat{D}}_x = -a_{14}\dfrac{\partial \tilde{\varphi}}{\partial x} - a_{15}\dfrac{\partial \tilde{\psi}}{\partial x} + a_1\tilde{\hat{\sigma}}_{xz}, \\ \tilde{\hat{B}}_x = -a_{15}\dfrac{\partial \tilde{\varphi}}{\partial x} - a_{16}\dfrac{\partial \tilde{\psi}}{\partial x} + a_2\tilde{\hat{\sigma}}_{xz}, \end{cases} \tag{6}$$

where a_i and ι_i in Eqs. (5) and (6) are presented in Appendix A. The full state vector $\tilde{\boldsymbol{f}}$ is taken as

$$\tilde{\boldsymbol{f}} = [\tilde{\boldsymbol{q}}, \tilde{\boldsymbol{p}}]^{\mathrm{T}} = \left[\{\tilde{u}_x, \tilde{u}_z, \tilde{\varphi}, \tilde{\psi}\}, \{\tilde{\hat{\sigma}}_{xz}, \tilde{\hat{\sigma}}_{zz}, \tilde{\hat{D}}_z, \tilde{\hat{B}}_z\}\right]^{\mathrm{T}}, \tag{7}$$

which lead to

$$\frac{\partial}{\partial z}\mathbf{I}_8\tilde{\boldsymbol{f}} = \boldsymbol{\mathcal{H}}\tilde{\boldsymbol{f}} + \tilde{\boldsymbol{f}}', \tag{8}$$

where $\mathbf{I}_n$ is an nth-order identity matrix; $\boldsymbol{\mathcal{H}}$ is a quasi-Hamiltonian operator, which can be found in Appendix A; $\tilde{\boldsymbol{f}}'$ is the non-homogeneous term, detailed as:

$$\tilde{\boldsymbol{f}}' = \left[0, \iota_1\tilde{T}, \iota_2\tilde{T}, \iota_3\tilde{T}, \iota_4\frac{\partial \tilde{T}}{\partial x} + \beta\iota_4\tilde{T}, 0, 0, 0\right]^{\mathrm{T}}. \tag{9}$$

The following unit symplectic matrix is introduced to derive the symplectic orthogonality as

$$\mathbf{J} = \begin{bmatrix} 0 & \mathbf{I}_4 \\ -\mathbf{I}_4 & 0 \end{bmatrix}, \tag{10}$$

and the symplectic inner product is defined as

$$\begin{aligned} \left\langle \tilde{\boldsymbol{f}}_1, \tilde{\boldsymbol{f}}_2 \right\rangle &= \int_{-l}^{l} \tilde{\boldsymbol{f}}_1^{\mathrm{T}}\mathbf{J}\tilde{\boldsymbol{f}}_2 \mathrm{d}x \\ &= \int_{-l}^{l} (\tilde{u}_{x1}\tilde{\hat{\sigma}}_{xz2} + \tilde{u}_{z1}\tilde{\hat{\sigma}}_{zz2} + \tilde{\varphi}_1\tilde{\hat{D}}_{z2} + \tilde{\psi}_1\tilde{\hat{B}}_{z2} - \tilde{\hat{\sigma}}_{xz1}\tilde{u}_{x2} - \tilde{\hat{\sigma}}_{zz1}\tilde{u}_{z2} - \tilde{\hat{D}}_{z1}\tilde{\varphi}_2 - \tilde{\hat{B}}_{z1}\tilde{\psi}_2)\mathrm{d}x, \end{aligned} \tag{11}$$

where subscript 1 or 2 denotes a specified state vector. Obviously, Eq. (11) satisfies the four conditions of symplectic inner product [72], which results in the construction of the symplectic space. Given the homogeneous lateral boundary conditions at $x = \pm l$,

$$\tilde{u}_x = 0, \quad \tilde{u}_z = 0, \quad \tilde{\varphi} = 0, \quad \tilde{\psi} = 0. \tag{12}$$

We can prove the following property via integration by parts:

$$\left\langle \tilde{\boldsymbol{f}}_1, \boldsymbol{\mathcal{H}}\tilde{\boldsymbol{f}}_2 \right\rangle = \left\langle \tilde{\boldsymbol{f}}_2, \boldsymbol{\mathcal{H}}\tilde{\boldsymbol{f}}_1 \right\rangle - \beta \left\langle \tilde{\boldsymbol{f}}_1^*, \tilde{\boldsymbol{f}}_2^* \right\rangle, \tag{13}$$

where $\tilde{\boldsymbol{f}}^*$ is the dual full state vector, as

$$\tilde{\boldsymbol{f}}^* = \left[\{\tilde{u}_x, \tilde{u}_z, \tilde{\varphi}, \tilde{\psi}\}, \{\tilde{\tilde{\sigma}}_{xx}^H, \tilde{\tilde{\sigma}}_{xz}, \tilde{\tilde{D}}_x, \tilde{\tilde{B}}_x\} \right]^{\mathrm{T}}, \tag{14}$$

and $\tilde{\tilde{\sigma}}_{xx}^H = -a_{13}\dfrac{\partial \tilde{u}_x}{\partial x} + a_4\tilde{\tilde{\sigma}}_{zz} - a_8\tilde{\tilde{D}}_z - a_{11}\tilde{\tilde{B}}_z$. Hence, the dual Hamiltonian transformation is established.

To construct the adjoint symplectic orthogonal relations of the eigenvectors, we transfer the dual full state vector in the dual symplectic space into the full state vector as

$$\begin{aligned}
\left\langle \tilde{\boldsymbol{f}}_1, \boldsymbol{\mathcal{H}}\tilde{\boldsymbol{f}}_2 \right\rangle &= \left\langle \tilde{\boldsymbol{f}}_2, \boldsymbol{\mathcal{H}}\tilde{\boldsymbol{f}}_1 \right\rangle - \beta \left\langle \tilde{\boldsymbol{f}}_1^*, \tilde{\boldsymbol{f}}_2^* \right\rangle \\
&= \left\langle \tilde{\boldsymbol{f}}_2, \boldsymbol{\mathcal{H}}\tilde{\boldsymbol{f}}_1 \right\rangle - \beta \left\langle \boldsymbol{\mathcal{A}}\tilde{\boldsymbol{f}}_1, \boldsymbol{\mathcal{A}}\tilde{\boldsymbol{f}}_2 \right\rangle \\
&= \left\langle \tilde{\boldsymbol{f}}_2, \boldsymbol{\mathcal{H}}\tilde{\boldsymbol{f}}_1 \right\rangle - \beta \int_{-l}^{l} (\boldsymbol{\mathcal{A}}\tilde{\boldsymbol{f}}_1)^{\mathrm{T}} \mathbf{J} (\boldsymbol{\mathcal{A}}\tilde{\boldsymbol{f}}_2) \mathrm{d}x \\
&= \left\langle \tilde{\boldsymbol{f}}_2, \boldsymbol{\mathcal{H}}\tilde{\boldsymbol{f}}_1 \right\rangle - \beta \int_{-l}^{l} \tilde{\boldsymbol{f}}_1^{\mathrm{T}} \mathbf{J}\mathbf{J}^{\mathcal{T}} \boldsymbol{\mathcal{A}}^{\mathcal{T}} \mathbf{J}\boldsymbol{\mathcal{A}}\tilde{\boldsymbol{f}}_2 \mathrm{d}x \\
&= \left\langle \tilde{\boldsymbol{f}}_2, \boldsymbol{\mathcal{H}}\tilde{\boldsymbol{f}}_1 \right\rangle - \beta \int_{-l}^{l} \tilde{\boldsymbol{f}}_1^{\mathrm{T}} \mathbf{J} (\boldsymbol{\mathcal{A}}\mathbf{J})^{\mathrm{T}} (\mathbf{J}\boldsymbol{\mathcal{A}}) \tilde{\boldsymbol{f}}_2 \mathrm{d}x,
\end{aligned} \tag{15}$$

which results in

$$\left\langle \tilde{\boldsymbol{f}}_1, (\boldsymbol{\mathcal{H}} + \beta\boldsymbol{\mathcal{B}})\tilde{\boldsymbol{f}}_2 \right\rangle = \left\langle \tilde{\boldsymbol{f}}_2, \boldsymbol{\mathcal{H}}\tilde{\boldsymbol{f}}_1 \right\rangle, \tag{16}$$

where $(\cdot)^{\mathcal{T}}$ represents the adjoint transpose of an operator matrix; $\boldsymbol{\mathcal{B}} = (\boldsymbol{\mathcal{A}}\mathbf{J})^{\mathrm{T}}(\mathbf{J}\boldsymbol{\mathcal{A}})$; $\boldsymbol{\mathcal{A}}$ can be deduced through the supplementary equations in Eq. (6), as

$$\boldsymbol{\mathcal{A}}=\begin{bmatrix} 1 & 0 & 0 & 0 & 0 & 0 & 0 & 0 \\ 0 & 1 & 0 & 0 & 0 & 0 & 0 & 0 \\ 0 & 0 & 1 & 0 & 0 & 0 & 0 & 0 \\ 0 & 0 & 0 & 1 & 0 & 0 & 0 & 0 \\ -a_{13}\dfrac{\partial}{\partial x} & 0 & 0 & 0 & 0 & a_4 & -a_8 & -a_{11} \\ 0 & 0 & 0 & 0 & 1 & 0 & 0 & 0 \\ 0 & 0 & -a_{14}\dfrac{\partial}{\partial x} & -a_{15}\dfrac{\partial}{\partial x} & a_1 & 0 & 0 & 0 \\ 0 & 0 & -a_{15}\dfrac{\partial}{\partial x} & -a_{16}\dfrac{\partial}{\partial x} & a_2 & 0 & 0 & 0 \end{bmatrix}. \tag{17}$$

It is worth noting that if the stress-free boundary conditions are taken instead, we will arrive at the Eq. (16) with another non-homogeneous term. Furthermore, the relation may also be valid for the non-homogeneous lateral boundary conditions, so long as the respective particular terms are derived to homogenize. As derived in Eq. (16), the dual operator of $\boldsymbol{\mathcal{H}}$ is $\boldsymbol{\mathcal{H}}+\beta\boldsymbol{\mathcal{B}}$, which leads to the dual adjoint symplectic orthogonality between the two sets of eigenvectors, as proved via Theorem 1, 2, and 3 in Appendix B. Triggered by symmetry breaking with respect to the coordinate system, this novel mathematical property is essential for dealing with the non-homogeneous state equations.

We first solve for the homogenous state equations, and the variables may be separated in the form of

$$\tilde{\boldsymbol{f}}(x,z)=\tilde{\boldsymbol{\Phi}}(x)\tilde{\xi}(z)=[\tilde{u}(x),\tilde{w}(x),\tilde{\phi}(x),\tilde{\psi}(x),\tilde{\tau}(x),\tilde{\sigma}(x),\tilde{D}(x),\tilde{B}(x)]^{\mathrm{T}}\tilde{\xi}(z), \tag{18}$$

which leads to

$$\frac{\frac{\partial}{\partial z}\tilde{\xi}(z)}{\tilde{\xi}(z)}=\left[\boldsymbol{\mathcal{H}}\tilde{\boldsymbol{\Phi}}(x)\right]\tilde{\boldsymbol{\Phi}}^{-1}(x), \tag{19}$$

and we have

$$\tilde{\xi}(z)=\mathrm{e}^{\mu z}, \tag{20}$$

together with the eigen equation

$$\boldsymbol{\mathcal{H}}\tilde{\boldsymbol{\Phi}}(x)=\mu\tilde{\boldsymbol{\Phi}}(x), \tag{21}$$

where μ is the eigenvalue, and $\tilde{\boldsymbol{\Phi}}(x)$ is the corresponding eigenvector in the frequency domain.

2.2. *The absence of special eigenvalues*

The zero and $-\beta$ eigenvalues are considered unique because solutions of the corresponding displacement and stress components show nonexponential decay in the z-direction. The state equations for zero-eigenvalue are established as

$$\begin{cases}
-\dfrac{\partial\tilde{w}}{\partial x}-a_1\dfrac{\partial\tilde{\phi}}{\partial x}-a_2\dfrac{\partial\tilde{\psi}}{\partial x}+a_3\tilde{\tau}=0,\\
-a_4\dfrac{\partial\tilde{u}}{\partial x}+a_5\tilde{\sigma}+a_6\tilde{D}+a_7\tilde{B}=0,\\
a_8\dfrac{\partial\tilde{u}}{\partial x}+a_6\tilde{\sigma}-a_9\tilde{D}+a_{10}\tilde{B}=0,\\
a_{11}\dfrac{\partial\tilde{u}}{\partial x}+a_7\tilde{\sigma}+a_{10}\tilde{D}-a_{12}\tilde{B}=0,\\
a_{13}\dfrac{\partial^2\tilde{u}}{\partial x^2}-a_4\dfrac{\partial\tilde{\sigma}}{\partial x}+a_8\dfrac{\partial\tilde{D}}{\partial x}+a_{11}\dfrac{\partial\tilde{B}}{\partial x}+\beta\left(a_{13}\dfrac{\partial\tilde{u}}{\partial x}-a_4\tilde{\sigma}+a_8\tilde{D}+a_{11}\tilde{B}\right)=0,\\
-\dfrac{\partial\tilde{\tau}}{\partial x}-\beta\tilde{\tau}=0,\\
a_{14}\dfrac{\partial^2\tilde{\phi}}{\partial x^2}+a_{15}\dfrac{\partial^2\tilde{\psi}}{\partial x^2}-a_1\dfrac{\partial\tilde{\tau}}{\partial x}+\beta\left(a_{14}\dfrac{\partial\tilde{\phi}}{\partial x}+a_{15}\dfrac{\partial\tilde{\psi}}{\partial x}-a_1\tilde{\tau}\right)=0,\\
a_{15}\dfrac{\partial^2\tilde{\phi}}{\partial x^2}+a_{16}\dfrac{\partial^2\tilde{\psi}}{\partial x^2}-a_2\dfrac{\partial\tilde{\tau}}{\partial x}+\beta\left(a_{15}\dfrac{\partial\tilde{\phi}}{\partial x}+a_{16}\dfrac{\partial\tilde{\psi}}{\partial x}-a_2\tilde{\tau}\right)=0,
\end{cases} \tag{22}$$

and the displacement component $\tilde{u}$ is derived from the second to fifth equations in Eq. (22). Hence, we obtain

$$\begin{aligned}
&-\tilde{c}_{11}^{\prime 0}\frac{\partial\tilde{u}}{\partial x}=\varsigma_1\mathrm{e}^{-\beta x},\\
&\tilde{u}=\frac{\varsigma_1}{\tilde{c}_{11}^{\prime 0}\beta}\mathrm{e}^{-\beta x}+\varsigma_2.
\end{aligned} \tag{23}$$

However, no feasible solution for $\varsigma_1(\neq 0)$ and $\varsigma_2(\neq 0)$ fulfills the homogeneous boundary conditions $\tilde{u}(\pm l)=0$, which indicates the absence of eigenvectors for zero eigenvalue. To elucidate the issue, the trivial solution $\varsigma_1 = 0$ and $\varsigma_2 = 0$ lead to the trivial eigenvector (i.e., all the state variables remain zero), which contributes null solutions to the symplectic expansion. Furthermore, the eigenvectors for $-\beta$ eigenvalue are not practical neither. Therefore, the Saint-Venant solutions do not exist with displacements and potentials constrained.

2.3. Eigen-solutions of general eigenvalues

Consider η as the eigenvalue in the x-direction, the determinant is derived as

$$\det\begin{bmatrix} -\mu & -\eta & -a_1\eta & -a_2\eta & a_3 & 0 & 0 & 0 \\ -a_4\eta & -\mu & 0 & 0 & 0 & a_5 & a_6 & a_7 \\ a_8\eta & 0 & -\mu & 0 & 0 & a_6 & -a_9 & a_{10} \\ a_{11}\eta & 0 & 0 & -\mu & 0 & a_7 & a_{10} & -a_{12} \\ a_{13}\left(\eta^2+\beta\eta\right) & 0 & 0 & 0 & -\mu & -a_4\left(\eta+\beta\right) & a_8\left(\eta+\beta\right) & a_{11}\left(\eta+\beta\right) \\ 0 & 0 & 0 & 0 & -\left(\eta+\beta\right) & -\mu & 0 & 0 \\ 0 & 0 & a_{14}\left(\eta^2+\beta\eta\right) & a_{15}\left(\eta^2+\beta\eta\right) & -a_1\left(\eta+\beta\right) & 0 & -\mu & 0 \\ 0 & 0 & a_{15}\left(\eta^2+\beta\eta\right) & a_{16}\left(\eta^2+\beta\eta\right) & -a_2\left(\eta+\beta\right) & 0 & 0 & -\mu \end{bmatrix} = 0, \tag{24}$$

which results in

$$\theta_8\eta^8 + \theta_7\eta^7 + \theta_6\eta^6 + \theta_5\eta^5 + \theta_4\eta^4 + \theta_3\eta^3 + \theta_2\eta^2 + \theta_1\eta + \theta_0 = 0, \tag{25}$$

where θ_i $(i = 0,\cdots,8)$ are parameters, shown in Appendix C; and μ is the nonzero eigenvalue. By replacing η with $\sqrt{\lambda} - \beta/2$, Eq. (25) is further simplified as

$$\begin{aligned} &\Lambda_0\lambda^4 + (\mu^2\Lambda_1 + \beta^2\Lambda_2)\lambda^3 + (\mu^4\Lambda_3 + \mu^2\beta^2\Lambda_4 + \beta^4\Lambda_5)\lambda^2 \\ &+(\mu^6\Lambda_6 + \mu^4\beta^2\Lambda_7 + \mu^2\beta^4\Lambda_8 + \beta^6\Lambda_9)\lambda \\ &+(\mu^8\Lambda_{10} + \mu^6\beta^2\Lambda_{11} + \mu^4\beta^4\Lambda_{12} + \mu^2\beta^6\Lambda_{13} + \beta^8\Lambda_{14}) = 0, \end{aligned} \tag{26}$$

where $\Lambda_k (k = 0,\cdots,14)$ are given in Appendix C. Thus, the eight roots of Eq. (25) are derived analytically as $\eta_t (t = 1,\cdots,8)$ with the assistance of Eq. (26). The eigenvectors for general eigenvalues are in the form of

$$\tilde{\boldsymbol{\Phi}}=\sum_{t=1}^{8}\mathrm{e}^{\eta_t x}[\tilde{A}_t,\tilde{B}_t,\tilde{C}_t,\tilde{D}_t,\tilde{E}_t,\tilde{F}_t,\tilde{G}_t,\tilde{H}_t]^{\mathrm{T}}, \tag{27}$$

where $\tilde{A}_t$, $\tilde{B}_t$, $\tilde{C}_t$, $\tilde{D}_t$, $\tilde{E}_t$, $\tilde{F}_t$, $\tilde{G}_t$, and $\tilde{H}_t$ are constants, which are represented in terms of $\tilde{E}_t$ with the substitution of Eq. (27) into Eq.(21), as

$$\begin{Bmatrix}\tilde{A}_t\\ \tilde{B}_t\\ \tilde{C}_t\\ \tilde{D}_t\\ \tilde{F}_t\\ \tilde{G}_t\\ \tilde{H}_t\end{Bmatrix}=\begin{bmatrix}-\mu & -\eta_t & -a_1\eta_t & -a_2\eta_t & 0 & 0 & 0\\ -a_4\eta_t & -\mu & 0 & 0 & a_5 & a_6 & a_7\\ a_8\eta_t & 0 & -\mu & 0 & a_6 & -a_9 & a_{10}\\ a_{11}\eta_t & 0 & 0 & -\mu & a_7 & a_{10} & -a_{12}\\ 0 & 0 & 0 & 0 & -\mu & 0 & 0\\ 0 & 0 & a_{14}(\eta_t^2+\beta\eta_t) & a_{15}(\eta_t^2+\beta\eta_t) & 0 & -\mu & 0\\ 0 & 0 & a_{15}(\eta_t^2+\beta\eta_t) & a_{16}(\eta_t^2+\beta\eta_t) & 0 & 0 & -\mu\end{bmatrix}^{-1}\begin{Bmatrix}-a_3\\ 0\\ 0\\ 0\\ (\eta_t+\beta)\\ a_1(\eta_t+\beta)\\ a_2(\eta_t+\beta)\end{Bmatrix}\tilde{E}_t \tag{28}$$
$$\equiv[\chi_{1t},\chi_{2t},\chi_{3t},\chi_{4t},\chi_{5t},\chi_{6t},\chi_{7t}]^{\mathrm{T}}\tilde{E}_t,$$

where $\chi_{jt}(j=1,\cdots,7;t=1,\cdots,8)$ are constants, as presented in Appendix C. Then, $\tilde{A}_t$, $\tilde{B}_t$, $\tilde{C}_t$, and $\tilde{D}_t$ in the homogeneous boundary conditions at $x=\pm l$ are replaced with $\tilde{E}_t$, as

$$\begin{cases}\tilde{u}\big|_{x=\pm l}=\sum_{t=1}^{8}\chi_{1t}\tilde{E}_t\mathrm{e}^{\pm l\eta_t}=0,\\ \tilde{w}\big|_{x=\pm l}=\sum_{t=1}^{8}\chi_{2t}\tilde{E}_t\mathrm{e}^{\pm l\eta_t}=0,\\ \tilde{\phi}\big|_{x=\pm l}=\sum_{t=1}^{8}\chi_{3t}\tilde{E}_t\mathrm{e}^{\pm l\eta_t}=0,\\ \tilde{\psi}\big|_{x=\pm l}=\sum_{t=1}^{8}\chi_{4t}\tilde{E}_t\mathrm{e}^{\pm l\eta_t}=0.\end{cases} \tag{29}$$

The determinant of coefficient matrix is established to vanish for nontrivial solutions. Hence we arrive at the following characteristic equation

$$\det\left[\chi_{\lceil\frac{i}{2}\rceil j}\mathrm{e}^{(-1)^{i+1}\eta_j l}\right]=0,\quad(i=1,\cdots,8;j=1,\cdots,8), \tag{30}$$

where the subscript $\lceil\frac{i}{2}\rceil$ is the ceiling function, which maps $\frac{i}{2}$ to the smallest integer greater than or equal to $\frac{i}{2}$. The i-th root μ_i of the characteristic equation are obtained, which lead to the derivation of the parameters for nontrivial solutions

$$\tilde{E}_{1i}=\mu_i,\quad \tilde{E}_{(t+1)i}=\varpi_{ti}\tilde{E}_{1i},\quad (t=1,\cdots,7),\tag{31}$$

where ϖ_{ti} are constants clarified in Appendix C. The eigen-solutions of general eigenvalues are constructed as

$$\tilde{\boldsymbol{f}}_{\mu,i}=\mathrm{e}^{\mu_i z}\tilde{\boldsymbol{\Phi}}_{\mu,i}.\tag{32}$$

2.4. Particular solution and complete solution

Having derived all the eigenvectors for homogeneous state equations, the non-homogeneous term $\tilde{\boldsymbol{f}}'$ in Eq. (8) is expanded as

$$\tilde{\boldsymbol{f}}'=\sum_{i=1}^{\infty}\left[\tilde{g}_{\mu,i}(z)\tilde{\boldsymbol{\Phi}}_{\mu,i}+\tilde{g}_{-\mu,i}(z)\tilde{\boldsymbol{\Phi}}_{-\mu,i}\right],\tag{33}$$

where

$$\begin{cases}\tilde{g}_{\mu,i}(z)=\left\langle\tilde{\boldsymbol{f}}',\tilde{\boldsymbol{\Omega}}_{-\mu,i}\right\rangle,\\ \tilde{g}_{-\mu,i}(z)=\left\langle\tilde{\boldsymbol{f}}',\tilde{\boldsymbol{\Omega}}_{\mu,i}\right\rangle.\end{cases}\tag{34}$$

Assume the particular solution is in the form of

$$\tilde{\boldsymbol{f}}^{p}=\sum_{i=1}^{\infty}\left[\tilde{\mathfrak{g}}_{\mu,i}(z)\tilde{\boldsymbol{\Phi}}_{\mu,i}+\tilde{\mathfrak{g}}_{-\mu,i}(z)\tilde{\boldsymbol{\Phi}}_{-\mu,i}\right],\tag{35}$$

which leads to

$$\begin{cases}\dfrac{\mathrm{d}\tilde{\mathfrak{g}}_{\mu,i}(z)}{\mathrm{d}z}=\mu_i\tilde{\mathfrak{g}}_{\mu,i}(z)+\tilde{g}_{\mu,i}(z),\\ \dfrac{\mathrm{d}\tilde{\mathfrak{g}}_{-\mu,i}(z)}{\mathrm{d}z}=-\mu_i\tilde{\mathfrak{g}}_{-\mu,i}(z)+\tilde{g}_{-\mu,i}(z),\end{cases}\tag{36}$$

after substituting the particular solution into the state equations, where $\tilde{\boldsymbol{\Omega}}_{\pm\mu,i}$ are shown in Appendix B. The complete solution is established according to the symplectic expansion, which can be expressed as

$$\begin{aligned}\tilde{\tilde{\boldsymbol{f}}}&=\tilde{\tilde{\boldsymbol{f}}}^{g}+\tilde{\tilde{\boldsymbol{f}}}^{p}\\ &=\sum_{i=1}^{\infty}(\tilde{m}_{\mu,i}\tilde{\tilde{\boldsymbol{f}}}_{\mu,i}+\tilde{m}_{-\mu,i}\tilde{\tilde{\boldsymbol{f}}}_{-\mu,i})+\sum_{i=1}^{\infty}\left[\tilde{\mathfrak{g}}_{\mu,i}(z)\boldsymbol{\mathcal{M}}\tilde{\boldsymbol{\Phi}}_{\mu,i}+\tilde{\mathfrak{g}}_{-\mu,i}(z)\boldsymbol{\mathcal{M}}\tilde{\boldsymbol{\Phi}}_{-\mu,i}\right]\\ &=\sum_{i=1}^{\infty}\left\{[\tilde{m}_{\mu,i}+\tilde{m}^{*}_{\mu,i}(z)]\tilde{\tilde{\boldsymbol{f}}}_{\mu,i}+[\tilde{m}_{-\mu,i}+\tilde{m}^{*}_{-\mu,i}(z)]\tilde{\tilde{\boldsymbol{f}}}_{-\mu,i}\right\},\end{aligned}\tag{37}$$

where $\tilde{\tilde{\boldsymbol{f}}}_{\mu,i}$ and $\tilde{\tilde{\boldsymbol{f}}}_{-\mu,i}$ are the eigen-solutions of general eigenvalues μ_i and $-\mu_i$, respectively, and

$$\begin{cases}\tilde{\mathfrak{g}}_{\mu,i}(z)=\mathrm{e}^{\mu_i z}\tilde{m}^*_{\mu,i}(z)=\mathrm{e}^{\mu_i z}\int_0^z \mathrm{e}^{-\mu_i\zeta}\tilde{g}(\zeta)\mathrm{d}\zeta,\\ \tilde{\mathfrak{g}}_{-\mu,i}(z)=\mathrm{e}^{-\mu_i z}\tilde{m}^*_{-\mu,i}(z)=\mathrm{e}^{-\mu_i z}\int_0^z \mathrm{e}^{\mu_i\zeta}\tilde{g}(\zeta)\mathrm{d}\zeta,\end{cases} \tag{38}$$

It is noteworthy that the eigen-solutions are distinct from the full state vectors $\tilde{\tilde{\boldsymbol{f}}}$, such that

$$\tilde{\tilde{\boldsymbol{f}}}=\boldsymbol{\mathcal{M}}\tilde{\boldsymbol{f}}, \tag{39}$$

where $\boldsymbol{\mathcal{M}}=\mathrm{diag}[1,1,1,1,\mathrm{e}^{\beta x},\mathrm{e}^{\beta x},\mathrm{e}^{\beta x},\mathrm{e}^{\beta x}]$.

To determine the parameters appeared in general solution, we first connect the full state vector with the complex eigen-solutions as

$$\begin{aligned}\tilde{\tilde{\boldsymbol{f}}}^g&=\tilde{\tilde{\boldsymbol{f}}}^g+\tilde{\tilde{\boldsymbol{f}}}^p\\&=\sum_{i=1}^{\infty}\Big[(\tilde{m}^{\mathrm{Re}}_{\mu,i}\mathrm{Re}\tilde{\tilde{\boldsymbol{f}}}_{\mu,i}+\tilde{m}^{\mathrm{Im}}_{\mu,i}\mathrm{Im}\tilde{\tilde{\boldsymbol{f}}}_{\mu,i})+(\tilde{m}^{\mathrm{Re}}_{-\mu,i}\mathrm{Re}\tilde{\tilde{\boldsymbol{f}}}_{-\mu,i}+\tilde{m}^{\mathrm{Im}}_{-\mu,i}\mathrm{Im}\tilde{\tilde{\boldsymbol{f}}}_{-\mu,i})\Big]+\tilde{\tilde{\boldsymbol{f}}}^p_{\mathrm{R}},\end{aligned} \tag{40}$$

where

$$\tilde{\tilde{\boldsymbol{f}}}^p_{\mathrm{R}}=\sum_{i=1}^{\infty}\Big\{2\,\mathrm{Re}[\tilde{m}^*_{\mu,i}(z)]\,\mathrm{Re}\,\tilde{\tilde{\boldsymbol{f}}}_{\mu,i}-2\,\mathrm{Im}[\tilde{m}^*_{\mu,i}(z)]\,\mathrm{Im}\,\tilde{\tilde{\boldsymbol{f}}}_{\mu,i}+2\,\mathrm{Re}[\tilde{m}^*_{-\mu,i}(z)]\,\mathrm{Re}\,\tilde{\tilde{\boldsymbol{f}}}_{-\mu,i}-2\,\mathrm{Im}[\tilde{m}^*_{-\mu,i}(z)]\,\mathrm{Im}\,\tilde{\tilde{\boldsymbol{f}}}_{-\mu,i}\Big\},$$

where $\tilde{m}^{\mathrm{Re}}_{\mu,i}$, $\tilde{m}^{\mathrm{Im}}_{\mu,i}$, $\tilde{m}^{\mathrm{Re}}_{-\mu,i}$, and $\tilde{m}^{\mathrm{Im}}_{-\mu,i}$ are the coefficients for superposition; $\mathrm{Re}[\cdot]$ and $\mathrm{Im}[\cdot]$ represent the real part and imaginary part, respectively.

The boundary conditions at $z=h$ is assumed as

$$\tilde{\tilde{u}}=0,\quad \tilde{\tilde{w}}=0,\quad \tilde{\tilde{\phi}}=0,\quad \tilde{\tilde{\psi}}=0. \tag{41}$$

If the indenter is perfectly insulated and frictionless, the mixed boundary-value conditions at $z=0$ are

$$\begin{cases}\tilde{\tilde{w}}=[d-\kappa(x)]/\omega, & x\in[a,b],\\ \tilde{\tilde{\sigma}}=0, & x\in[-l,a]\cup[b,l],\end{cases}\quad \tilde{\tilde{\tau}}=0,\quad \tilde{\tilde{D}}=0,\quad \tilde{\tilde{B}}=0, \tag{42}$$

where d is the maximum indentation depth, $\kappa(x)$ represents the indenter shape function, and $x\in[a,b]$ is the contact region.

To solve the mixed boundary-value problems, the Hamiltonian mixed energy variational principle [77] in frequency domain is introduced

$$\begin{aligned}&\delta\left\{\int_0^h\int_{-l}^{l}\left[\tilde{\boldsymbol{p}}^{\mathrm{T}}\frac{\partial\tilde{\boldsymbol{q}}}{\partial z}-H(\tilde{\boldsymbol{q}},\tilde{\boldsymbol{p}})\right]\mathrm{d}x\mathrm{d}z-\int_{\Gamma_{\bar{\tilde{q}}_h}}\left[\tilde{\boldsymbol{p}}^{\mathrm{T}}(\tilde{\boldsymbol{q}}-\bar{\tilde{\boldsymbol{q}}}_h)\right]\mathrm{d}x\right.\\&\left.-\int_{\Gamma_{\bar{\tilde{p}}_h}}\left[\bar{\tilde{\boldsymbol{p}}}_h{}^{\mathrm{T}}\tilde{\boldsymbol{q}}\right]\mathrm{d}x+\int_{\Gamma_{\bar{\tilde{q}}_0}}\left[\tilde{\boldsymbol{p}}^{\mathrm{T}}(\tilde{\boldsymbol{q}}-\bar{\tilde{\boldsymbol{q}}}_0)\right]\mathrm{d}x+\int_{\Gamma_{\bar{\tilde{p}}_0}}\left[\bar{\tilde{\boldsymbol{p}}}_0{}^{\mathrm{T}}\tilde{\boldsymbol{q}}\right]\mathrm{d}x\right\}=0,\end{aligned}\tag{43}$$

which can be further simplified as

$$\begin{aligned}&\int_{\Gamma_{\bar{\tilde{p}}_h}}\left[(\delta\tilde{\boldsymbol{q}})^{\mathrm{T}}(\tilde{\boldsymbol{p}}-\bar{\tilde{\boldsymbol{p}}}_h)\right]\mathrm{d}x-\int_{\Gamma_{\bar{\tilde{q}}_h}}\left[(\delta\tilde{\boldsymbol{p}})^{\mathrm{T}}(\tilde{\boldsymbol{q}}-\bar{\tilde{\boldsymbol{q}}}_h)\right]\mathrm{d}x\\&+\int_{\Gamma_{\bar{\tilde{q}}_0}}\left[(\delta\tilde{\boldsymbol{p}})^{\mathrm{T}}(\tilde{\boldsymbol{q}}-\bar{\tilde{\boldsymbol{q}}}_0)\right]\mathrm{d}x-\int_{\Gamma_{\bar{\tilde{p}}_0}}\left[(\delta\tilde{\boldsymbol{q}})^{\mathrm{T}}(\tilde{\boldsymbol{p}}-\bar{\tilde{\boldsymbol{p}}}_0)\right]\mathrm{d}x=0,\end{aligned}\tag{44}$$

because the adjoint vectors satisfy the canonical equation. It is noted that the non-conservative system is transformed into a conservative system through Laplace transform such that the variational principle is feasible to this problem [73]. The boundary with determined displacement $\bar{\tilde{\boldsymbol{q}}}_h$ at $z=h$ is defined as $\Gamma_{\bar{\tilde{q}}_h}$ in frequency domain, and the remaining symbols denote analogous meanings. Substituting Eq. (40) into Eq. (44) yields the relation as

$$\begin{aligned}&\int_{\Gamma_{\bar{\tilde{p}}_h}}\left[(\sum_{i=1}^{\infty}\delta\tilde{m}_i\tilde{\boldsymbol{q}}_i)^{\mathrm{T}}(\tilde{\boldsymbol{p}}_{\mathrm{R}}^p+\sum_{j=1}^{\infty}\tilde{m}_j\tilde{\boldsymbol{p}}_j-\bar{\tilde{\boldsymbol{p}}}_h)\right]\mathrm{d}x-\int_{\Gamma_{\bar{\tilde{q}}_h}}\left[(\sum_{i=1}^{\infty}\delta\tilde{m}_i\tilde{\boldsymbol{p}}_i)^{\mathrm{T}}(\tilde{\boldsymbol{q}}_{\mathrm{R}}^p+\sum_{j=1}^{\infty}\tilde{m}_j\tilde{\boldsymbol{q}}_j-\bar{\tilde{\boldsymbol{q}}}_h)\right]\mathrm{d}x\\&+\int_{\Gamma_{\bar{\tilde{q}}_0}}\left[(\sum_{i=1}^{\infty}\delta\tilde{m}_i\tilde{\boldsymbol{p}}_i)^{\mathrm{T}}(\tilde{\boldsymbol{q}}_{\mathrm{R}}^p+\sum_{j=1}^{\infty}\tilde{m}_j\tilde{\boldsymbol{q}}_j-\bar{\tilde{\boldsymbol{q}}}_0)\right]\mathrm{d}x-\int_{\Gamma_{\bar{\tilde{p}}_0}}\left[(\sum_{i=1}^{\infty}\delta\tilde{m}_i\tilde{\boldsymbol{q}}_i)^{\mathrm{T}}(\tilde{\boldsymbol{p}}_{\mathrm{R}}^p+\sum_{j=1}^{\infty}\tilde{m}_j\tilde{\boldsymbol{p}}_j-\bar{\tilde{\boldsymbol{p}}}_0)\right]\mathrm{d}x=0,\end{aligned}\tag{45}$$

where $\tilde{\boldsymbol{f}}_{\mathrm{R}}^p=[\tilde{\boldsymbol{q}}_{\mathrm{R}}^p,\tilde{\boldsymbol{p}}_{\mathrm{R}}^p]^{\mathrm{T}}$. Without loss of generality, we may assume

$$\begin{aligned}\tilde{\mathscr{A}}_{ij}&=\int_{\Gamma_{\bar{\tilde{p}}_h}}\left[(\tilde{\boldsymbol{q}}_i)^{\mathrm{T}}\tilde{\boldsymbol{p}}_j\right]\mathrm{d}x-\int_{\Gamma_{\bar{\tilde{q}}_h}}\left[(\tilde{\boldsymbol{p}}_i)^{\mathrm{T}}\tilde{\boldsymbol{q}}_j\right]\mathrm{d}x+\int_{\Gamma_{\bar{\tilde{q}}_0}}\left[(\tilde{\boldsymbol{p}}_i)^{\mathrm{T}}\tilde{\boldsymbol{q}}_j\right]\mathrm{d}x-\int_{\Gamma_{\bar{\tilde{p}}_0}}\left[(\tilde{\boldsymbol{q}}_i)^{\mathrm{T}}\tilde{\boldsymbol{p}}_j\right]\mathrm{d}x,\\\tilde{\mathscr{H}}_i&=\int_{\Gamma_{\bar{\tilde{p}}_h}}\left[(\tilde{\boldsymbol{q}}_i)^{\mathrm{T}}\bar{\tilde{\boldsymbol{p}}}_h\right]\mathrm{d}x-\int_{\Gamma_{\bar{\tilde{q}}_h}}\left[(\tilde{\boldsymbol{p}}_i)^{\mathrm{T}}\bar{\tilde{\boldsymbol{q}}}_h\right]\mathrm{d}x+\int_{\Gamma_{\bar{\tilde{q}}_0}}\left[(\tilde{\boldsymbol{p}}_i)^{\mathrm{T}}\bar{\tilde{\boldsymbol{q}}}_0\right]\mathrm{d}x-\int_{\Gamma_{\bar{\tilde{p}}_0}}\left[(\tilde{\boldsymbol{q}}_i)^{\mathrm{T}}\bar{\tilde{\boldsymbol{p}}}_0\right]\mathrm{d}x,\\\tilde{\mathscr{K}}_i&=\int_{\Gamma_{\bar{\tilde{p}}_h}}\left[(\tilde{\boldsymbol{q}}_i)^{\mathrm{T}}\tilde{\boldsymbol{p}}_{\mathrm{R}}^p\right]\mathrm{d}x-\int_{\Gamma_{\bar{\tilde{q}}_h}}\left[(\tilde{\boldsymbol{p}}_i)^{\mathrm{T}}\tilde{\boldsymbol{q}}_{\mathrm{R}}^p\right]\mathrm{d}x+\int_{\Gamma_{\bar{\tilde{q}}_0}}\left[(\tilde{\boldsymbol{p}}_i)^{\mathrm{T}}\tilde{\boldsymbol{q}}_{\mathrm{R}}^p\right]\mathrm{d}x-\int_{\Gamma_{\bar{\tilde{p}}_0}}\left[(\tilde{\boldsymbol{q}}_i)^{\mathrm{T}}\tilde{\boldsymbol{p}}_{\mathrm{R}}^p\right]\mathrm{d}x,\end{aligned}\tag{46}$$

which leads to

$$\tilde{\tilde{\mathscr{A}}}_{ij}\tilde{m}_j = \tilde{\tilde{\mathscr{H}}}_i - \tilde{\tilde{\mathscr{K}}}_i, \tag{47}$$

where

$$\tilde{m}_k = \frac{\det \tilde{\tilde{\mathscr{A}}}_{ij;k}}{\det \tilde{\tilde{\mathscr{A}}}_{ij}}, \tag{48}$$

$\tilde{\tilde{\mathscr{A}}}_{ij;k}$ is the matrix formed by replacing the k-th column of $\tilde{\tilde{\mathscr{A}}}_{ij}$ by the column vector $\tilde{\tilde{\mathscr{H}}}_i - \tilde{\tilde{\mathscr{K}}}_i$. Applying inverse Laplace transform, we obtain the complete solution in the temporal domain as

$$\widehat{\boldsymbol{f}} = \mathcal{L}^{-1}[\tilde{\tilde{\boldsymbol{f}}}]. \tag{49}$$

3. Numerical Examples and Discussion

As shown in the previous section, the complete solution is formulated in symplectic expansion in Eq. (40), which is a combination of general and particular solutions of a quasi-Hamiltonian operator. After transforming a non-conservative system into a conservative one via Laplace transform, all constants for superposition can be derived through the Hamiltonian mixed energy variational principle.

In the subsequent sections, we will give two simple numerical examples involving viscoelasticity, where the above solutions are computed numerically by analyzing the distribution of eigenvalues. We also conduct finite element analysis (FEA) to verify the analytical solutions. In particular, the first example demonstrates stress relaxation effect. An indentation curve with viscoelastic and inhomogeneous effects is also discussed. The second example displays the results under the action of multiple indenters. The same material parameters are chosen for both examples.

3.1. Viscoelastic plane

Considering the application of a rigid flat punch on the surface of a finite-sized horizontally graded viscoelastic plane with length $2l = 20(\mathrm{m})$ and width $h = 10(\mathrm{m})$, as illustrated in Fig. 2. Without loss of generality, a two-dimensional contact region within the domain $x \in [-0.5, 0.5]$ (m) and with the maximum indentation depth $d = 0.02(\mathrm{m})$ is assumed. The temperature is set as $T = 273.15(\mathrm{K})$.

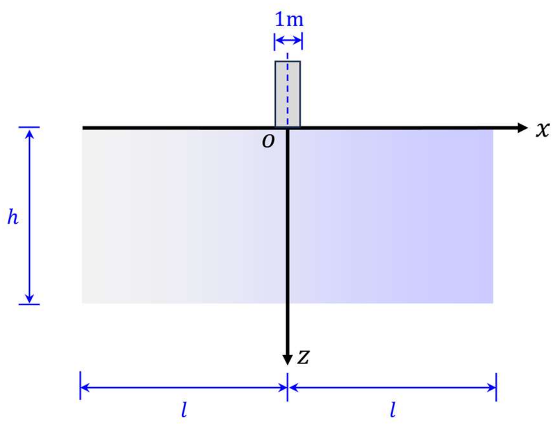

Fig. 2. Application of a rigid flat punch symmetrically with respect to the z-axis on the surface of a horizontally graded viscoelastic plane.

Following the generalized Maxwell model, the constitutive relations are given by

$$\begin{cases} s_{ij} = 2G(x,t) * \mathrm{d}\hat{e}_{ij}(t) = 2\int_0^t G(x,t-\tau)\dfrac{\mathrm{d}\hat{e}_{ij}(\tau)}{\mathrm{d}\tau}\mathrm{d}\tau, \\ \sigma_{kk} = 3K(x,t) * \mathrm{d}\hat{\varepsilon}_{ij}(t) = 3\int_0^t K(x,t-\tau)\dfrac{\mathrm{d}\hat{\varepsilon}_{kk}(\tau)}{\mathrm{d}\tau}\mathrm{d}\tau, \end{cases} \tag{50}$$

where

$$\begin{cases} s_{ij} = \sigma_{ij} - \dfrac{1}{3}\sigma_{kk}\delta_{ij}, \\ \hat{e}_{ij} = \hat{\varepsilon}_{ij} - \dfrac{1}{3}\hat{\varepsilon}_{kk}\delta_{ij}, \end{cases} \tag{51}$$

in which σ_{ij}, s_{ij}, $\hat{\varepsilon}_{ij}$, and $\hat{e}_{ij}$ are the stress, deviatoric stress, strain, and deviatoric strain components, respectively; δ_{ij} is the Kronecker delta. The shear relaxation modulus and the bulk relaxation modulus are $G(x,t)$ and $K(x,t)$, respectively, and they are assumed to vary exponentially along the x-direction, i.e.,

$$\begin{cases} G(x,t) = \mathfrak{G}(t)\mathrm{e}^{\beta x} = [\mathfrak{G}_\infty + \sum_{i=1}^{N}\mathfrak{G}_i \mathrm{e}^{-\frac{t}{\hat{\tau}_{1i}}}]\mathrm{e}^{\beta x}, \\ K(x,t) = \mathfrak{K}(t)\mathrm{e}^{\beta x} = [\mathfrak{K}_\infty + \sum_{i=1}^{N}\mathfrak{K}_i \mathrm{e}^{-\frac{t}{\hat{\tau}_{2i}}}]\mathrm{e}^{\beta x}, \end{cases} \tag{52}$$

where $\hat{\tau}_{1i} = \hat{\eta}_i / \mathfrak{G}_i$ and $\hat{\tau}_{2i} = \hat{\eta}_i / \mathfrak{K}_i$; while $\mathfrak{G}_\infty$, $\mathfrak{G}_i$, $\mathfrak{K}_\infty$, $\mathfrak{K}_i$, and $\hat{\eta}_i$ are viscous parameters. For simplicity, we assume that

$$K(x,t) = \frac{2(1+\nu)}{3(1-2\nu)}G(x,t) = \frac{1}{3(1-2\nu)}E(x,t), \tag{53}$$

where $E(x,t)$ is the Young's relaxation modulus and ν is the Poisson's ratio. If $K(x,t)$ and $G(x,t)$ are proportional, then Poisson's ratio keeps constants and Young's relaxation modulus remains proportional to $K(x,t)$. Furthermore, the relation in Eq. (53) also indicates that

$$\hat{\tau}_{1i} = \hat{\tau}_{2i} = \hat{\tau}_i = \hat{\eta}_i / \mathfrak{G}_i, \tag{54}$$

as shown in Fig. 3. The values of essential parameters are listed in Table 1.

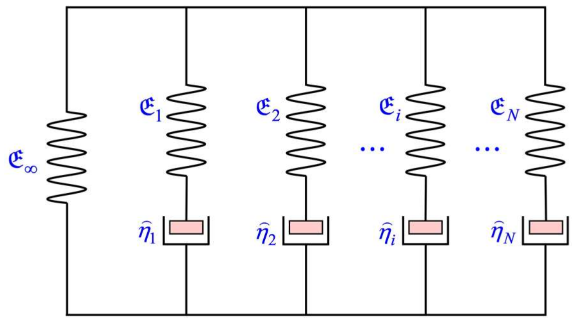

Fig. 3. Generalized Maxwell model where $\mathfrak{E}_\infty$ and $\mathfrak{E}_i$ are viscous parameters in Young's relaxation modulus.

Table 1. General and branch parameters in the viscoelastic case.

General parameters	Poisson's ratio $\nu = 0.25$	Instantaneous shear modulus $\mathfrak{G}_0 = 27.46(\text{Pa})$	Material gradient index $\beta = 0.1\ (\text{m}^{-1})$
Branch parameters	Shear modulus-1	$\mathfrak{G}_1 = 0.04\mathfrak{G}_0(\text{Pa})$	$\widehat{\tau}_1 = 0.003(\text{s})$
	Shear modulus-2	$\mathfrak{G}_2 = 0.08\mathfrak{G}_0(\text{Pa})$	$\widehat{\tau}_2 = 0.03(\text{s})$
	Shear modulus-3	$\mathfrak{G}_3 = 0.09\mathfrak{G}_0(\text{Pa})$	$\widehat{\tau}_3 = 0.3(\text{s})$
	Shear modulus-4	$\mathfrak{G}_4 = 0.25\mathfrak{G}_0(\text{Pa})$	$\widehat{\tau}_4 = 1.2(\text{s})$

It warrants noting that the constant $\mathfrak{G}_\infty$ is rather difficult to be determined in an experiment, because it reveals the shear modulus as the time approaches infinity. However, the following form is taken instead

$$\mathfrak{G}(t) = \mathfrak{G}_0(1 - \sum_{i=1}^{N} r_i) + \sum_{i=1}^{N} \mathfrak{G}_0 r_i \mathrm{e}^{-t/\widehat{\tau}_i}, \tag{55}$$

where $r_i = \mathfrak{G}_i / \mathfrak{G}_0$, and

$$\mathfrak{G}_0 = \mathfrak{G}(0) = \mathfrak{G}_\infty + \sum_{i=1}^{N} \mathfrak{G}_i. \tag{56}$$

We may further simplify Eq. (50) as

$$
\begin{aligned}
\sigma_{ij}(t) &= [2\mathfrak{G}(t) * \mathrm{d}\hat{e}_{ij}(t)]\mathrm{e}^{\beta x} + \frac{1}{3}[3\mathfrak{K}(t) * \mathrm{d}\hat{\varepsilon}_{kk}(t)]\delta_{ij}\mathrm{e}^{\beta x} \\
&= \{2\mathfrak{G}(t) * \mathrm{d}\hat{\varepsilon}_{ij}(t) + [\mathfrak{K}(t) - \frac{2}{3}\mathfrak{G}(t)] * \mathrm{d}\hat{\varepsilon}_{kk}(t)\delta_{ij}\}\mathrm{e}^{\beta x},
\end{aligned} \tag{57}
$$

which leads to state equations in the frequency domain (with tilde above the variables) according to the definition of Laplace transform in Eq. (3), as

$$
\frac{\partial}{\partial z}\begin{Bmatrix} \tilde{u}_z \\ \tilde{u}_x \\ \tilde{\tilde{\sigma}}_{zz} \\ \tilde{\tilde{\sigma}}_{xz} \end{Bmatrix} = \left[\begin{array}{cc|cc} 0 & -\dfrac{\mathfrak{A}_2}{\mathfrak{A}_1}\dfrac{\partial}{\partial x} & \dfrac{1}{\omega\mathfrak{A}_1} & 0 \\ -\dfrac{\partial}{\partial x} & 0 & 0 & \dfrac{1}{\omega\tilde{\mathfrak{G}}} \\ \hline 0 & 0 & 0 & -\left(\dfrac{\partial}{\partial x}+\beta\right) \\ 0 & -\omega\dfrac{\mathfrak{A}_1^2-\mathfrak{A}_2^2}{\mathfrak{A}_1}\left(\dfrac{\partial^2}{\partial x^2}+\beta\dfrac{\partial}{\partial x}\right) & -\dfrac{\mathfrak{A}_2}{\mathfrak{A}_1}\left(\dfrac{\partial}{\partial x}+\beta\right) & 0 \end{array}\right]\begin{Bmatrix} \tilde{u}_z \\ \tilde{u}_x \\ \tilde{\tilde{\sigma}}_{zz} \\ \tilde{\tilde{\sigma}}_{xz} \end{Bmatrix}, \tag{58}
$$

where $\tilde{\tilde{\sigma}}_{ij} = \tilde{\sigma}_{ij}\mathrm{e}^{-\beta x}$ are the modified stress components; $\tilde{u}_x$ and $\tilde{u}_z$ are the displacement components in the x- and z-directions, respectively; $\tilde{\mathfrak{G}}$ and $\tilde{\mathfrak{K}}$ are given by

$$
\begin{cases} \tilde{\mathfrak{G}} = \dfrac{1}{\omega}\mathfrak{G}_0(1-\sum\limits_{i=1}^{N} r_i) + \sum\limits_{i=1}^{N}\dfrac{\mathfrak{G}_0 r_i}{\omega + 1/\tau_i}, \\ \tilde{\mathfrak{K}} = \dfrac{2(1+\nu)}{3(1-2\nu)}\tilde{\mathfrak{G}}, \end{cases} \tag{59}
$$

and

$$
\mathfrak{A}_1 = 4\tilde{\mathfrak{G}}\frac{\tilde{\mathfrak{K}}+\tilde{\mathfrak{G}}/3}{\tilde{\mathfrak{K}}+4\tilde{\mathfrak{G}}/3}, \quad \mathfrak{A}_2 = 2\tilde{\mathfrak{G}}\frac{\tilde{\mathfrak{K}}-2\tilde{\mathfrak{G}}/3}{\tilde{\mathfrak{K}}+4\tilde{\mathfrak{G}}/3}. \tag{60}
$$

The homogeneous boundary conditions at $x = \pm l$ yield

$$
\omega\frac{\mathfrak{A}_1^2-\mathfrak{A}_2^2}{\mathfrak{A}_1}\frac{\partial\tilde{u}_x}{\partial x} + \frac{\mathfrak{A}_2}{\mathfrak{A}_1}\tilde{\tilde{\sigma}}_{zz} = 0, \quad \tilde{\tilde{\sigma}}_{xz} = 0, \tag{61}
$$

and the boundary conditions at z-direction are

$$
z = h, \quad \begin{cases} \tilde{u}_z = 0, \\ \tilde{u}_x = 0, \end{cases} \quad z = 0, \quad \begin{cases} \tilde{\tilde{\sigma}}_{xz} = 0, & x \in [-l,l]. \\ \tilde{u}_z = d/\omega, & x \in [a,b]. \\ \tilde{\tilde{\sigma}}_{zz} = 0, & x \in [-l,a]\cup[b,l]. \end{cases} \tag{62}
$$

The eigen-solutions for zero eigenvalue are obtained via the method of variable separation, as

$$
\begin{aligned}
&\tilde{\boldsymbol{f}}_{0,1}^{(0)}=\tilde{\boldsymbol{\Phi}}_{0,1}^{(0)}=[\frac{1}{\omega},0,0,0]^{\mathrm{T}}, \qquad \tilde{\boldsymbol{f}}_{0,2}^{(0)}=\tilde{\boldsymbol{\Phi}}_{0,2}^{(0)}=[0,\frac{1}{\omega},0,0]^{\mathrm{T}},\\
&\tilde{\boldsymbol{f}}_{0,1}^{(1)}=\tilde{\boldsymbol{\Phi}}_{0,1}^{(1)}+z\tilde{\boldsymbol{\Phi}}_{0,1}^{(0)}=[\frac{z}{\omega},-\frac{\mathfrak{A}_2}{\omega\mathfrak{A}_1}x,\frac{\mathfrak{A}_1^2-\mathfrak{A}_2^2}{\mathfrak{A}_1},0]^{\mathrm{T}}, \quad \tilde{\boldsymbol{f}}_{0,2}^{(1)}=\tilde{\boldsymbol{\Phi}}_{0,2}^{(1)}+z\tilde{\boldsymbol{\Phi}}_{0,2}^{(0)}=[-\frac{x}{\omega},\frac{z}{\omega},0,0]^{\mathrm{T}},\\
&\tilde{\boldsymbol{f}}_{0,2}^{(2)}=\tilde{\boldsymbol{\Phi}}_{0,2}^{(2)}+z\tilde{\boldsymbol{\Phi}}_{0,2}^{(1)}+\frac{z^2}{2}\tilde{\boldsymbol{\Phi}}_{0,2}^{(0)}=[-\frac{xz}{\omega},\frac{1}{2\omega}(\frac{\mathfrak{A}_2}{\mathfrak{A}_1}x^2+z^2),-\frac{\mathfrak{A}_1^2-\mathfrak{A}_2^2}{\mathfrak{A}_1}x,0]^{\mathrm{T}},\\
&\tilde{\boldsymbol{f}}_{0}^{(3)}=\tilde{\boldsymbol{\Phi}}_{0}^{(3)}+z\tilde{\boldsymbol{\Phi}}_{0,2}^{(2)}+\frac{z^2}{2!}\tilde{\boldsymbol{\Phi}}_{0,2}^{(1)}+\frac{z^3}{3!}\tilde{\boldsymbol{\Phi}}_{0,2}^{(0)}+\zeta_0(z\tilde{\boldsymbol{\Phi}}_{0,1}^{(1)}+\frac{z^2}{2!}\tilde{\boldsymbol{\Phi}}_{0,1}^{(0)}),
\end{aligned}
\tag{63}
$$

where

$$
\tilde{\boldsymbol{\Phi}}_0^{(3)}=\begin{Bmatrix}\mathfrak{X}\\0\\0\\\dfrac{\left(\mathfrak{A}_1^2-\mathfrak{A}_2^2\right)\left(-\beta\zeta_0+\beta l\mathrm{e}^{-\beta x}\operatorname{csch}(\beta l)+\beta x-1\right)}{\mathfrak{A}_1\beta^2}\end{Bmatrix},
\tag{64}
$$

and

$$
\zeta_0=l\coth(\beta l)-\frac{1}{\beta},
$$

$$
\begin{aligned}
\mathfrak{X}=\frac{1}{2\mathfrak{A}_1\beta^3\tilde{\mathfrak{G}}\omega}\Big\{&\mathfrak{A}_1^2\left[(\coth(\beta l)-1)\mathrm{e}^{\beta l}(2\beta l+\sinh(\beta l)(2\beta\zeta_0+\beta x(-2\beta\zeta_0+\beta x-2)+2))-2\beta l\operatorname{csch}(\beta l)\mathrm{e}^{-\beta x}\right]\\
&+\mathfrak{A}_2^2\left[-2\beta l\mathrm{e}^{\beta l}\coth(\beta l)+\beta\left(2l\mathrm{e}^{\beta l}-2\zeta_0+x(2\beta\zeta_0-\beta x+2)\right)+2\beta l\mathrm{e}^{-\beta x}\operatorname{csch}(\beta l)-2\right]-\beta^3\mathfrak{A}_2\tilde{\mathfrak{G}}x^2(\frac{x}{3}-\zeta_0)\Big\}.
\end{aligned}
$$

For general eigenvalues, the corresponding eigen-solutions are constructed as

$$
\tilde{\boldsymbol{f}}_{\mu,n}=\mathrm{e}^{\mu_n z}\tilde{\boldsymbol{\Phi}}_n=\mathrm{e}^{\mu_n z}\sum_{i=1}^{4}\left(\mathrm{e}^{\eta_{in}x}[\tilde{\mathcal{A}}_{in},\tilde{\mathcal{B}}_{in},\tilde{\mathcal{C}}_{in},\tilde{\mathcal{D}}_{in}]^{\mathrm{T}}\right),
\tag{65}
$$

where $\tilde{\mathcal{A}}_{in}$, $\tilde{\mathcal{B}}_{in}$, $\tilde{\mathcal{C}}_{in}$, and $\tilde{\mathcal{D}}_{in}$ are constants, which are represented in a compact form in Appendix D; η_{in} are

$$
\begin{aligned}
\eta_{1n}&=-\frac{1}{2}\beta+\frac{1}{2}\sqrt{\beta^2-4\mu_n^2-2\mu_n\beta\sqrt{2(-2\tilde{\mathfrak{G}}+3\tilde{\mathfrak{K}})/(\tilde{\mathfrak{G}}+3\tilde{\mathfrak{K}})}},\\
\eta_{2n}&=-\frac{1}{2}\beta-\frac{1}{2}\sqrt{\beta^2-4\mu_n^2-2\mu_n\beta\sqrt{2(-2\tilde{\mathfrak{G}}+3\tilde{\mathfrak{K}})/(\tilde{\mathfrak{G}}+3\tilde{\mathfrak{K}})}},\\
\eta_{3n}&=-\frac{1}{2}\beta+\frac{1}{2}\sqrt{\beta^2-4\mu_n^2+2\mu_n\beta\sqrt{2(-2\tilde{\mathfrak{G}}+3\tilde{\mathfrak{K}})/(\tilde{\mathfrak{G}}+3\tilde{\mathfrak{K}})}},\\
\eta_{4n}&=-\frac{1}{2}\beta-\frac{1}{2}\sqrt{\beta^2-4\mu_n^2+2\mu_n\beta\sqrt{2(-2\tilde{\mathfrak{G}}+3\tilde{\mathfrak{K}})/(\tilde{\mathfrak{G}}+3\tilde{\mathfrak{K}})}},
\end{aligned}
\tag{66}
$$

which are derived through the following characteristic equation

$$
\begin{aligned}
&(\eta_1-\eta_2)(\eta_3-\eta_4)+(\eta_1-\eta_4)(\eta_2-\eta_3)\cosh[(\eta_1-\eta_2-\eta_3+\eta_4)l]\\
&+(\eta_1-\eta_3)(\eta_4-\eta_2)\cosh[(\eta_1-\eta_2+\eta_3-\eta_4)l]=0.
\end{aligned}
\tag{67}
$$

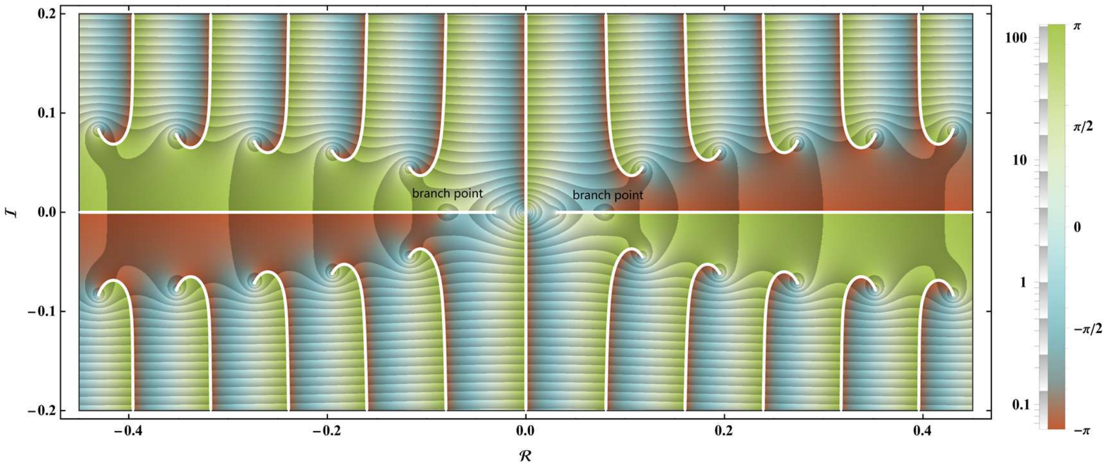

Fig. 4. The left-hand side of Eq. (67) on the complex plane (real axis $\Re(\mu) \in [-0.45, 0.45]$ and imaginary axis $\Im(\mu) \in [-0.2, 0.2]$). All zeros and branch points are illustrated as circles. The material parameters are selected as in Table1.

As presented in Fig. 4, roots in the $\tilde{\alpha}$-set and $\tilde{\beta}$-set show symmetry about both the real and imaginary axes. We may take the roots according to Chen and Chen [76], which leads to the derivation of the general solutions in Fig. 5. To verify, finite element analysis using COMSOL Multiphysics [78] is conducted. A comparison with FE numerical solutions is shown in Fig. 5.

(a)

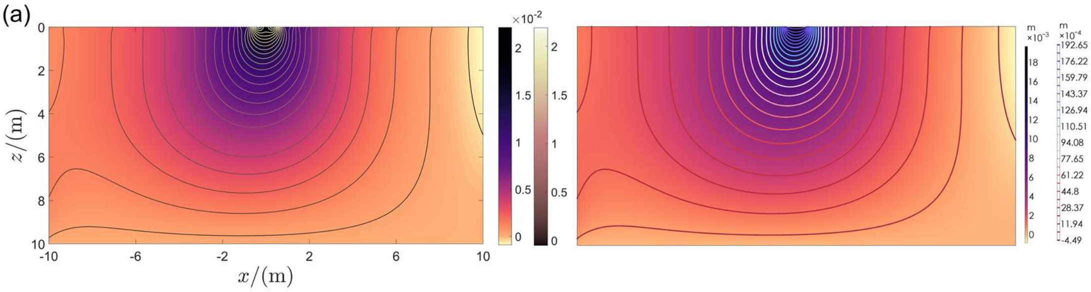

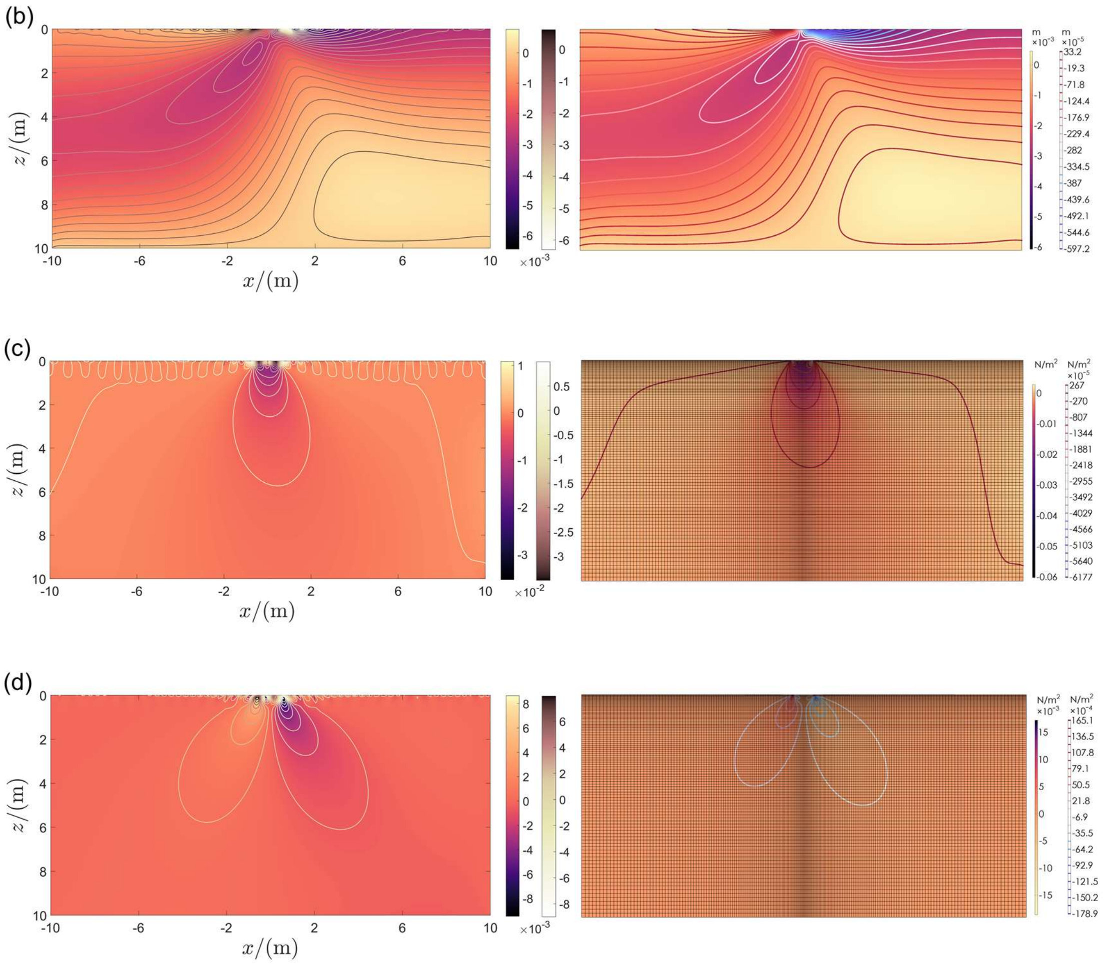

Fig. 5. Comparison between analytical solutions and FEA numerical solutions using COMSOL Multiphysics [78] for deformation and stress distribution for $t = 0.1(\mathrm{s})$ in the domain. There are 61 eigenvalues derived through symplectic analysis on the left while FEA solutions are shown on the right. The penalty method in FEA is used with 20,381 nodes, and a highly refined FE mesh is used on the surface, particularly within the contact region. The mesh for displacement remains similar to stress distribution, which is omitted here. The comparison cases illustrated include **(a)** vertical displacement; **(b)** horizontal displacement; **(c)** normal stress; and **(d)** shear stress. The material parameters are selected as in Table1.

It is evident from Fig. 5 that a comparison of contour plots between symplectic analytical solutions and FEA shows excellent and precise agreement, with the exception of solution oscillation at the boundaries. The oscillating behavior at $z=0$ is instigated by the Gibbs phenomenon and coupled with geometric singularities as elucidated in Chen and Chen [76]. While away from the surface, solution oscillation diminishes significantly due to decaying characteristics of the solution, as illustrated in Fig. 5(c) and Fig. 5(d). Furthermore, displacement comparison is more accurate than stress in between symplectic solutions and FEA result, which indicates the symplectic expansion is unable to capture singularities in the stress concentration perfectly. In addition, it is crucial to emphasize that the contact analysis of viscoelastic planes is inherently quasi-static, necessitating computational methodologies to yield convergent solutions to ensure reliability. Although the penalty method is comparatively less precise than the augmented Lagrangian method, it shows greater robustness and thus rendering it an advantageous choice for dealing with intricate multi-physics and time-dependent problems.

Referring to normal stress as an example, stress relaxation occurs gradually as shown in Fig. 6. In viscoelastic problems, this phenomenon arises due to variation in the material modulus, consequently influencing solely the magnitude of stress without altering its initial distribution, i.e., the stress distribution across distinct moments exhibits a notable similarity.

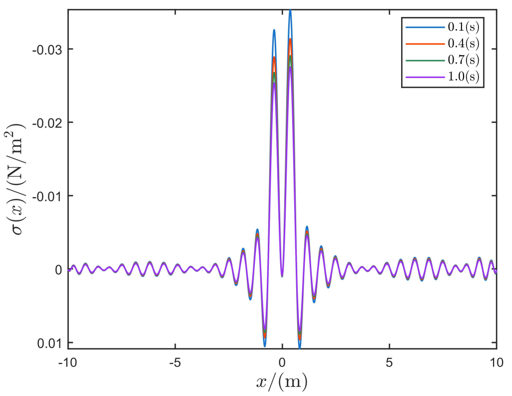

Fig. 6. Stress relaxation phenomenon for normal stress at $z = 0$. The material parameters are selected as in Table1.

The force-displacement curve is illustrated in Fig. 7. A flat punch loads in 0-4 seconds and unloads in 4-8 seconds near the lateral boundary ($x \in [8.5, 9.5](\mathrm{m})$) of a finite viscoelastic plane in the first two cases (displayed with solid lines). The inhomogeneity significantly influences the indentation curve. We also find that the viscoelastic indentation curve is a hysteresis loop, in comparison with the case of a homogeneous elastic medium. Additionally, in a finite-sized plane, the boundary effect is clear, i.e., the indenters applied near the lateral boundaries are with relatively lower reaction forces.

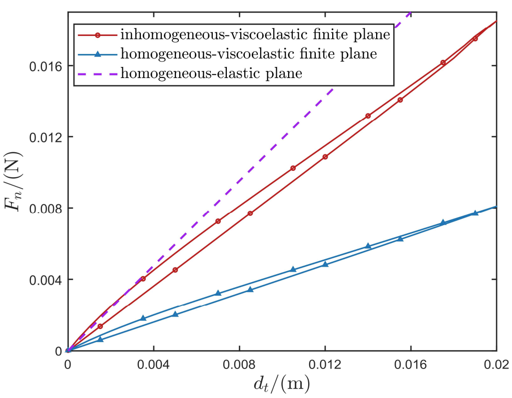

Fig. 7. Force-displacement curve of different cases.

3.2. Case of multi-indenter

Identical parameters as those in Section 3.1 are adopted in here, except the contact regions and the maximum indentation depths of the two rigid punches applied on the viscoelastic plane. The indenter on the left-hand side acts on $x \in [-5.5, -4.5]$ (m) with $d_1 = 0.02(\mathrm{m})$, while the other is applied on $x \in [1.5, 2.5]$ (m) with $d_2 = 0.03(\mathrm{m})$. At $t = 0.2(\mathrm{s})$, the displacement and stress distribution on the surface of the plane are shown in Fig. 8.

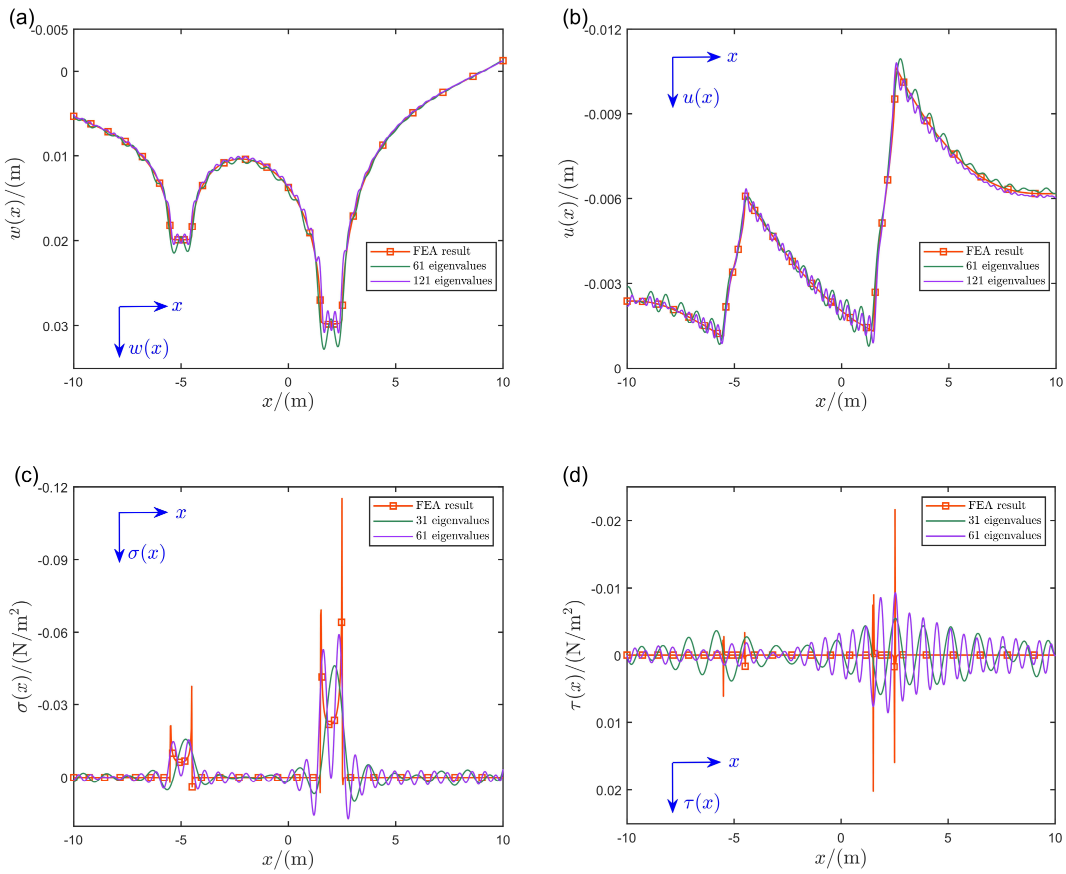

Fig. 8. Comparison between symplectic solution and FEA on the surface along the x-axis: **(a)** vertical displacement; **(b)** horizontal displacement; **(c)** normal stress; and **(d)**

shear stress. The material parameters are selected as in Table1.

With the presence of more eigenvalues, the analytical symplectic solution converges to the FEA result as shown in Figs. 8(a) and (b). The presence of singularities in Figs. 8(c) and (d) causes less accurate approximation for stress distribution. Nevertheless, the analytical symplectic result is still sufficiently precise and accurate in an overall sense of analysis. The FEA simulation result at $t = 0.2(\mathrm{s})$ is presented in Fig. 9, where the penalty method in COMSOL is applied. It is noted that one indenter significantly influences the other for displacement distribution, whereas its impact on stress distribution is relatively localized, which also coincides with the decaying characteristics of stresses derived in the symplectic solution.

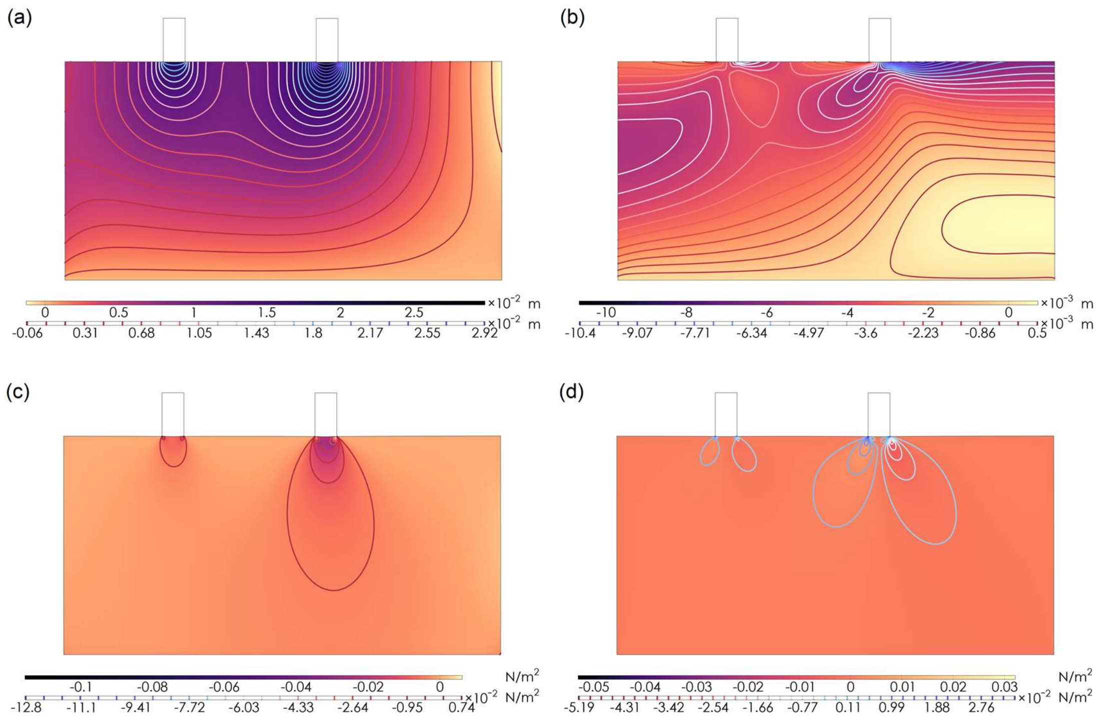

Fig. 9. FEA numerical solution for displacement and stress distribution in the whole domain for **(a)** vertical displacement; **(b)** horizontal displacement; **(c)** normal stress; and **(d)** shear stress. Refined mesh with 50,761 nodes adopted on the surface, especially within the contact region. The material parameters are selected as in Table1.

4. Concluding Remarks

A new symplectic framework analytical approach for contact analysis of a finite-sized magneto-electro-thermo-viscoelastic plane with an exponential material gradient in the horizontal direction has been established in this work. Through Laplace transform, the constitutive relations can be linearized and thus the viscoelastic multi-physical problem can be transformed into an elastic problem with multi-physics field coupling in the frequency domain. The non-homogeneous state equations are derived by rearranging the variables into a matrix form, leading to the construction of the dual Hamiltonian transformation under specific lateral boundary conditions. To deal with the non-homogeneous terms, a novel adjoint symplectic orthogonality is introduced and precisely proven, which reveals the consequence of symmetry breaking in the symplectic space. It warrants noting that two sets of bases that are distinct from the classical case are involved in the orthogonal relations. As a result of the homogeneous displacement constraint, zero is no longer an eigenvalue of the problem and it indicates the absence of special eigenvectors. Subsequently, the general eigenvectors are derived analytically. In the symplectic expansion, the general and particular solutions are constructed, thus jointly constituting the complete solution space. The symplectic analytical solutions are verified in the entire domain by comparing with FEA result. The comparison shows highly accurate result and excellent agreement. In additional to for the behavior reported in our previous work, new and significant stress relaxation phenomenon is observed in this study through analytical symplectic solution. Furthermore, an example of a multi-indenter is considered where the behaviors not only coincide with the analytical solution, but also reveals significant stress locality within a specified domain. It should be highlighted that the frequency variable should be collocated to satisfy physical reality in the temporal domain when applying inverse Laplace transform for the eigenvectors.

If the direction of material gradient is arbitrary within the plane, it may be divided into vertical and horizontal components that leads to the combination of the shift Hamiltonian transformation [79,80] and dual Hamiltonian transformation. In essence, the symplectic methodology has shown remarkable proficiency in addressing specific intricate problems pertaining to contact analysis, thus forging a path for future endeavors and advancing the frontiers of the relevant area.

CRediT authorship contribution statement

Lizichen Chen: Writing – original draft, Validation, Methodology, Investigation, Conceptualization. **C. W. Lim**: Writing – review & editing.

Weiqiu Chen: Writing – review & editing, Supervision, Funding acquisition.

Declaration of competing interest

The authors declare that they have no known competing financial interests or personal relationships that could have appeared to influence the work reported in this paper.

Data availability

Data will be made available on request.

Acknowledgments

The work was supported by the National Natural Science Foundation of China (Nos. 12192211 and 12192210), the 111 Project, PR China (No. B21034), and the specialized research projects of Huanjiang Laboratory, Zhuji, Zhejiang Province.

Appendix A. Constants and operator matrix in the basic formulations

The constants for governing equations are

$$
\begin{array}{lll}
a_1 = e_{15}^0 / \tilde{c}_{44}'^0, & a_2 = q_{15}^0 / \tilde{c}_{44}'^0, & a_3 = 1 / \tilde{c}_{44}'^0 \\
a_4 = (\tilde{c}_{13}'^0 b_1 + e_{31}^0 b_2 + q_{31}^0 b_3) / b_0, & a_5 = b_1 / b_0, & a_6 = b_2 / b_0 \\
a_7 = b_3 / b_0, & a_8 = (-\tilde{c}_{13}'^0 b_2 + e_{31}^0 b_4 - q_{31}^0 b_5) / b_0, & a_9 = b_4 / b_0 \\
a_{10} = b_5 / b_0, & a_{11} = (-\tilde{c}_{13}'^0 b_3 + q_{31}^0 b_6 - e_{31}^0 b_5) / b_0, & a_{12} = b_6 / b_0 \\
a_{13} = -\tilde{c}_{11}'^0 + \tilde{c}_{13}'^0 a_4 - e_{31}^0 a_8 - q_{31}^0 a_{11}, & a_{14} = \varepsilon_{11}^0 + (e_{15}^0)^2 / \tilde{c}_{44}'^0, & a_{15} = d_{11}^0 + e_{15}^0 q_{15}^0 / \tilde{c}_{44}'^0 \\
a_{16} = \gamma_{11}^0 + (q_{15}^0)^2 / \tilde{c}_{44}'^0, & a_{17} = \tilde{c}_{13}'^0 / \tilde{c}_{11}'^0, & a_{18} = e_{31}^0 / \tilde{c}_{11}'^0 \\
a_{19} = q_{31}^0 / \tilde{c}_{11}'^0, & b_0 = \tilde{c}_{33}'^0 b_1 + e_{33}^0 b_2 + q_{33}^0 b_3, & b_1 = \gamma_{33}^0 \varepsilon_{33}^0 - (d_{33}^0)^2 \\
b_2 = e_{33}^0 \gamma_{33}^0 - q_{33}^0 d_{33}^0, & b_3 = \varepsilon_{33}^0 q_{33}^0 - e_{33}^0 d_{33}^0, & b_4 = \tilde{c}_{33}'^0 \gamma_{33}^0 + (q_{33}^0)^2 \\
b_5 = \tilde{c}_{33}'^0 d_{33}^0 + e_{33}^0 q_{33}^0, & b_6 = \tilde{c}_{33}'^0 \varepsilon_{33}^0 + (e_{33}^0)^2, & \iota_1 = \mathfrak{a}_3^0 b_1 - \mathfrak{b}_3^0 b_2 - \mathfrak{c}_3^0 b_3 \\
\iota_2 = \mathfrak{a}_3^0 b_2 + \mathfrak{b}_3^0 b_4 - \mathfrak{c}_3^0 b_5, & \iota_3 = \mathfrak{a}_3^0 b_3 - \mathfrak{b}_3^0 b_5 + \mathfrak{c}_3^0 b_6, & \iota_4 = \mathfrak{a}_1^0 - \tilde{c}_{13}'^0 \iota_1 - e_{31}^0 \iota_2 - q_{31}^0 \iota_3
\end{array}
$$

and the operator matrix is in the form of:

$$
\boldsymbol{\mathcal{H}}=\left[\begin{array}{cccc:cccc}
0 & -\frac{\partial}{\partial x} & -a_1\frac{\partial}{\partial x} & -a_2\frac{\partial}{\partial x} & a_3 & 0 & 0 & 0\\
-a_4\frac{\partial}{\partial x} & 0 & 0 & 0 & 0 & a_5 & a_6 & a_7\\
a_8\frac{\partial}{\partial x} & 0 & 0 & 0 & 0 & a_6 & -a_9 & a_{10}\\
a_{11}\frac{\partial}{\partial x} & 0 & 0 & 0 & 0 & a_7 & a_{10} & -a_{12}\\
\hdashline
a_{13}\left(\frac{\partial^2}{\partial x^2}+\beta\frac{\partial}{\partial x}\right) & 0 & 0 & 0 & 0 & -a_4\left(\frac{\partial}{\partial x}+\beta\right) & a_8\left(\frac{\partial}{\partial x}+\beta\right) & a_{11}\left(\frac{\partial}{\partial x}+\beta\right)\\
0 & 0 & 0 & 0 & -\left(\frac{\partial}{\partial x}+\beta\right) & 0 & 0 & 0\\
0 & 0 & a_{14}\left(\frac{\partial^2}{\partial x^2}+\beta\frac{\partial}{\partial x}\right) & a_{15}\left(\frac{\partial^2}{\partial x^2}+\beta\frac{\partial}{\partial x}\right) & -a_1\left(\frac{\partial}{\partial x}+\beta\right) & 0 & 0 & 0\\
0 & 0 & a_{15}\left(\frac{\partial^2}{\partial x^2}+\beta\frac{\partial}{\partial x}\right) & a_{16}\left(\frac{\partial^2}{\partial x^2}+\beta\frac{\partial}{\partial x}\right) & -a_2\left(\frac{\partial}{\partial x}+\beta\right) & 0 & 0 & 0
\end{array}\right]
$$

If we denote $\boldsymbol{\mathcal{H}}=\left[\begin{array}{c:c}\mathbf{A} & \mathbf{B}\\ \hdashline \mathbf{C} & \mathbf{D}\end{array}\right]$, then $\mathbf{A}=-\lim\limits_{\beta\to 0}\mathbf{D}^{\mathcal{T}}$, $\mathbf{B}=\mathbf{B}^{\mathcal{T}}$, and $\mathbf{C}=\mathbf{C}^{\mathcal{T}}_{\beta\to-\beta}$ (i.e., $\mathbf{C}=\mathbf{C}^{\mathrm{T}}$), which indicate the operator $\boldsymbol{\mathcal{H}}$ is a quasi-Hamiltonian operator.

Appendix B. Dual symplectic orthogonality

Theorem. 1. If μ is an eigenvalue of operator matrix $\mathcal{H}$, then $-\mu$ is the eigenvalue of $\mathcal{H}+\beta\mathcal{B}$ with the same multiplicity.

Proof. We can deduce that

$$\mathcal{H}^{\mathcal{T}} = \mathbf{J}(\mathcal{H}+\beta\mathcal{B})\mathbf{J} \tag{B.1}$$

through the generalized canonical Hamilton transformation. The characteristic polynomial is defined as $|\mu\mathbf{I}-\mathcal{H}|$, which leads to

$$\begin{aligned}
|\mu\mathbf{I}-\mathcal{H}| &= |(\mu\mathbf{I}-\mathcal{H})\mathbf{J}| \\
&= |\mu\mathbf{J}\mathbf{J}-\mathbf{J}\mathcal{H}\mathbf{J}| \\
&= |\mu\mathbf{J}\mathbf{J}-\mathbf{J}(\mathcal{H}+\beta\mathcal{B})\mathbf{J}+\mathbf{J}\beta\mathcal{B}\mathbf{J}| \\
&= |\mu\mathbf{J}\mathbf{J}+\mathbf{J}\beta\mathcal{B}\mathbf{J}-\mathcal{H}^{\mathcal{T}}| \\
&= |-\mu\mathbf{I}-(\beta\mathcal{B})^{\mathcal{T}}-\mathcal{H}^{\mathcal{T}}| \\
&= |-\mu\mathbf{I}-(\beta\mathcal{B}+\mathcal{H})^{\mathcal{T}}| \\
&= |-\mu\mathbf{I}-(\beta\mathcal{B}+\mathcal{H})|
\end{aligned} \tag{B.2}$$

Q.E.D.

Theorem. 2. Let $\boldsymbol{\Phi}_i^{(0)},\boldsymbol{\Phi}_i^{(1)},\boldsymbol{\Phi}_i^{(2)},\cdots,\boldsymbol{\Phi}_i^{(m)}$ and $\boldsymbol{\Omega}_j^{(0)},\boldsymbol{\Omega}_j^{(1)},\boldsymbol{\Omega}_j^{(2)},\cdots,\boldsymbol{\Omega}_j^{(n)}$ are the basic eigenvectors and Jordan form eigenvectors of the eigenvalues

μ_i and μ_j, respectively. For $\mu_i + \mu_j \neq 0$, the canonical symplectic orthogonality between the eigenvectors are

$$\left\langle \boldsymbol{\Phi}_i^{(\mathfrak{s})}, \boldsymbol{\Omega}_j^{(\mathfrak{t})} \right\rangle = 0, (\mathfrak{s} = 0,1,\cdots,m; \mathfrak{t} = 0,1,\cdots,n) \tag{B.3}$$

Proof. Following the procedures of mathematical induction, we denote $\mathfrak{r} = \mathfrak{s} + \mathfrak{t}$.

(1) For $\mathfrak{r} = 0$, i.e., $\mathfrak{s} = 0; \mathfrak{t} = 0$, with $\boldsymbol{\mathcal{H}}\boldsymbol{\Phi}_i^{(0)} = \mu_i \boldsymbol{\Phi}_i^{(0)}$ and $(\boldsymbol{\mathcal{H}} + \beta\boldsymbol{\mathcal{B}})\boldsymbol{\Omega}_j^{(0)} = \mu_j \boldsymbol{\Omega}_j^{(0)}$, the symplectic inner products:

$$\begin{aligned} &\left\langle \boldsymbol{\Phi}_i^{(0)}, (\boldsymbol{\mathcal{H}} + \beta\boldsymbol{\mathcal{B}})\boldsymbol{\Omega}_j^{(0)} \right\rangle = \left\langle \boldsymbol{\Phi}_i^{(0)}, \mu_j \boldsymbol{\Omega}_j^{(0)} \right\rangle = \mu_j \left\langle \boldsymbol{\Phi}_i^{(0)}, \boldsymbol{\Omega}_j^{(0)} \right\rangle \\ &\left\langle \boldsymbol{\Omega}_j^{(0)}, \boldsymbol{\mathcal{H}}\boldsymbol{\Phi}_i^{(0)} \right\rangle = \left\langle \boldsymbol{\Omega}_j^{(0)}, \mu_i \boldsymbol{\Phi}_i^{(0)} \right\rangle = \mu_i \left\langle \boldsymbol{\Omega}_j^{(0)}, \boldsymbol{\Phi}_i^{(0)} \right\rangle = -\mu_i \left\langle \boldsymbol{\Phi}_i^{(0)}, \boldsymbol{\Omega}_j^{(0)} \right\rangle \end{aligned} \tag{B.4}$$

with $\left\langle \tilde{\boldsymbol{f}}_1, (\boldsymbol{\mathcal{H}} + \beta\boldsymbol{\mathcal{B}})\tilde{\boldsymbol{f}}_2 \right\rangle = \left\langle \tilde{\boldsymbol{f}}_2, \boldsymbol{\mathcal{H}}\tilde{\boldsymbol{f}}_1 \right\rangle$, we obtain

$$(\mu_i + \mu_j)\left\langle \boldsymbol{\Phi}_i^{(0)}, \boldsymbol{\Omega}_j^{(0)} \right\rangle = 0 \tag{B.5}$$

which leads to $\left\langle \boldsymbol{\Phi}_i^{(0)}, \boldsymbol{\Omega}_j^{(0)} \right\rangle = 0$ under the assumption of $\mu_i + \mu_j \neq 0$.

(2) Assume Eq. (B.3) is valid for $\mathfrak{r} = \mathfrak{k}$, and for the case of $\mathfrak{r} = \mathfrak{k} + 1$:

$$\begin{aligned} &\boldsymbol{\mathcal{H}}\boldsymbol{\Phi}_i^{(\mathfrak{s})} = \mu_i \boldsymbol{\Phi}_i^{(\mathfrak{s})} + \boldsymbol{\Phi}_i^{(\mathfrak{s}-1)} \\ &(\boldsymbol{\mathcal{H}} + \beta\boldsymbol{\mathcal{B}})\boldsymbol{\Omega}_j^{(\mathfrak{t})} = \mu_j \boldsymbol{\Omega}_j^{(\mathfrak{t})} + \boldsymbol{\Omega}_j^{(\mathfrak{t}-1)} \end{aligned} \tag{B.6}$$

from which the symplectic inner products are

$$\begin{aligned}&\left\langle \boldsymbol{\Phi}_i^{(\mathfrak{s})},(\boldsymbol{\mathcal{H}}+\beta\boldsymbol{\mathcal{B}})\boldsymbol{\Omega}_j^{(\mathfrak{t})}\right\rangle=\left\langle \boldsymbol{\Phi}_i^{(\mathfrak{s})},\mu_j\boldsymbol{\Omega}_j^{(\mathfrak{t})}\right\rangle+\left\langle \boldsymbol{\Phi}_i^{(\mathfrak{s})},\boldsymbol{\Omega}_j^{(\mathfrak{t}-1)}\right\rangle=\mu_j\left\langle \boldsymbol{\Phi}_i^{(\mathfrak{s})},\boldsymbol{\Omega}_j^{(\mathfrak{t})}\right\rangle\\&\left\langle \boldsymbol{\Omega}_j^{(\mathfrak{t})},\boldsymbol{\mathcal{H}}\boldsymbol{\Phi}_i^{(\mathfrak{s})}\right\rangle=\left\langle \boldsymbol{\Omega}_j^{(\mathfrak{t})},\mu_i\boldsymbol{\Phi}_i^{(\mathfrak{s})}\right\rangle+\left\langle \boldsymbol{\Omega}_j^{(\mathfrak{t})},\boldsymbol{\Phi}_i^{(s-1)}\right\rangle=\mu_i\left\langle \boldsymbol{\Omega}_j^{(\mathfrak{t})},\boldsymbol{\Phi}_i^{(\mathfrak{s})}\right\rangle=-\mu_i\left\langle \boldsymbol{\Phi}_i^{(\mathfrak{s})},\boldsymbol{\Omega}_j^{(\mathfrak{t})}\right\rangle\end{aligned}\tag{B.7}$$

we finally arrive at

$$\left\langle \boldsymbol{\Phi}_i^{(\mathfrak{s})},\boldsymbol{\Omega}_j^{(\mathfrak{t})}\right\rangle=0\tag{B.8}$$

Q.E.D.

Theorem. 3. Let μ and $-\mu$ be the canonical symplectic adjoint eigenvalues of the operator $\boldsymbol{\mathcal{H}}$ and $\boldsymbol{\mathcal{H}}+\beta\boldsymbol{\mathcal{B}}$ with multiplicity $\mathfrak{m}$, respectively. The respective adjoint symplectic orthonormal vector sets are $\left\{\boldsymbol{\Phi}^{(0)},\boldsymbol{\Phi}^{(1)},\cdots,\boldsymbol{\Phi}^{(\mathfrak{m}-1)}\right\}$ and $\left\{\boldsymbol{\Omega}^{(0)},\boldsymbol{\Omega}^{(1)},\cdots,\boldsymbol{\Omega}^{(\mathfrak{m}-1)}\right\}$, such that

$$\left\langle \boldsymbol{\Phi}^{(i)},\boldsymbol{\Omega}^{(j)}\right\rangle=\begin{cases}(-1)^i\mathscr{C}\neq 0 & (i+j=\mathfrak{m}-1)\\ 0 & (i+j\neq\mathfrak{m}-1)\end{cases}\tag{B.9}$$

Proof. Following the procedures of mathematical induction,

(1) If $i=0$, when $j\leq\mathfrak{m}-2$,

$$\begin{aligned}&\left\langle \boldsymbol{\Phi}^{(0)},(\boldsymbol{\mathcal{H}}+\beta\boldsymbol{\mathcal{B}})\boldsymbol{\Omega}^{(j+1)}\right\rangle=-\mu\left\langle \boldsymbol{\Phi}^{(0)},\boldsymbol{\Omega}^{(j+1)}\right\rangle+\left\langle \boldsymbol{\Phi}^{(0)},\boldsymbol{\Omega}^{(j)}\right\rangle\\&\left\langle \boldsymbol{\Omega}^{(j+1)},\boldsymbol{\mathcal{H}}\boldsymbol{\Phi}^{(0)}\right\rangle=\mu\left\langle \boldsymbol{\Omega}^{(j+1)},\boldsymbol{\Phi}^{(0)}\right\rangle=-\mu\left\langle \boldsymbol{\Phi}^{(0)},\boldsymbol{\Omega}^{(j+1)}\right\rangle\end{aligned}\tag{B.10}$$

with $\left\langle \boldsymbol{\Phi}^{(0)}, (\boldsymbol{\mathcal{H}}+\beta\boldsymbol{\mathcal{B}})\boldsymbol{\Omega}^{(j+1)} \right\rangle = \left\langle \boldsymbol{\Omega}^{(j+1)}, \boldsymbol{\mathcal{H}}\boldsymbol{\Phi}^{(0)} \right\rangle$, we can derive $\left\langle \boldsymbol{\Phi}^{(0)}, \boldsymbol{\Omega}^{(j)} \right\rangle = 0$.

So $\left\langle \boldsymbol{\Phi}^{(0)}, \boldsymbol{\Omega}^{(j)} \right\rangle = \mathscr{C} \neq 0$, when $j = \mathfrak{m}-1$. Otherwise, $\boldsymbol{\Phi}^{(0)} \equiv 0$, which is contradictory.

(2) Assume Eq. (B.9) is valid for $i = \mathfrak{k}$. Then for $i = \mathfrak{k}+1$, we first denote $\mathscr{d} = -\frac{1}{\mathscr{C}}\left\langle \boldsymbol{\Phi}^{(\mathfrak{k}+1)}, \boldsymbol{\Omega}^{(\mathfrak{m}-1)} \right\rangle$, and $\widehat{\boldsymbol{\Phi}}^{(\mathfrak{k}+1+\mathfrak{p})} = \boldsymbol{\Phi}^{(\mathfrak{k}+1+\mathfrak{p})} + \mathscr{d}\boldsymbol{\Phi}^{(\mathfrak{p})}$ $(\mathfrak{p} = 1, 2, \cdots, \mathfrak{m}-\mathfrak{k}-2)$, then the set $\left\{ \boldsymbol{\Phi}^{(0)}, \cdots, \boldsymbol{\Phi}^{(\mathfrak{k})}, \widehat{\boldsymbol{\Phi}}^{(\mathfrak{k}+1)}, \cdots, \widehat{\boldsymbol{\Phi}}^{(\mathfrak{m}-1)} \right\}$ also satisfies the eigen equation. The symplectic inner product:

$$\left\langle \widehat{\boldsymbol{\Phi}}^{(\mathfrak{k}+1)}, \boldsymbol{\Omega}^{(\mathfrak{m}-1)} \right\rangle = \left\langle \boldsymbol{\Phi}^{(\mathfrak{k}+1)}, \boldsymbol{\Omega}^{(\mathfrak{m}-1)} \right\rangle + \mathscr{d}\left\langle \boldsymbol{\Phi}^{(0)}, \boldsymbol{\Omega}^{(\mathfrak{m}-1)} \right\rangle = 0 \tag{B.11}$$

For $j \leq \mathfrak{m}-2$,

$$\begin{aligned}
&\left\langle \widehat{\boldsymbol{\Phi}}^{(\mathfrak{k}+1)}, (\boldsymbol{\mathcal{H}}+\beta\boldsymbol{\mathcal{B}})\boldsymbol{\Omega}^{(j+1)} \right\rangle = -\mu\left\langle \widehat{\boldsymbol{\Phi}}^{(\mathfrak{k}+1)}, \boldsymbol{\Omega}^{(j+1)} \right\rangle + \left\langle \widehat{\boldsymbol{\Phi}}^{(\mathfrak{k}+1)}, \boldsymbol{\Omega}^{(j)} \right\rangle \\
&\left\langle \boldsymbol{\Omega}^{(j+1)}, \boldsymbol{\mathcal{H}}\widehat{\boldsymbol{\Phi}}^{(\mathfrak{k}+1)} \right\rangle = \mu\left\langle \boldsymbol{\Omega}^{(j+1)}, \widehat{\boldsymbol{\Phi}}^{(\mathfrak{k}+1)} \right\rangle + \left\langle \boldsymbol{\Omega}^{(j+1)}, \boldsymbol{\Phi}^{(\mathfrak{k})} \right\rangle \\
&\qquad\qquad\qquad\qquad = -\mu\left\langle \widehat{\boldsymbol{\Phi}}^{(\mathfrak{k}+1)}, \boldsymbol{\Omega}^{(j+1)} \right\rangle - \left\langle \boldsymbol{\Phi}^{(\mathfrak{k})}, \boldsymbol{\Omega}^{(j+1)} \right\rangle
\end{aligned} \tag{B.12}$$

Consider $\left\langle \widehat{\boldsymbol{\Phi}}^{(\mathfrak{k}+1)}, (\boldsymbol{\mathcal{H}}+\beta\boldsymbol{\mathcal{B}})\boldsymbol{\Omega}^{(j+1)} \right\rangle = \left\langle \boldsymbol{\Omega}^{(j+1)}, \boldsymbol{\mathcal{H}}\widehat{\boldsymbol{\Phi}}^{(\mathfrak{k}+1)} \right\rangle$, then $\left\langle \widehat{\boldsymbol{\Phi}}^{(\mathfrak{k}+1)}, \boldsymbol{\Omega}^{(j)} \right\rangle = -\left\langle \boldsymbol{\Phi}^{(\mathfrak{k})}, \boldsymbol{\Omega}^{(j+1)} \right\rangle$.

Since Eq. (B.9) is tenable for $i = \mathfrak{k}$, when $i = \mathfrak{k}+1$,

$$\left\langle \widehat{\boldsymbol{\Phi}}^{(\mathfrak{k}+1)}, \boldsymbol{\Omega}^{(j)} \right\rangle = -\left\langle \boldsymbol{\Phi}^{(\mathfrak{k})}, \boldsymbol{\Omega}^{(j+1)} \right\rangle = \begin{cases} (-1)^{(\mathfrak{k}+1)}\mathscr{C} \neq 0 & (\mathfrak{k}+j = \mathfrak{m}-2) \\ 0 & (\mathfrak{k}+j \neq \mathfrak{m}-2) \end{cases}$$

Q.E.D.

Appendix C. Parameters for algebraic equations and relations

The parameters in Eq. (25) are detailed as:

$$\begin{aligned}\theta_8 =& \Big(a_4^2\left(a_{10}^2-a_9a_{12}\right)+2a_4a_6\left(a_{10}a_{11}+a_8a_{12}\right)+a_6^2a_{11}^2+a_5a_9a_{11}^2+2a_5a_8a_{10}a_{11}+a_5a_8^2a_{12}+a_{12}a_{13}\left(a_6^2+a_5a_9\right)\\&-a_5a_{10}^2a_{13}+a_7^2\left(a_8^2+a_9a_{13}\right)+2a_4a_7\left(a_8a_{10}+a_9a_{11}\right)+2a_6a_7\left(a_{10}a_{13}-a_8a_{11}\right)\Big)\left(a_{15}^2-a_{14}a_{16}\right)\end{aligned} \tag{C.1}$$

$$\theta_7 = 4\beta\theta_8 \tag{C.2}$$

$$\begin{aligned}\theta_6 =& \mu^2\Big(2a_8a_{10}a_{11}a_{16}a_1^2-a_{10}^2a_{13}a_{16}a_1^2+\Big(a_{12}a_8^2+a_9\left(a_{11}^2+a_{12}a_{13}\right)\Big)a_{16}a_1^2-a_2a_9a_{11}^2a_{15}a_1-4a_2a_8a_{10}a_{11}a_{15}a_1-a_2a_8^2a_{12}a_{15}a_1\\&+2a_2a_{10}^2a_{13}a_{15}a_1-a_2a_9a_{12}a_{13}a_{15}a_1+2\Big(a_4\left(a_8a_{10}+a_9a_{11}\right)+a_7\left(a_8^2+a_9a_{13}\right)+a_6\left(a_{10}a_{13}-a_8a_{11}\right)\Big)a_{15}a_1-a_2\Big(a_{12}a_8^2+a_9\left(a_{11}^2+a_{12}a_{13}\right)\Big)a_{15}a_1\\&-2\Big(a_4\left(a_{10}a_{11}+a_8a_{12}\right)+a_7\left(a_{10}a_{13}-a_8a_{11}\right)+a_6\left(a_{11}^2+a_{12}a_{13}\right)\Big)a_{16}a_1-2\Big(a_7\left(a_8a_{10}+a_9a_{11}\right)+a_6\left(a_{10}a_{11}+a_8a_{12}\right)+a_4\left(a_{10}^2-a_9a_{12}\right)\Big)a_{15}^2\\&+a_3\Big(a_{12}a_8^2+2a_{10}a_{11}a_8-a_{10}^2a_{13}+a_9\left(a_{11}^2+a_{12}a_{13}\right)\Big)a_{15}^2+a_2^2a_9a_{11}^2a_{14}+2a_2^2a_8a_{10}a_{11}a_{14}+a_2^2a_8^2a_{12}a_{14}-a_2^2a_{10}^2a_{13}a_{14}+a_2^2a_9a_{12}a_{13}a_{14}\\&+\Big(a_9a_4^2-2a_6a_8a_4-a_5a_8^2-\left(a_6^2+a_5a_9\right)a_{13}\Big)a_{14}-2a_2\Big(a_4\left(a_8a_{10}+a_9a_{11}\right)+a_7\left(a_8^2+a_9a_{13}\right)+a_6\left(a_{10}a_{13}-a_8a_{11}\right)\Big)a_{14}\\&-2\Big(a_{10}a_4^2+\left(a_7a_8+a_6a_{11}\right)a_4+a_5a_8a_{11}+\left(a_6a_7-a_5a_{10}\right)a_{13}\Big)a_{15}+2a_2\Big(a_4\left(a_{10}a_{11}+a_8a_{12}\right)+a_7\left(a_{10}a_{13}-a_8a_{11}\right)+a_6\left(a_{11}^2+a_{12}a_{13}\right)\Big)a_{15}\\&+\Big(a_{12}a_4^2-2a_7a_{11}a_4-a_5a_{11}^2-\left(a_7^2+a_5a_{12}\right)a_{13}\Big)a_{16}+2\Big(a_7\left(a_8a_{10}+a_9a_{11}\right)+a_6\left(a_{10}a_{11}+a_8a_{12}\right)+a_4\left(a_{10}^2-a_9a_{12}\right)\Big)a_{14}a_{16}\\&-a_3\Big(a_{12}a_8^2+2a_{10}a_{11}a_8-a_{10}^2a_{13}+a_9\left(a_{11}^2+a_{12}a_{13}\right)\Big)a_{14}a_{16}\Big)+6\beta^2\theta_8\end{aligned} \tag{C.3}$$

$$\theta_5 = 3\beta\mu^2\Upsilon_0+4\beta^3\theta_8 \tag{C.4}$$

$$
\begin{aligned}
\theta_4 = {} & \mu^4\Upsilon_1 + \beta^2\mu^2 \bigg(6a_8a_{10}a_{11}a_{16}a_1^2 - 3a_{10}^2a_{13}a_{16}a_1^2 + 3\Big(a_{12}a_8^2 + a_9\left(a_{11}^2 + a_{12}a_{13}\right)\Big)a_{16}a_1^2 - 3a_2a_9a_{11}^2a_{15}a_1 - 12a_2a_8a_{10}a_{11}a_{15}a_1 \\
& -3a_2a_8^2a_{12}a_{15}a_1 + 6a_2a_{10}^2a_{13}a_{15}a_1 - 3a_2a_9a_{12}a_{13}a_{15}a_1 + 6a_{15}a_1a_4\left(a_8a_{10}+a_9a_{11}\right) + 6a_{15}a_1\Big(a_7\left(a_8^2+a_9a_{13}\right) + a_6\left(a_{10}a_{13} - a_8a_{11}\right)\Big) \\
& -3a_2\Big(a_{12}a_8^2 + a_9\left(a_{11}^2+a_{12}a_{13}\right)\Big)a_{15}a_1 - 6\Big(a_4\left(a_{10}a_{11}+a_8a_{12}\right) + a_7\left(a_{10}a_{13}-a_8a_{11}\right) + a_6\left(a_{11}^2+a_{12}a_{13}\right)\Big)a_{16}a_1 \\
& -7\Big(a_7\left(a_8a_{10}+a_9a_{11}\right) + a_6\left(a_{10}a_{11}+a_8a_{12}\right) + a_4\left(a_{10}^2 - a_9a_{12}\right)\Big)a_{15}^2 + 3a_3\Big(a_{12}a_8^2 + 2a_{10}a_{11}a_8 - a_{10}^2a_{13} + a_9\left(a_{11}^2+a_{12}a_{13}\right)\Big)a_{15}^2 \\
& +3a_2^2a_9a_{11}^2a_{14} + 6a_2^2a_8a_{10}a_{11}a_{14} + 3a_2^2a_8^2a_{12}a_{14} - 3a_2^2a_{10}^2a_{13}a_{14} + 3a_2^2a_9a_{12}a_{13}a_{14} - 3\Big(-a_9a_4^2 + 2a_6a_8a_4 + a_5a_8^2 + \left(a_6^2+a_5a_9\right)a_{13}\Big)a_{14} \\
& -6a_2\Big(a_4\left(a_8a_{10}+a_9a_{11}\right) + a_7\left(a_8^2+a_9a_{13}\right) + a_6\left(a_{10}a_{13}-a_8a_{11}\right)\Big)a_{14} - 6\Big(a_{10}a_4^2 + \left(a_7a_8+a_6a_{11}\right)a_4 + a_5a_8a_{11} + \left(a_6a_7 - a_5a_{10}\right)a_{13}\Big)a_{15} \\
& +6a_2\Big(a_4\left(a_{10}a_{11}+a_8a_{12}\right) + a_7\left(a_{10}a_{13}-a_8a_{11}\right) + a_6\left(a_{11}^2+a_{12}a_{13}\right)\Big)a_{15} - 3\Big(-a_{12}a_4^2 + 2a_7a_{11}a_4 + a_5a_{11}^2 + \left(a_7^2+a_5a_{12}\right)a_{13}\Big)a_{16} \\
& +7\Big(a_7\left(a_8a_{10}+a_9a_{11}\right) + a_6\left(a_{10}a_{11}+a_8a_{12}\right) + a_4\left(a_{10}^2-a_9a_{12}\right)\Big)a_{14}a_{16} - 3a_3\Big(a_{12}a_8^2 + 2a_{10}a_{11}a_8 - a_{10}^2a_{13} + a_9\left(a_{11}^2+a_{12}a_{13}\right)\Big)a_{14}a_{16}\bigg) + \beta^4\theta_8
\end{aligned}
\tag{C.5}
$$

$$
\begin{aligned}
\theta_3 = {} & 2\beta\mu^4\Upsilon_1 + \beta^3\mu^2 \bigg(2a_8a_{10}a_{11}a_{16}a_1^2 - a_{10}^2a_{13}a_{16}a_1^2 + \Big(a_{12}a_8^2 + a_9\left(a_{11}^2 + a_{12}a_{13}\right)\Big)a_{16}a_1^2 - a_2a_9a_{11}^2a_{15}a_1 - 4a_2a_8a_{10}a_{11}a_{15}a_1 \\
& -a_2a_8^2a_{12}a_{15}a_1 + 2a_2a_{10}^2a_{13}a_{15}a_1 - a_2a_9a_{12}a_{13}a_{15}a_1 + 2\Big(a_4\left(a_8a_{10}+a_9a_{11}\right) + a_7\left(a_8^2+a_9a_{13}\right) + a_6\left(a_{10}a_{13}-a_8a_{11}\right)\Big)a_{15}a_1 \\
& -a_2\Big(a_{12}a_8^2 + a_9\left(a_{11}^2+a_{12}a_{13}\right)\Big)a_{15}a_1 - 2\Big(a_4\left(a_{10}a_{11}+a_8a_{12}\right) + a_7\left(a_{10}a_{13}-a_8a_{11}\right) + a_6\left(a_{11}^2+a_{12}a_{13}\right)\Big)a_{16}a_1 - 4a_{15}^2a_7\left(a_8a_{10}+a_9a_{11}\right) \\
& -4a_{15}^2\Big(a_6\left(a_{10}a_{11}+a_8a_{12}\right) + a_4\left(a_{10}^2-a_9a_{12}\right)\Big)a_{15}^2 + a_3\Big(a_{12}a_8^2 + 2a_{10}a_{11}a_8 - a_{10}^2a_{13} + a_9\left(a_{11}^2+a_{12}a_{13}\right)\Big)a_{15}^2 + a_2^2a_9a_{11}^2a_{14} + 2a_2^2a_8a_{10}a_{11}a_{14} + a_2^2a_8^2a_{12}a_{14} \\
& -a_2^2a_{10}^2a_{13}a_{14} + a_2^2a_9a_{12}a_{13}a_{14} + \Big(a_9a_4^2 - 2a_6a_8a_4 - a_5a_8^2 - \left(a_6^2+a_5a_9\right)a_{13}\Big)a_{14} - 2a_2\Big(a_4\left(a_8a_{10}+a_9a_{11}\right) + a_7\left(a_8^2+a_9a_{13}\right) + a_6\left(a_{10}a_{13}-a_8a_{11}\right)\Big)a_{14} \\
& -2\Big(a_{10}a_4^2 + \left(a_7a_8+a_6a_{11}\right)a_4 + a_5a_8a_{11} + \left(a_6a_7-a_5a_{10}\right)a_{13}\Big)a_{15} + 2a_2\Big(a_4\left(a_{10}a_{11}+a_8a_{12}\right) + a_7\left(a_{10}a_{13}-a_8a_{11}\right) + a_6\left(a_{11}^2+a_{12}a_{13}\right)\Big)a_{15} \\
& +\Big(a_{12}a_4^2 - 2a_7a_{11}a_4 - a_5a_{11}^2 - \left(a_7^2+a_5a_{12}\right)a_{13}\Big)a_{16} + 4\Big(a_7\left(a_8a_{10}+a_9a_{11}\right) + a_6\left(a_{10}a_{11}+a_8a_{12}\right) + a_4\left(a_{10}^2-a_9a_{12}\right)\Big)a_{14}a_{16} \\
& -a_3\Big(a_{12}a_8^2 + 2a_{10}a_{11}a_8 - a_{10}^2a_{13} + a_9\left(a_{11}^2+a_{12}a_{13}\right)\Big)a_{14}a_{16}\bigg)
\end{aligned}
\tag{C.6}
$$

$$
\begin{aligned}
\theta_2 = {} & \mu^6 \Upsilon_2 + \beta^2 \mu^4 \Big(\big(a_8^2 + a_9 a_{13} \big) a_1^2 + \big(-2a_6 a_{13} + 2a_2 \left(a_8 a_{11} - a_{10} a_{13} \right) - 3\big(a_8 a_{10} + a_9 a_{11} \big) a_{15} + 3\big(a_{10} a_{11} + a_8 a_{12} \big) a_{16} \big) a_1 \\
& + a_4^2 + a_2^2 a_{11}^2 + a_{10}^2 a_{15}^2 - a_9 a_{12} a_{15}^2 - a_5 a_{13} - 2a_2 a_7 a_{13} + a_2^2 a_{12} a_{13} + a_8 \left(3a_6 - a_3 a_8 \right) a_{14} + 3a_2 a_8 a_{10} a_{14} + 3a_2 a_9 a_{11} a_{14} \\
& - a_3 a_9 a_{13} a_{14} + 3a_7 a_8 a_{15} + 3a_6 a_{11} a_{15} - 2a_3 a_8 a_{11} a_{15} - 3a_2 a_{10} a_{11} a_{15} - 3a_2 a_8 a_{12} a_{15} + 2a_3 a_{10} a_{13} a_{15} \\
& - \Big(-3a_7 a_{11} + a_3 \left(a_{11}^2 + a_{12} a_{13} \right) + \left(a_{10}^2 - a_9 a_{12} \right) a_{14} \Big) a_{16} - a_4 \left(2a_1 a_8 + 2a_2 a_{11} + 3a_9 a_{14} - 6a_{10} a_{15} + 3a_{12} a_{16} \right) \Big) \\
& + \beta^4 \mu^2 \Big(\Big(-a_7 \left(a_8 a_{10} + a_9 a_{11} \right) - a_6 \left(a_{10} a_{11} + a_8 a_{12} \right) - a_4 \left(a_{10}^2 - a_9 a_{12} \right) \Big) a_{15}^2 + \Big(a_7 \left(a_8 a_{10} + a_9 a_{11} \right) + a_6 \left(a_{10} a_{11} + a_8 a_{12} \right) + a_4 \left(a_{10}^2 - a_9 a_{12} \right) \Big) a_{14} a_{16} \Big)
\end{aligned} \tag{C.7}
$$

$$
\begin{aligned}
\theta_1 = {} & \beta \mu^6 \Upsilon_2 + \beta^3 \mu^4 \Big(\big(a_6 a_8 - a_4 a_9 \big) a_{14} + a_2 a_8 a_{10} a_{14} + a_2 a_9 a_{11} a_{14} - a_1 a_8 a_{10} a_{15} + \big(a_7 a_8 + a_4 a_{10} \big) a_{15} - a_1 a_9 a_{11} a_{15} \\
& - a_2 a_{10} a_{11} a_{15} + \big(a_4 a_{10} + a_6 a_{11} \big) a_{15} - a_2 a_8 a_{12} a_{15} + a_1 a_{10} a_{11} a_{16} + a_1 a_8 a_{12} a_{16} + \big(a_7 a_{11} - a_4 a_{12} \big) a_{16} \Big)
\end{aligned} \tag{C.8}
$$

$$
\theta_0 = \big(a_1 a_8 + a_2 a_{11} - a_4 \big) \beta^2 \mu^6 + \mu^8 \tag{C.9}
$$

The parameters in Eq. (26) are detailed as:

$$
\Lambda_0 = \theta_8 \tag{C.10}
$$

$$
\begin{aligned}
\Lambda_1 = {} & a_9 a_{11}^2 a_{14} a_2^2 + 2a_8 a_{10} a_{11} a_{14} a_2^2 + a_8^2 a_{12} a_{14} a_2^2 - a_{10}^2 a_{13} a_{14} a_2^2 + a_9 a_{12} a_{13} a_{14} a_2^2 - 2a_7 a_8^2 a_{14} a_2 + 2a_6 a_8 a_{11} a_{14} a_2 - 2a_7 a_9 a_{13} a_{14} a_2 \\
& - 2a_6 a_{10} a_{13} a_{14} a_2 + 2a_6 a_{11}^2 a_{15} a_2 - 2a_1 a_9 a_{11}^2 a_{15} a_2 - 2a_7 a_8 a_{11} a_{15} a_2 - 4a_1 a_8 a_{10} a_{11} a_{15} a_2 - 2a_1 a_8^2 a_{12} a_{15} a_2 + 2a_1 a_{10}^2 a_{13} a_{15} a_2 + 2a_7 a_{10} a_{13} a_{15} a_2 \\
& + 2a_6 a_{12} a_{13} a_{15} a_2 - 2a_1 a_9 a_{12} a_{13} a_{15} a_2 + a_3 a_9 a_{11}^2 a_{15}^2 - 2a_7 a_8 a_{10} a_{15}^2 - 2a_7 a_9 a_{11} a_{15}^2 - 2a_6 a_{10} a_{11} a_{15}^2 + 2a_3 a_8 a_{10} a_{11} a_{15}^2 + a_3 a_8^2 a_{12} a_{15}^2 - 2a_6 a_8 a_{12} a_{15}^2 \\
& - a_3 a_{10}^2 a_{13} a_{15}^2 + a_3 a_9 a_{12} a_{13} a_{15}^2 - a_5 a_8^2 a_{14} - a_6^2 a_{13} a_{14} - a_5 a_9 a_{13} a_{14} + 2a_1 a_7 a_8^2 a_{15} - 2a_5 a_8 a_{11} a_{15} - 2a_1 a_6 a_8 a_{11} a_{15} - 2a_6 a_7 a_{13} a_{15} + 2a_1 a_7 a_9 a_{13} a_{15} \\
& + 2a_5 a_{10} a_{13} a_{15} + 2a_1 a_6 a_{10} a_{13} a_{15} \left(a_9 a_{14} - 2a_{10} a_{15} + a_{12} a_{16} \right) a_4^2 + 2\Big(-a_6 \left(a_8 a_{14} + a_{11} a_{15} \right) + a_2 \Big(\big(a_{10} a_{11} + a_8 a_{12} \big) a_{15} - \big(a_8 a_{10} + a_9 a_{11} \big) a_{14} \Big) \\
& + a_{15} \Big(-a_7 a_8 + a_1 \left(a_8 a_{10} + a_9 a_{11} \right) + \left(a_9 a_{12} - a_{10}^2 \right) a_{15} \Big) - \Big(a_7 a_{11} + a_1 \left(a_{10} a_{11} + a_8 a_{12} \right) + \left(a_9 a_{12} - a_{10}^2 \right) a_{14} \Big) a_{16} \Big) a_4 + a_5 a_{11}^2 + a_7^2 a_{13} + a_5 a_{12} a_{13} \\
& - \Bigg(- \Big(\Big(a_{12} a_8^2 + 2a_{10} a_{11} a_8 - a_{10}^2 a_{13} + a_9 \left(a_{11}^2 + a_{12} a_{13} \right) \Big) a_1^2 \Big) + 2\Big(a_7 \left(a_{10} a_{13} - a_8 a_{11} \right) + a_6 \left(a_{11}^2 + a_{12} a_{13} \right) \Big) a_1 + \Big(-2a_7 \left(a_8 a_{10} + a_9 a_{11} \right) \\
& - 2a_6 \left(a_{10} a_{11} + a_8 a_{12} \right) + a_3 \Big(a_{12} a_8^2 + 2a_{10} a_{11} a_8 + a_9 a_{11}^2 + \left(a_9 a_{12} - a_{10}^2 \right) a_{13} \Big) \Big) a_{14} \Bigg) a_{16}
\end{aligned} \tag{C.11}
$$

$$\Lambda_2 = -\theta_8 \tag{C.12}$$

$$\begin{aligned}\Lambda_3 = &\left(a_8^2 + a_9 a_{13}\right) a_1^2 + 2\left(-a_6 a_{13} + a_2\left(a_8 a_{11} - a_{10} a_{13}\right) - \left(a_8 a_{10} + a_9 a_{11}\right) a_{15} + \left(a_{10} a_{11} + a_8 a_{12}\right) a_{16}\right) a_1 + a_4^2 + a_2^2 a_{11}^2 + a_{10}^2 a_{15}^2 - a_9 a_{12} a_{15}^2 \\ &- a_5 a_{13} - 2 a_2 a_7 a_{13} + a_2^2 a_{12} a_{13} + a_8\left(2 a_6 - a_3 a_8\right) a_{14} + 2 a_2 a_8 a_{10} a_{14} + 2 a_2 a_9 a_{11} a_{14} - a_3 a_9 a_{13} a_{14} + 2 a_7 a_8 a_{15} + 2 a_6 a_{11} a_{15} - 2 a_3 a_8 a_{11} a_{15} \\ &- 2 a_2 a_{10} a_{11} a_{15} - 2 a_2 a_8 a_{12} a_{15} + 2 a_3 a_{10} a_{13} a_{15} - \left(-2 a_7 a_{11} + a_3\left(a_{11}^2 + a_{12} a_{13}\right) + \left(a_{10}^2 - a_9 a_{12}\right) a_{14}\right) a_{16} - 2 a_4\left(a_1 a_8 + a_2 a_{11} + a_9 a_{14} - 2 a_{10} a_{15} + a_{12} a_{16}\right)\end{aligned} \tag{C.13}$$

$$\begin{aligned}\Lambda_4 = &\Big(-3 a_9 a_{11}^2 a_{14} a_2^2 - 6 a_8 a_{10} a_{11} a_{14} a_2^2 - 3 a_8^2 a_{12} a_{14} a_2^2 + 3 a_{10}^2 a_{13} a_{14} a_2^2 - 3 a_9 a_{12} a_{13} a_{14} a_2^2 + 6 a_7 a_8^2 a_{14} a_2 - 6 a_6 a_8 a_{11} a_{14} a_2 + 6 a_7 a_9 a_{13} a_{14} a_2 \\ &+ 6 a_6 a_{10} a_{13} a_{14} a_2 - 6 a_6 a_{11}^2 a_{15} a_2 + 6 a_1 a_9 a_{11}^2 a_{15} a_2 + 6 a_7 a_8 a_{11} a_{15} a_2 + 12 a_1 a_8 a_{10} a_{11} a_{15} a_2 + 6 a_1 a_8^2 a_{12} a_{15} a_2 - 6 a_1 a_{10}^2 a_{13} a_{15} a_2 - 6 a_7 a_{10} a_{13} a_{15} a_2 \\ &- 6 a_6 a_{12} a_{13} a_{15} a_2 + 6 a_1 a_9 a_{12} a_{13} a_{15} a_2 - 3 a_3 a_9 a_{11}^2 a_{15}^2 + 2 a_7 a_8 a_{10} a_{15}^2 + 2 a_7 a_9 a_{11} a_{15}^2 + 2 a_6 a_{10} a_{11} a_{15}^2 - 6 a_3 a_8 a_{10} a_{11} a_{15}^2 - 3 a_3 a_8^2 a_{12} a_{15}^2 + 2 a_6 a_8 a_{12} a_{15}^2 \\ &+ 3 a_3 a_{10}^2 a_{13} a_{15}^2 - 3 a_3 a_9 a_{12} a_{13} a_{15}^2 + 3 a_5 a_8^2 a_{14} + 3 a_6^2 a_{13} a_{14} + 3 a_5 a_9 a_{13} a_{14} - 6 a_1 a_7 a_8^2 a_{15} + 6 a_5 a_8 a_{11} a_{15} + 6 a_1 a_6 a_8 a_{11} a_{15} + 6 a_6 a_7 a_{13} a_{15} - 6 a_1 a_7 a_9 a_{13} a_{15} \\ &- 6 a_5 a_{10} a_{13} a_{15} - 6 a_1 a_6 a_{10} a_{13} a_{15} - 3\left(a_9 a_{14} - 2 a_{10} a_{15} + a_{12} a_{16}\right) a_4^2 + 2\Big(3 a_6\left(a_8 a_{14} + a_{11} a_{15}\right) + a_{15}\Big(3 a_7 a_8 - 3 a_1\left(a_8 a_{10} + a_9 a_{11}\right) + \left(a_{10}^2 - a_9 a_{12}\right) a_{15}\Big) \\ &+ 3 a_2\left(\left(a_8 a_{10} + a_9 a_{11}\right) a_{14} - \left(a_{10} a_{11} + a_8 a_{12}\right) a_{15}\right) + \Big(3\left(a_7 + a_1 a_{10}\right) a_{11} + 3 a_1 a_8 a_{12} + \left(a_9 a_{12} - a_{10}^2\right) a_{14}\Big) a_{16}\Big) a_4 + \Big(-3 a_1^2 a_{12} a_8^2 \\ &+ 3 a_{11}\left(\left(a_5 + a_1\left(2 a_6 - a_1 a_9\right)\right) a_{11} - 2 a_1 a_8\left(a_7 + a_1 a_{10}\right)\right) + 3\Big(\left(a_7 + a_1 a_{10}\right)^2 + \left(a_5 + a_1\left(2 a_6 - a_1 a_9\right)\right) a_{12}\Big) a_{13} \\ &+ \Big(-2 a_7\left(a_8 a_{10} + a_9 a_{11}\right) - 2 a_6\left(a_{10} a_{11} + a_8 a_{12}\right) + 3 a_3\left(a_{12} a_8^2 + 2 a_{10} a_{11} a_8 + a_9 a_{11}^2 + \left(a_9 a_{12} - a_{10}^2\right) a_{13}\right)\Big) a_{14}\Big) a_{16}\Big) / 4\end{aligned} \tag{C.14}$$

$$\Lambda_5 = 3\theta_8 / 8 \tag{C.15}$$

$$\Lambda_6 = \Upsilon_2 \tag{C.16}$$

$$\begin{aligned}\Lambda_7 = &\Big(-\left(\left(a_8^2 + a_9 a_{13}\right) a_1^2\right) + 2\left(\left(a_6 + a_2 a_{10}\right) a_{13} - a_2 a_8 a_{11}\right) a_1 - a_4^2 - a_2^2 a_{11}^2 - a_{10}^2 a_{15}^2 + a_9 a_{12} a_{15}^2 + 2 a_4\left(a_1 a_8 + a_2 a_{11}\right) + a_5 a_{13} + 2 a_2 a_7 a_{13} \\ &- a_2^2 a_{12} a_{13} + a_3 a_8^2 a_{14} + a_3 a_9 a_{13} a_{14} + 2 a_3 a_8 a_{11} a_{15} - 2 a_3 a_{10} a_{13} a_{15} + \left(a_3\left(a_{11}^2 + a_{12} a_{13}\right) + \left(a_{10}^2 - a_9 a_{12}\right) a_{14}\right) a_{16}\Big) / 2\end{aligned} \tag{C.17}$$

$$
\begin{aligned}
\Lambda_8 = \Big(& 3a_9 a_{11}^2 a_{14} a_2^2 + 6a_8 a_{10} a_{11} a_{14} a_2^2 + 3a_8^2 a_{12} a_{14} a_2^2 - 3a_{10}^2 a_{13} a_{14} a_2^2 + 3a_9 a_{12} a_{13} a_{14} a_2^2 - 6a_7 a_8^2 a_{14} a_2 + 6a_6 a_8 a_{11} a_{14} a_2 - 6a_7 a_9 a_{13} a_{14} a_2 \\
& -6a_6 a_{10} a_{13} a_{14} a_2 + 6a_6 a_{11}^2 a_{15} a_2 - 6a_1 a_9 a_{11}^2 a_{15} a_2 - 6a_7 a_8 a_{11} a_{15} a_2 - 12a_1 a_8 a_{10} a_{11} a_{15} a_2 - 6a_1 a_8^2 a_{12} a_{15} a_2 + 6a_1 a_{10}^2 a_{13} a_{15} a_2 + 6a_7 a_{10} a_{13} a_{15} a_2 \\
& +6a_6 a_{12} a_{13} a_{15} a_2 - 6a_1 a_9 a_{12} a_{13} a_{15} a_2 + 3a_3 a_9 a_{11}^2 a_{15}^2 + 2a_7 a_8 a_{10} a_{15}^2 + 2a_7 a_9 a_{11} a_{15}^2 + 2a_6 a_{10} a_{11} a_{15}^2 + 6a_3 a_8 a_{10} a_{11} a_{15}^2 + 3a_3 a_8^2 a_{12} a_{15}^2 + 2a_6 a_8 a_{12} a_{15}^2 \\
& -3a_3 a_{10}^2 a_{13} a_{15}^2 + 3a_3 a_9 a_{12} a_{13} a_{15}^2 - 3a_6^2 a_{13} a_{14} + 6a_1 a_7 a_8^2 a_{15} - 6a_1 a_6 a_8 a_{11} a_{15} - 6a_6 a_7 a_{13} a_{15} + 6a_1 a_7 a_9 a_{13} a_{15} + 6a_1 a_6 a_{10} a_{13} a_{15} + 3\left(a_9 a_{14} - 2a_{10} a_{15} + a_{12} a_{16}\right) a_4^2 \\
& +2\Big(-3a_6 \left(a_8 a_{14} + a_{11} a_{15}\right) + 3a_2 \left(\left(a_{10} a_{11} + a_8 a_{12}\right) a_{15} - \left(a_8 a_{10} + a_9 a_{11}\right) a_{14}\right) + a_{15} \Big(-3a_7 a_8 + 3a_1 \left(a_8 a_{10} + a_9 a_{11}\right) + \left(a_{10}^2 - a_9 a_{12}\right) a_{15}\Big) \\
& -\Big(3\left(a_7 + a_1 a_{10}\right) a_{11} + 3a_1 a_8 a_{12} + \left(a_{10}^2 - a_9 a_{12}\right) a_{14}\Big) a_{16}\Big) a_4 - \Big(-3a_1^2 a_{12} a_8^2 - 3a_1 a_{11} \Big(2a_8 \left(a_7 + a_1 a_{10}\right) + \left(a_1 a_9 - 2a_6\right) a_{11}\Big) + 3\Big(\left(a_7 + a_1 a_{10}\right)^2 + a_1 \left(2a_6 - a_1 a_9\right) a_{12}\Big) a_{13} \\
& +\Big(2a_7 \left(a_8 a_{10} + a_9 a_{11}\right) + 2a_6 \left(a_{10} a_{11} + a_8 a_{12}\right) + 3a_3 \Big(a_{12} a_8^2 + 2a_{10} a_{11} a_8 + a_9 a_{11}^2 + \left(a_9 a_{12} - a_{10}^2\right) a_{13}\Big)\Big) a_{14}\Big) a_{16} \\
& -3a_5 \Big(a_{14} a_8^2 + 2a_{11} a_{15} a_8 + a_{11}^2 a_{16} + a_{13} \left(a_9 a_{14} - 2a_{10} a_{15} + a_{12} a_{16}\right)\Big)\Big) / 16
\end{aligned}
\tag{C.18}
$$

$$
\Lambda_9 = -\theta_8 / 16 \tag{C.19}
$$

$$
\Lambda_{10} = 1 \tag{C.20}
$$

$$
\Lambda_{11} = \left(-2a_4 + 2a_1 a_8 + 2a_2 a_{11} + a_3 a_{13} - a_9 a_{14} + 2a_{10} a_{15} - a_{12} a_{16}\right) / 4 \tag{C.21}
$$

$$
\begin{aligned}
\Lambda_{12} = \Big(& \left(a_8^2 + a_9 a_{13}\right) a_1^2 + 2\left(-a_6 a_{13} + a_2 \left(a_8 a_{11} - a_{10} a_{13}\right) + \left(a_8 a_{10} + a_9 a_{11}\right) a_{15} - \left(a_{10} a_{11} + a_8 a_{12}\right) a_{16}\right) a_1 + a_4^2 + a_2^2 a_{11}^2 + a_{10}^2 a_{15}^2 - a_9 a_{12} a_{15}^2 \\
& -a_5 a_{13} - 2a_2 a_7 a_{13} + a_2^2 a_{12} a_{13} - a_8 \left(2a_6 + a_3 a_8\right) a_{14} - 2a_2 a_8 a_{10} a_{14} - 2a_2 a_9 a_{11} a_{14} - a_3 a_9 a_{13} a_{14} - 2a_7 a_8 a_{15} - 2a_6 a_{11} a_{15} - 2a_3 a_8 a_{11} a_{15} \\
& +2a_2 a_{10} a_{11} a_{15} + 2a_2 a_8 a_{12} a_{15} + 2a_3 a_{10} a_{13} a_{15} - \Big(2a_7 a_{11} + a_3 \left(a_{11}^2 + a_{12} a_{13}\right) + \left(a_{10}^2 - a_9 a_{12}\right) a_{14}\Big) a_{16} - 2a_4 \left(a_1 a_8 + a_2 a_{11} - a_9 a_{14} + 2a_{10} a_{15} - a_{12} a_{16}\right)\Big) / 16
\end{aligned}
\tag{C.22}
$$

$$
\begin{aligned}
\Lambda_{13} = \Big(& -a_9 a_{11}^2 a_{14} a_2^2 - 2a_8 a_{10} a_{11} a_{14} a_2^2 - a_8^2 a_{12} a_{14} a_2^2 + a_{10}^2 a_{13} a_{14} a_2^2 - a_9 a_{12} a_{13} a_{14} a_2^2 + 2a_7 a_8^2 a_{14} a_2 - 2a_6 a_8 a_{11} a_{14} a_2 + 2a_7 a_9 a_{13} a_{14} a_2 \\
& +2a_6 a_{10} a_{13} a_{14} a_2 - 2a_6 a_{11}^2 a_{15} a_2 + 2a_1 a_9 a_{11}^2 a_{15} a_2 + 2a_7 a_8 a_{11} a_{15} a_2 + 4a_1 a_8 a_{10} a_{11} a_{15} a_2 + 2a_1 a_8^2 a_{12} a_{15} a_2 - 2a_1 a_{10}^2 a_{13} a_{15} a_2 - 2a_7 a_{10} a_{13} a_{15} a_2 \\
& -2a_6 a_{12} a_{13} a_{15} a_2 + 2a_1 a_9 a_{12} a_{13} a_{15} a_2 - a_3 a_9 a_{11}^2 a_{15}^2 - 2a_7 a_8 a_{10} a_{15}^2 - 2a_7 a_9 a_{11} a_{15}^2 - 2a_6 a_{10} a_{11} a_{15}^2 - 2a_3 a_8 a_{10} a_{11} a_{15}^2 - a_3 a_8^2 a_{12} a_{15}^2 - 2a_6 a_8 a_{12} a_{15}^2 \\
& +a_3 a_{10}^2 a_{13} a_{15}^2 - a_3 a_9 a_{12} a_{13} a_{15}^2 + a_5 a_8^2 a_{14} + a_6^2 a_{13} a_{14} + a_5 a_9 a_{13} a_{14} - 2a_1 a_7 a_8^2 a_{15} + 2a_5 a_8 a_{11} a_{15} + 2a_1 a_6 a_8 a_{11} a_{15} + 2a_6 a_7 a_{13} a_{15} - 2a_1 a_7 a_9 a_{13} a_{15} \\
& -2a_5 a_{10} a_{13} a_{15} - 2a_1 a_6 a_{10} a_{13} a_{15} - \left(a_9 a_{14} - 2a_{10} a_{15} + a_{12} a_{16}\right) a_4^2 + 2\Big(a_6 \left(a_8 a_{14} + a_{11} a_{15}\right) - a_{15} \Big(-a_7 a_8 + a_1 \left(a_8 a_{10} + a_9 a_{11}\right) + \left(a_{10}^2 - a_9 a_{12}\right) a_{15}\Big) \\
& +a_2 \left(\left(a_8 a_{10} + a_9 a_{11}\right) a_{14} - \left(a_{10} a_{11} + a_8 a_{12}\right) a_{15}\right) + \Big(a_7 a_{11} + a_1 \left(a_{10} a_{11} + a_8 a_{12}\right) + \left(a_{10}^2 - a_9 a_{12}\right) a_{14}\Big) a_{16}\Big) a_4 + a_5 a_{11}^2 + a_7^2 a_{13} + a_5 a_{12} a_{13} \\
& +\Big(-\Big(\Big(a_{12} a_8^2 + 2a_{10} a_{11} a_8 - a_{10}^2 a_{13} + a_9 \left(a_{11}^2 + a_{12} a_{13}\right)\Big) a_1^2\Big) + 2\Big(a_7 \left(a_{10} a_{13} - a_8 a_{11}\right) + a_6 \left(a_{11}^2 + a_{12} a_{13}\right)\Big) a_1 + \Big(2a_7 \left(a_8 a_{10} + a_9 a_{11}\right) \\
& +2a_6 \left(a_{10} a_{11} + a_8 a_{12}\right) + a_3 \Big(a_{12} a_8^2 + 2a_{10} a_{11} a_8 + a_9 a_{11}^2 + \left(a_9 a_{12} - a_{10}^2\right) a_{13}\Big)\Big) a_{14}\Big) a_{16}\Big) / 64
\end{aligned}
\tag{C.23}
$$

$$
\Lambda_{14} = \theta_8 / 256 \tag{C.24}
$$

The parameters in Eq. (28) yield:

$$
\chi_{1t} = (\eta_t^6 \Upsilon_3 + 3\eta_t^5 \beta \Upsilon_3 + \eta_t^4 (3\beta^2 \Upsilon_3 + \mu^2 \Upsilon_4) + \eta_t^3 (\beta^3 \Upsilon_3 + 2\beta\mu^2 \Upsilon_4) + \eta_t^2 (\mu^4 \Upsilon_5 + \beta^2 \mu^2 \Upsilon_4) + \eta_t \beta \mu^4 \Upsilon_5 + a_3 \mu^6) / (\mu \Theta) \tag{C.25}
$$

$$
\begin{aligned}
\chi_{2t} = \Big(& \eta_t^5 \Upsilon_8 + \eta_t^4 \beta \Upsilon_9 + \eta_t^3 \Big(\mu^2 \Big(- \Big(\big(a_6 a_8 - a_4 a_9 \big) a_1^2 \Big) - a_5 a_8 a_1 - a_2 \big(a_7 a_8 + 2 a_4 a_{10} \big) a_1 - a_6 \big(a_4 + a_2 a_{11} \big) a_1 + a_7 a_9 a_{15} a_1 + a_6 a_{10} a_{15} a_1 \\
& - a_7 a_{10} a_{16} a_1 - a_6 a_{12} a_{16} a_1 - a_2 a_4 a_7 - a_2 a_5 a_{11} - a_2^2 a_7 a_{11} + a_2^2 a_4 a_{12} - a_6^2 a_{14} + a_3 a_6 a_8 a_{14} - a_3 a_4 a_9 a_{14} - a_5 a_9 a_{14} - a_2 a_7 a_9 a_{14} - a_2 a_6 a_{10} a_{14} \\
& - 2 a_6 a_7 a_{15} + a_3 a_7 a_8 a_{15} + 2 a_3 a_4 a_{10} a_{15} + 2 a_5 a_{10} a_{15} + a_2 a_7 a_{10} a_{15} + a_3 a_6 a_{11} a_{15} + a_2 a_6 a_{12} a_{15} - a_7^2 a_{16} + a_3 a_7 a_{11} a_{16} - a_3 a_4 a_{12} a_{16} - a_5 a_{12} a_{16} \Big) \\
& + \beta^2 \Big(- \Big(\Big(a_7 \big(a_8 a_{10} + a_9 a_{11} \big) + a_6 \big(a_{10} a_{11} + a_8 a_{12} \big) + a_4 \big(a_{10}^2 - a_9 a_{12} \big) \Big) a_{16} a_1^2 \Big) + a_4 a_7 a_9 a_{15} a_1 + a_6^2 a_{11} a_{15} a_1 - a_6 \Big(a_8 \big(a_7 - 2 a_2 a_{12} \big) - a_{10} \big(a_4 + 2 a_2 a_{11} \big) \Big) a_{15} a_1 \\
& + 2 a_2 \Big(a_7 \big(a_8 a_{10} + a_9 a_{11} \big) + a_4 \big(a_{10}^2 - a_9 a_{12} \big) \Big) a_{15} a_1 - a_7^2 a_8 a_{16} a_1 - a_4 a_7 a_{10} a_{16} a_1 + a_6 a_7 a_{11} a_{16} a_1 - a_4 a_6 a_{12} a_{16} a_1 - a_5 a_{11} \big(a_{10} a_{16} - a_9 a_{15} \big) a_1 \\
& - a_5 a_8 \big(a_{12} a_{16} - a_{10} a_{15} \big) a_1 - a_3 a_4 a_{10}^2 a_{15}^2 + 3 a_7^2 a_9 a_{15}^2 + 6 a_6 a_7 a_{10} a_{15}^2 - a_3 a_6 a_{10} a_{11} a_{15}^2 - a_3 a_7 \big(a_8 a_{10} + a_9 a_{11} \big) a_{15}^2 + 3 a_6^2 a_{12} a_{15}^2 - a_3 a_6 a_8 a_{12} a_{15}^2 \\
& + a_3 a_4 a_9 a_{12} a_{15}^2 + 3 a_5 a_9 a_{12} a_{15}^2 - a_2^2 a_4 a_{10}^2 a_{14} + a_2 a_6 a_7 a_8 a_{14} - a_2 a_4 a_7 a_9 a_{14} - a_2 a_4 a_6 a_{10} a_{14} - a_2^2 a_7 a_8 a_{10} a_{14} - a_2 a_6^2 a_{11} a_{14} - a_2^2 a_7 a_9 a_{11} a_{14} \\
& - a_2^2 a_6 a_{10} a_{11} a_{14} - a_2^2 a_6 a_8 a_{12} a_{14} + a_2^2 a_4 a_9 a_{12} a_{14} + a_2 a_7^2 a_8 a_{15} + a_2 a_4 a_7 a_{10} a_{15} - a_2 a_6 a_7 a_{11} a_{15} + a_2 a_4 a_6 a_{12} a_{15} - a_2 a_5 a_{11} \big(a_9 a_{14} - a_{10} a_{15} \big) \\
& - a_2 a_5 a_8 \big(a_{10} a_{14} - a_{12} a_{15} \big) + a_3 a_4 a_{10}^2 a_{14} a_{16} + a_3 a_6 a_{10} a_{11} a_{14} a_{16} + a_3 a_7 \big(a_8 a_{10} + a_9 a_{11} \big) a_{14} a_{16} + a_3 a_6 a_8 a_{12} a_{14} a_{16} - a_3 a_4 a_9 a_{12} a_{14} a_{16} - 3 a_5 a_9 a_{12} a_{14} a_{16} \\
& - 3 \big(a_{12} a_6^2 + 2 a_7 a_{10} a_6 + a_7^2 a_9 \big) a_{14} a_{16} - 3 a_5 a_{10}^2 \big(a_{15}^2 - a_{14} a_{16} \big) \Big) \Big) + \eta_t^2 \Big(\beta \mu^2 \Big(- \Big(\big(a_6 a_8 - a_4 a_9 \big) a_1^2 \Big) - a_5 a_8 a_1 - a_2 \big(a_7 a_8 + 2 a_4 a_{10} \big) a_1 - a_6 \big(a_4 + a_2 a_{11} \big) a_1 \\
& + 2 a_7 a_9 a_{15} a_1 + 2 a_6 a_{10} a_{15} a_1 - 2 a_7 a_{10} a_{16} a_1 - 2 a_6 a_{12} a_{16} a_1 - a_2 a_4 a_7 - a_2 a_5 a_{11} - a_2^2 a_7 a_{11} + a_2^2 a_4 a_{12} - 2 a_6^2 a_{14} + a_3 a_6 a_8 a_{14} - a_3 a_4 a_9 a_{14} - 2 a_5 a_9 a_{14} \\
& - 2 a_2 a_7 a_9 a_{14} - 2 a_2 a_6 a_{10} a_{14} - 4 a_6 a_7 a_{15} + a_3 a_7 a_8 a_{15} + 2 a_3 a_4 a_{10} a_{15} + 4 a_5 a_{10} a_{15} + 2 a_2 a_7 a_{10} a_{15} + a_3 a_6 a_{11} a_{15} + 2 a_2 a_6 a_{12} a_{15} - 2 a_7^2 a_{16} + a_3 a_7 a_{11} a_{16} \\
& - a_3 a_4 a_{12} a_{16} - 2 a_5 a_{12} a_{16} \Big) + \beta^3 \Big(- a_5 \big(a_{15}^2 - a_{14} a_{16} \big) a_{10}^2 + 2 a_6 a_7 a_{15}^2 a_{10} + a_7^2 a_9 a_{15}^2 + a_6^2 a_{12} a_{15}^2 + a_5 a_9 a_{12} a_{15}^2 - a_5 a_9 a_{12} a_{14} a_{16} + \big(- a_{12} a_6^2 - 2 a_7 a_{10} a_6 - a_7^2 a_9 \big) a_{14} a_{16} \Big) \Big) \\
& + \eta_t \Big(\mu^4 \big(- a_3 a_4 - a_5 - a_1 a_6 - a_2 a_7 \big) + \beta^2 \mu^2 \Big(- a_2 a_{10} a_{14} a_6 - 2 a_7 a_{15} a_6 + a_1 a_{10} a_{15} a_6 + a_2 a_{12} a_{15} a_6 - a_1 a_{12} a_{16} a_6 - a_6^2 a_{14} - a_5 a_9 a_{14} - a_2 a_7 a_9 a_{14} \\
& + a_1 a_7 a_9 a_{15} + 2 a_5 a_{10} a_{15} + a_2 a_7 a_{10} a_{15} - a_7^2 a_{16} - a_1 a_7 a_{10} a_{16} - a_5 a_{12} a_{16} \Big) \Big) - \beta \mu^4 \big(a_5 + a_1 a_6 + a_2 a_7 \big) \Big) / \Theta
\end{aligned} \tag{C.26}
$$

$$
\begin{aligned}
\chi_{3t} = \Big(& \eta_t^5 \Upsilon_{10} + 2 \eta_t^4 \beta \Upsilon_{10} + \eta_t^3 \big(\beta^2 \Upsilon_{10} + \mu^2 \Upsilon_{11} \big) + \eta_t^2 \mu^2 \beta \Big(- \Big(\big(a_{10} a_{11} + a_8 a_{12} \big) a_2^2 \Big) - a_6 a_{11} a_2 + \Big(2 a_7 a_8 + \big(a_4 + a_1 a_8 \big) a_{10} + a_1 a_9 a_{11} \Big) a_2 \\
& + 2 \big(a_{10}^2 - a_9 a_{12} \big) a_{15} a_2 + a_4 a_6 + a_5 a_8 + a_1 a_6 a_8 - a_1 a_4 a_9 + 2 a_7 a_9 a_{15} + 2 a_6 a_{10} a_{15} - 2 a_7 a_{10} a_{16} - 2 a_6 a_{12} a_{16} - 2 a_1 \big(a_{10}^2 - a_9 a_{12} \big) a_{16} \\
& + a_3 a_{11} \big(a_{10} a_{16} - a_9 a_{15} \big) + a_3 a_8 \big(a_{12} a_{16} - a_{10} a_{15} \big) \Big) + \eta_t \Big(\mu^4 \big(- a_6 + a_3 a_8 + a_1 a_9 - a_2 a_{10} \big) + \beta^2 \mu^2 \Big(a_7 a_9 a_{15} + a_6 a_{10} a_{15} + a_2 \big(a_{10}^2 - a_9 a_{12} \big) a_{15} \\
& - a_7 a_{10} a_{16} - a_6 a_{12} a_{16} - a_1 \big(a_{10}^2 - a_9 a_{12} \big) a_{16} \Big) \Big) + \mu^4 \beta \big(- a_6 + a_1 a_9 - a_2 a_{10} \big) \Big) / \Theta
\end{aligned} \tag{C.27}
$$

$$
\begin{aligned}
\chi_{4t} =& \Big(\eta_t^5\Upsilon_{12} + 2\eta_t^4\beta\Upsilon_{12} + \eta_t^3\left(\mu^2\Upsilon_{13} + \beta^2\Upsilon_{12}\right) + \eta_t^2\mu^2\beta\Big(-\left(\left(a_8a_{10} + a_9a_{11}\right)a_1^2\right) - a_7a_8a_1 + a_{10}\left(a_4 + a_2a_{11}\right)a_1 + \left(2a_6a_{11} + a_2a_8a_{12}\right)a_1 \\
& + 2a_{10}^2a_{15}a_1 - 2a_9a_{12}a_{15}a_1 + a_4a_7 + a_5a_{11} + a_2a_7a_{11} - a_2a_4a_{12} - 2a_2a_{10}^2a_{14} - 2a_7a_9a_{14} - 2a_6a_{10}a_{14} + a_3a_8a_{10}a_{14} + a_3a_9a_{11}a_{14} + 2a_2a_9a_{12}a_{14} \\
& + 2a_7a_{10}a_{15} - a_3a_{10}a_{11}a_{15} + 2a_6a_{12}a_{15} - a_3a_8a_{12}a_{15}\Big) + \eta_t\Big(\mu^4\left(-a_7 - a_1a_{10} + a_3a_{11} + a_2a_{12}\right) + \beta^2\mu^2\Big(-a_2a_{14}a_{10}^2 + a_1a_{15}a_{10}^2 - a_6a_{14}a_{10} \\
& + a_7a_{15}a_{10} - a_7a_9a_{14} + a_2a_9a_{12}a_{14} + a_6a_{12}a_{15} - a_1a_9a_{12}a_{15}\Big)\Big) + \mu^4\beta\left(-a_7 - a_1a_{10} + a_2a_{12}\right)\Big) / \Theta
\end{aligned}
\tag{C.28}
$$

$$
\chi_{5t} = -(\beta + \eta_t) / \mu \tag{C.29}
$$

$$
\begin{aligned}
\chi_{6t} =& \Big(\eta_t^7\Upsilon_{14} + 3\eta_t^6\beta\Upsilon_{14} + \eta_t^5\left(3\beta^2\Upsilon_{14} + \mu^2\Upsilon_{15}\right) + \eta_t^4\Big(\beta^3\Upsilon_{14} + 2\beta\mu^2\Big(-2\left(a_{10}a_{11} + a_8a_{12}\right)a_{16}a_1^2 - 2\Big(2a_8\left(a_7 - a_2a_{12}\right) - \left(a_6 + 2a_2a_{10}\right)a_{11}\Big)a_{15}a_1 \\
& - 2a_7a_{11}a_{16}a_1 - 2a_4\left(a_{10}a_{15} - a_{12}a_{16}\right)a_1 + 3a_7a_{10}a_{15}^2 - 2a_3a_{10}a_{11}a_{15}^2 + 3a_6a_{12}a_{15}^2 - 2a_3a_8a_{12}a_{15}^2 + 2a_5a_8a_{14} - 2a_6\left(a_2a_{11} - a_4\right)a_{14} \\
& - 2a_2^2\left(a_{10}a_{11} + a_8a_{12}\right)a_{14} + 2a_4a_7a_{15} + 2a_5a_{11}a_{15} + 2a_2a_7\left(2a_8a_{14} + a_{11}a_{15}\right) + 2a_2a_4\left(a_{10}a_{14} - a_{12}a_{15}\right) - 3a_7a_{10}a_{14}a_{16} + 2a_3a_{10}a_{11}a_{14}a_{16} \\
& - 3a_6a_{12}a_{14}a_{16} + 2a_3a_8a_{12}a_{14}a_{16}\Big) + \eta_t^3\Big(\mu^4\Big(-a_8a_1^2 + a_4a_1 - a_2a_{11}a_1 + a_{10}a_{15}a_1 - a_{12}a_{16}a_1 - a_6a_{14} + a_3a_8a_{14} - a_7a_{15} + a_3a_{11}a_{15} - a_2\left(a_{10}a_{14} - a_{12}a_{15}\right)\Big) \\
& + \beta^2\mu^2\Big(-\left(\left(a_{10}a_{11} + a_8a_{12}\right)a_{16}a_1^2\right) - \Big(2a_8\left(a_7 - a_2a_{12}\right) - \left(a_6 + 2a_2a_{10}\right)a_{11}\Big)a_{15}a_1 - a_7a_{11}a_{16}a_1 - a_4\left(a_{10}a_{15} - a_{12}a_{16}\right)a_1 + 3a_7a_{10}a_{15}^2 - a_3a_{10}a_{11}a_{15}^2 \\
& + 3a_6a_{12}a_{15}^2 - a_3a_8a_{12}a_{15}^2 + a_5a_8a_{14} - a_6\left(a_2a_{11} - a_4\right)a_{14} - a_2^2\left(a_{10}a_{11} + a_8a_{12}\right)a_{14} + a_4a_7a_{15} + a_5a_{11}a_{15} + a_2a_7\left(2a_8a_{14} + a_{11}a_{15}\right) + a_2a_4\left(a_{10}a_{14} - a_{12}a_{15}\right) \\
& - 3a_7a_{10}a_{14}a_{16} + a_3a_{10}a_{11}a_{14}a_{16} - 3a_6a_{12}a_{14}a_{16} + a_3a_8a_{12}a_{14}a_{16}\Big)\Big) + \eta_t^2\Big(\beta\mu^4\Big(-a_8a_1^2 + a_4a_1 - a_2a_{11}a_1 + 2a_{10}a_{15}a_1 - 2a_{12}a_{16}a_1 - 2a_6a_{14} + a_3a_8a_{14} \\
& - 2a_7a_{15} + a_3a_{11}a_{15} - 2a_2\left(a_{10}a_{14} - a_{12}a_{15}\right)\Big) + \beta^3\mu^2\left(a_7a_{10}a_{15}^2 + a_6a_{12}a_{15}^2 - a_7a_{10}a_{14}a_{16} - a_6a_{12}a_{14}a_{16}\right)\Big) + \eta_t\Big(\beta^2\mu^4\Big(-a_6a_{14} - a_7a_{15} + a_1a_{10}a_{15} \\
& - a_2\left(a_{10}a_{14} - a_{12}a_{15}\right) - a_1a_{12}a_{16}\Big) - \mu^6 a_1\Big) - \beta\mu^6 a_1\Big) / (\mu\Theta)
\end{aligned}
\tag{C.30}
$$

$$
\begin{aligned}
\chi_{7t} = &\Big(\eta_t^7\Upsilon_{16} + 3\eta_t^6\beta\Upsilon_{16} + \eta_t^5\big(3\beta^2\Upsilon_{16} + \mu^2\Upsilon_{17}\big) + \eta_t^4\big(\beta^3\Upsilon_{16} + \beta\mu^2\big(-2(a_8a_{10} + a_9a_{11})a_{14}a_2^2 - 2a_6a_8a_{14}a_2 + 4a_1(a_8a_{10} + a_9a_{11})a_{15}a_2 \\
&+2(a_7a_8 - 2a_6a_{11})a_{15}a_2 - 2a_4(a_{10}a_{15} - a_9a_{14})a_2 + 3a_7a_9a_{15}^2 + 3a_6a_{10}a_{15}^2 - 2a_3(a_8a_{10} + a_9a_{11})a_{15}^2 + 2a_5a_8a_{15} + 2a_6(a_4 + a_1a_8)a_{15} \\
&-2a_1a_4a_9a_{15} - 2(a_1a_8 - a_4)(a_7 + a_1a_{10})a_{16} + 4a_1a_6a_{11}a_{16} - 2(a_1^2a_9 - a_5)a_{11}a_{16} - 3a_7a_9a_{14}a_{16} - 3a_6a_{10}a_{14}a_{16} + 2a_3(a_8a_{10} + a_9a_{11})a_{14}a_{16}\big)\big) \\
&+\eta_t^3\big(\mu^4\big(-a_{11}a_2^2 + a_4a_2 - a_1a_8a_2 - a_9a_{14}a_2 + a_{10}a_{15}a_2 - a_6a_{15} + a_3a_8a_{15} + a_1a_9a_{15} + (-a_7 - a_1a_{10})a_{16} + a_3a_{11}a_{16}\big) + \beta^2\mu^2\big(-\big((a_8a_{10} + a_9a_{11})a_{14}a_2^2\big) \\
&+2a_1(a_8a_{10} + a_9a_{11})a_{15}a_2 + (a_7a_8 - 2a_6a_{11})a_{15}a_2 - a_4(a_{10}a_{15} - a_9a_{14})a_2 + 3a_7a_9a_{15}^2 + 3a_6a_{10}a_{15}^2 - a_3(a_8a_{10} + a_9a_{11})a_{15}^2 - a_2a_6a_8a_{14} + a_5a_8a_{15} \\
&+a_6(a_4 + a_1a_8)a_{15} - a_1a_4a_9a_{15} + (a_4 - a_1a_8)(a_7 + a_1a_{10})a_{16} + 2a_1a_6a_{11}a_{16} + (a_5 - a_1^2a_9)a_{11}a_{16} - 3a_7a_9a_{14}a_{16} - 3a_6a_{10}a_{14}a_{16} + a_3(a_8a_{10} + a_9a_{11})a_{14}a_{16}\big)\big) \\
&+\eta_t^2\big(\beta^3\mu^2\big(a_7a_9a_{15}^2 + a_6a_{10}a_{15}^2 - a_7a_9a_{14}a_{16} - a_6a_{10}a_{14}a_{16}\big) + \beta\mu^4\big(-a_{11}a_2^2 + a_4a_2 - a_1a_8a_2 - 2a_9a_{14}a_2 + 2a_{10}a_{15}a_2 - 2a_6a_{15} + a_3a_8a_{15} + 2a_1a_9a_{15} \\
&-2(a_7 + a_1a_{10})a_{16} + a_3a_{11}a_{16}\big)\big) + \eta_t\big(\beta^2\mu^4\big(-a_2a_9a_{14} - a_6a_{15} + a_1a_9a_{15} + a_2a_{10}a_{15} + (-a_7 - a_1a_{10})a_{16}\big) - \mu^6a_2\big) - \beta\mu^6a_2\Big) / (\mu\Theta)
\end{aligned}
\tag{C.31}
$$

where

$$
\begin{aligned}
\Theta = &\,\eta_t^6\Upsilon_6 + 2\eta_t^5\beta\Upsilon_6 + \eta_t^4(\beta^2\Upsilon_6 + \mu^2\Upsilon_7) + \eta_t^3\beta^2\mu\Upsilon_7 + \eta_t^2(\mu^4(-a_4 + a_1a_8 + a_2a_{11} + a_9a_{14} - 2a_{10}a_{15} + a_{12}a_{16}) \\
&+\beta^2\mu^2(a_{15}^2a_{10}^2 - a_{14}a_{16}a_{10}^2 - a_9a_{12}a_{15}^2 + a_9a_{12}a_{14}a_{16})) + \eta_t\beta\mu^4(a_9a_{14} - 2a_{10}a_{15} + a_{12}a_{16}) + \mu^6
\end{aligned}
\tag{C.32}
$$

$$
\Upsilon_0 = \theta_6 - 6\beta^2\theta_8 \tag{C.33}
$$

$$
\begin{aligned}
\Upsilon_1 = &\Big(\big(a_8^2 + a_9a_{13}\big)a_1^2 + 2\big(-a_6a_{13} + a_2(a_8a_{11} - a_{10}a_{13}) - (a_8a_{10} + a_9a_{11})a_{15} + (a_{10}a_{11} + a_8a_{12})a_{16}\big)a_1 + a_4^2 + a_2^2a_{11}^2 + a_{10}^2a_{15}^2 \\
&-a_9a_{12}a_{15}^2 - a_5a_{13} - 2a_2a_7a_{13} + a_2^2a_{12}a_{13} + a_8(2a_6 - a_3a_8)a_{14} + 2a_2a_8a_{10}a_{14} + 2a_2a_9a_{11}a_{14} - a_3a_9a_{13}a_{14} + 2a_7a_8a_{15} + 2a_6a_{11}a_{15} \\
&-2a_3a_8a_{11}a_{15} - 2a_2a_{10}a_{11}a_{15} - 2a_2a_8a_{12}a_{15} + 2a_3a_{10}a_{13}a_{15} - \big(-2a_7a_{11} + a_3(a_{11}^2 + a_{12}a_{13}) + (a_{10}^2 - a_9a_{12})a_{14}\big)a_{16} \\
&-2a_4(a_1a_8 + a_2a_{11} + a_9a_{14} - 2a_{10}a_{15} + a_{12}a_{16})\Big)
\end{aligned}
\tag{C.34}
$$

$$
\Upsilon_2 = -2a_4 + 2a_1a_8 + 2a_2a_{11} - a_3a_{13} + a_9a_{14} - 2a_{10}a_{15} + a_{12}a_{16} \tag{C.35}
$$

$$
\Upsilon_3 = a_5a_{15}^2a_{10}^2 - a_5a_{14}a_{16}a_{10}^2 - 2a_6a_7a_{15}^2a_{10} - a_7^2a_9a_{15}^2 - a_6^2a_{12}a_{15}^2 - a_5a_9a_{12}a_{15}^2 + a_5a_9a_{12}a_{14}a_{16} + \big(a_{12}a_6^2 + 2a_7a_{10}a_6 + a_7^2a_9\big)a_{14}a_{16} \tag{C.36}
$$

$$\begin{aligned}\Upsilon_4 =& \left(a_{10}^2 - a_9 a_{12}\right) a_{16} a_1^2 - 2a_6 a_{10} a_{15} a_1 - 2a_2 \left(a_{10}^2 - a_9 a_{12}\right) a_{15} a_1 + 2a_6 a_{12} a_{16} a_1 + 2a_7 \left(a_{10} a_{16} - a_9 a_{15}\right) a_1 + a_3 a_{10}^2 a_{15}^2 - a_3 a_9 a_{12} a_{15}^2 \\ & + a_6^2 a_{14} + a_2^2 a_{10}^2 a_{14} + a_5 a_9 a_{14} + 2a_2 a_7 a_9 a_{14} + 2a_2 a_6 a_{10} a_{14} - a_2^2 a_9 a_{12} a_{14} + 2a_6 a_7 a_{15} - 2a_5 a_{10} a_{15} - 2a_2 a_7 a_{10} a_{15} - 2a_2 a_6 a_{12} a_{15} + a_7^2 a_{16} \\ & + a_5 a_{12} a_{16} - a_3 a_{10}^2 a_{14} a_{16} + a_3 a_9 a_{12} a_{14} a_{16}\end{aligned} \tag{C.37}$$

$$\Upsilon_5 = -a_9 a_1^2 + 2a_6 a_1 + 2a_2 a_{10} a_1 + a_5 + 2a_2 a_7 - a_2^2 a_{12} + a_3 a_9 a_{14} - 2a_3 a_{10} a_{15} + a_3 a_{12} a_{16} \tag{C.38}$$

$$\begin{aligned}\Upsilon_6 =& -a_4 a_{15}^2 a_{10}^2 + a_4 a_{14} a_{16} a_{10}^2 - a_7 a_8 a_{15}^2 a_{10} - a_6 a_{11} a_{15}^2 a_{10} + a_7 a_8 a_{14} a_{16} a_{10} + a_6 a_{11} a_{14} a_{16} a_{10} - a_7 a_9 a_{11} a_{15}^2 \\ & - a_6 a_8 a_{12} a_{15}^2 + a_4 a_9 a_{12} a_{15}^2 + a_7 a_9 a_{11} a_{14} a_{16} + a_6 a_8 a_{12} a_{14} a_{16} - a_4 a_9 a_{12} a_{14} a_{16}\end{aligned} \tag{C.39}$$

$$\begin{aligned}\Upsilon_7 =& a_{15}^2 a_{10}^2 - a_{14} a_{16} a_{10}^2 + 2a_4 a_{15} a_{10} - a_9 a_{12} a_{15}^2 + a_6 a_8 a_{14} - a_4 a_9 a_{14} + a_7 a_8 a_{15} + a_6 a_{11} a_{15} + a_2 a_{11} \left(a_9 a_{14} - a_{10} a_{15}\right) \\ & + a_2 a_8 \left(a_{10} a_{14} - a_{12} a_{15}\right) + a_7 a_{11} a_{16} - a_4 a_{12} a_{16} + a_9 a_{12} a_{14} a_{16} + a_1 a_{11} \left(a_{10} a_{16} - a_9 a_{15}\right) + a_1 a_8 \left(a_{12} a_{16} - a_{10} a_{15}\right)\end{aligned} \tag{C.40}$$

$$\begin{aligned}\Upsilon_8 =& -\left(\left(a_7 \left(a_8 a_{10} + a_9 a_{11}\right) + a_6 \left(a_{10} a_{11} + a_8 a_{12}\right) + a_4 \left(a_{10}^2 - a_9 a_{12}\right)\right) a_{16} a_1^2\right) + a_4 a_7 a_9 a_{15} a_1 + a_6^2 a_{11} a_{15} a_1 \\ & - a_6 \left(a_8 \left(a_7 - 2a_2 a_{12}\right) - a_{10} \left(a_4 + 2a_2 a_{11}\right)\right) a_{15} a_1 + 2a_2 \left(a_7 \left(a_8 a_{10} + a_9 a_{11}\right) + a_4 \left(a_{10}^2 - a_9 a_{12}\right)\right) a_{15} a_1 - a_7^2 a_8 a_{16} a_1 \\ & - a_4 a_7 a_{10} a_{16} a_1 + a_6 a_7 a_{11} a_{16} a_1 - a_4 a_6 a_{12} a_{16} a_1 - a_5 a_{11} \left(a_{10} a_{16} - a_9 a_{15}\right) a_1 - a_5 a_8 \left(a_{12} a_{16} - a_{10} a_{15}\right) a_1 - a_3 a_4 a_{10}^2 a_{15}^2 \\ & + a_7^2 a_9 a_{15}^2 + 2a_6 a_7 a_{10} a_{15}^2 - a_3 a_6 a_{10} a_{11} a_{15}^2 - a_3 a_7 \left(a_8 a_{10} + a_9 a_{11}\right) a_{15}^2 + a_6^2 a_{12} a_{15}^2 - a_3 a_6 a_8 a_{12} a_{15}^2 + a_3 a_4 a_9 a_{12} a_{15}^2 \\ & + a_5 a_9 a_{12} a_{15}^2 - a_2^2 a_4 a_{10}^2 a_{14} + a_2 a_6 a_7 a_8 a_{14} - a_2 a_4 a_7 a_9 a_{14} - a_2 a_4 a_6 a_{10} a_{14} - a_2^2 a_7 a_8 a_{10} a_{14} - a_2 a_6^2 a_{11} a_{14} - a_2^2 a_7 a_9 a_{11} a_{14} \\ & - a_2^2 a_6 a_{10} a_{11} a_{14} - a_2^2 a_6 a_8 a_{12} a_{14} + a_2^2 a_4 a_9 a_{12} a_{14} + a_2 a_7^2 a_8 a_{15} + a_2 a_4 a_7 a_{10} a_{15} - a_2 a_6 a_7 a_{11} a_{15} + a_2 a_4 a_6 a_{12} a_{15} \\ & - a_2 a_5 a_{11} \left(a_9 a_{14} - a_{10} a_{15}\right) - a_2 a_5 a_8 \left(a_{10} a_{14} - a_{12} a_{15}\right) + a_3 a_4 a_{10}^2 a_{14} a_{16} + a_3 a_6 a_{10} a_{11} a_{14} a_{16} + a_3 a_7 \left(a_8 a_{10} + a_9 a_{11}\right) a_{14} a_{16} \\ & + a_3 a_6 a_8 a_{12} a_{14} a_{16} - a_3 a_4 a_9 a_{12} a_{14} a_{16} - a_5 a_9 a_{12} a_{14} a_{16} + \left(-a_{12} a_6^2 - 2a_7 a_{10} a_6 - a_7^2 a_9\right) a_{14} a_{16} - a_5 a_{10}^2 \left(a_{15}^2 - a_{14} a_{16}\right)\end{aligned} \tag{C.41}$$

$$
\begin{aligned}
\Upsilon_9 = & -2\left(a_7\left(a_8a_{10}+a_9a_{11}\right)+a_6\left(a_{10}a_{11}+a_8a_{12}\right)+a_4\left(a_{10}^2-a_9a_{12}\right)\right)a_{16}a_1^2+2a_1\left(\left(-a_6a_7a_8+a_5a_{10}a_8+a_4a_7a_9+a_4a_6a_{10}+\left(a_6^2+a_5a_9\right)a_{11}\right)a_{15}\right.\\
& \left.-\left(a_8a_7^2+\left(a_4a_{10}-a_6a_{11}\right)a_7+a_5a_{10}a_{11}+\left(a_4a_6+a_5a_8\right)a_{12}\right)a_{16}\right)-2a_2^2\left(a_7\left(a_8a_{10}+a_9a_{11}\right)+a_6\left(a_{10}a_{11}+a_8a_{12}\right)+a_4\left(a_{10}^2-a_9a_{12}\right)\right)a_{14}\\
& +2a_2\left(\left(a_8a_7^2+\left(\left(a_4+2a_1a_8\right)a_{10}-\left(a_6-2a_1a_9\right)a_{11}\right)a_7+a_{10}\left(2a_1a_4a_{10}+\left(a_5+2a_1a_6\right)a_{11}\right)+\left(\left(a_5+2a_1a_6\right)a_8+a_4\left(a_6-2a_1a_9\right)\right)a_{12}\right)a_{15}\right.\\
& \left.-\left(-a_6a_7a_8+a_5a_{10}a_8+a_4a_7a_9+a_4a_6a_{10}+\left(a_6^2+a_5a_9\right)a_{11}\right)a_{14}\right)+\left(3a_9a_7^2+\left(6a_6a_{10}-2a_3\left(a_8a_{10}+a_9a_{11}\right)\right)a_7-3a_5a_{10}^2+3\left(a_6^2+a_5a_9\right)a_{12}\right.\\
& \left.-2a_3\left(a_6\left(a_{10}a_{11}+a_8a_{12}\right)+a_4\left(a_{10}^2-a_9a_{12}\right)\right)\right)\left(a_{15}^2-a_{14}a_{16}\right)
\end{aligned}
\tag{C.42}
$$

$$
\begin{aligned}
\Upsilon_{10} = & -a_{11}a_{15}a_6^2+a_7a_8a_{15}a_6-a_2a_{10}a_{11}a_{15}a_6-a_2a_8a_{12}a_{15}a_6-\left(a_7-a_1a_{10}\right)a_{11}a_{16}a_6+a_1a_8a_{12}a_{16}a_6+a_4\left(a_{12}a_{16}-a_{10}a_{15}\right)a_6-a_4a_7a_9a_{15}-a_2a_7\left(a_8a_{10}+a_9a_{11}\right)a_{15}\\
& -a_2a_4\left(a_{10}^2-a_9a_{12}\right)a_{15}+a_7^2a_8a_{16}+a_7\left(a_4+a_1a_8\right)a_{10}a_{16}+a_1a_7a_9a_{11}a_{16}+a_1a_4\left(a_{10}^2-a_9a_{12}\right)a_{16}-a_5a_{11}\left(a_9a_{15}-a_{10}a_{16}\right)-a_5a_8\left(a_{10}a_{15}-a_{12}a_{16}\right)
\end{aligned}
\tag{C.43}
$$

$$
\begin{aligned}
\Upsilon_{11} = & -\left(\left(a_{10}a_{11}+a_8a_{12}\right)a_2^2\right)-a_6a_{11}a_2+\left(2a_7a_8+\left(a_4+a_1a_8\right)a_{10}+a_1a_9a_{11}\right)a_2+\left(a_{10}^2-a_9a_{12}\right)a_{15}a_2+a_4a_6+a_5a_8+a_1a_6a_8\\
& -a_1a_4a_9+a_7a_9a_{15}+a_6a_{10}a_{15}-a_7a_{10}a_{16}-a_6a_{12}a_{16}-a_1\left(a_{10}^2-a_9a_{12}\right)a_{16}+a_3a_{11}\left(a_{10}a_{16}-a_9a_{15}\right)+a_3a_8\left(a_{12}a_{16}-a_{10}a_{15}\right)
\end{aligned}
\tag{C.44}
$$

$$
\begin{aligned}
\Upsilon_{12} = & \, a_{11}a_{14}a_6^2+a_4a_{10}a_{14}a_6+a_2a_{10}a_{11}a_{14}a_6+a_2a_8a_{12}a_{14}a_6-a_1a_{10}a_{11}a_{15}a_6-a_4a_{12}a_{15}a_6-a_1a_8a_{12}a_{15}a_6+a_2a_4a_{10}^2a_{14}\\
& -a_6a_7a_8a_{14}+a_5a_8a_{10}a_{14}+a_2a_7a_8a_{10}a_{14}+a_5a_9a_{11}a_{14}+a_2a_7a_9a_{11}a_{14}-a_2a_4a_9a_{12}a_{14}-a_1a_4a_{10}^2a_{15}-a_7^2a_8a_{15}-a_1a_7a_8a_{10}a_{15}\\
& +a_7\left(a_6-a_1a_9\right)a_{11}a_{15}-a_5a_{10}a_{11}a_{15}-a_5a_8a_{12}a_{15}+a_1a_4a_9a_{12}a_{15}+a_4a_7\left(a_9a_{14}-a_{10}a_{15}\right)
\end{aligned}
\tag{C.45}
$$

$$
\begin{aligned}
\Upsilon_{13} = & -\left(\left(a_8a_{10}+a_9a_{11}\right)a_1^2\right)-a_7a_8a_1+a_{10}\left(a_4+a_2a_{11}\right)a_1+\left(2a_6a_{11}+a_2a_8a_{12}\right)a_1+a_{10}^2a_{15}a_1-a_9a_{12}a_{15}a_1+a_4a_7+a_5a_{11}+a_2a_7a_{11}\\
& -a_2a_4a_{12}-a_2a_{10}^2a_{14}-a_7a_9a_{14}-a_6a_{10}a_{14}+a_3a_8a_{10}a_{14}+a_3a_9a_{11}a_{14}+a_2a_9a_{12}a_{14}+a_7a_{10}a_{15}-a_3a_{10}a_{11}a_{15}+a_6a_{12}a_{15}-a_3a_8a_{12}a_{15}
\end{aligned}
\tag{C.46}
$$

$$
\begin{aligned}
\Upsilon_{14} = & \, a_8a_{14}a_{16}a_7^2-a_4a_{10}a_{15}^2a_7+a_6a_{11}a_{15}^2a_7+a_4a_{10}a_{14}a_{16}a_7-a_6a_{11}a_{14}a_{16}a_7-a_7^2a_8a_{15}^2-a_5a_{10}a_{11}a_{15}^2\\
& -a_4a_6a_{12}a_{15}^2-a_5a_8a_{12}a_{15}^2+a_5a_{10}a_{11}a_{14}a_{16}+a_4a_6a_{12}a_{14}a_{16}+a_5a_8a_{12}a_{14}a_{16}
\end{aligned}
\tag{C.47}
$$

$$
\begin{aligned}
\Upsilon_{15} = &-\Big(\left(a_{10}a_{11} + a_8 a_{12}\right)a_{16}a_1^2\Big) - \Big(2a_8\left(a_7 - a_2 a_{12}\right) - \left(a_6 + 2a_2 a_{10}\right)a_{11}\Big)a_{15}a_1 - a_7 a_{11}a_{16}a_1 - a_4\left(a_{10}a_{15} - a_{12}a_{16}\right)a_1 + a_7 a_{10}a_{15}^2 \\
&- a_3 a_{10}a_{11}a_{15}^2 + a_6 a_{12}a_{15}^2 - a_3 a_8 a_{12}a_{15}^2 + a_5 a_8 a_{14} - a_6\left(a_2 a_{11} - a_4\right)a_{14} - a_2^2\left(a_{10}a_{11} + a_8 a_{12}\right)a_{14} + a_4 a_7 a_{15} + a_5 a_{11}a_{15} \\
&+ a_2 a_7\left(2a_8 a_{14} + a_{11}a_{15}\right) + a_2 a_4\left(a_{10}a_{14} - a_{12}a_{15}\right) - a_7 a_{10}a_{14}a_{16} + a_3 a_{10}a_{11}a_{14}a_{16} - a_6 a_{12}a_{14}a_{16} + a_3 a_8 a_{12}a_{14}a_{16}
\end{aligned}
\tag{C.48}
$$

$$
\begin{aligned}
\Upsilon_{16} = &-a_{11}\left(a_{15}^2 - a_{14}a_{16}\right)a_6^2 + a_7 a_8 a_{15}^2 a_6 - a_4 a_{10}a_{15}^2 a_6 - a_7 a_8 a_{14}a_{16}a_6 + a_4 a_{10}a_{14}a_{16}a_6 \\
&- a_4 a_7 a_9 a_{15}^2 - a_5\left(a_8 a_{10} + a_9 a_{11}\right)a_{15}^2 + a_4 a_7 a_9 a_{14}a_{16} + a_5\left(a_8 a_{10} + a_9 a_{11}\right)a_{14}a_{16}
\end{aligned}
\tag{C.49}
$$

$$
\begin{aligned}
\Upsilon_{17} = &-\Big(\left(a_8 a_{10} + a_9 a_{11}\right)a_{14}a_2^2\Big) + 2a_1\left(a_8 a_{10} + a_9 a_{11}\right)a_{15}a_2 + \left(a_7 a_8 - 2a_6 a_{11}\right)a_{15}a_2 - a_4\left(a_{10}a_{15} - a_9 a_{14}\right)a_2 + a_7 a_9 a_{15}^2 + a_6 a_{10}a_{15}^2 \\
&- a_3\left(a_8 a_{10} + a_9 a_{11}\right)a_{15}^2 - a_2 a_6 a_8 a_{14} + a_5 a_8 a_{15} + a_6\left(a_4 + a_1 a_8\right)a_{15} - a_1 a_4 a_9 a_{15} + \left(a_4 - a_1 a_8\right)\left(a_7 + a_1 a_{10}\right)a_{16} + 2a_1 a_6 a_{11}a_{16} \\
&+ \left(a_5 - a_1^2 a_9\right)a_{11}a_{16} - a_7 a_9 a_{14}a_{16} - a_6 a_{10}a_{14}a_{16} + a_3\left(a_8 a_{10} + a_9 a_{11}\right)a_{14}a_{16}
\end{aligned}
$$

(C.50)

The parameters in Eq. (31) are expressed as:

$$
\begin{Bmatrix} \varpi_{1i} \\ \varpi_{2i} \\ \varpi_{3i} \\ \varpi_{4i} \\ \varpi_{5i} \\ \varpi_{6i} \\ \varpi_{7i} \end{Bmatrix} = -
\begin{bmatrix}
\chi_{12i}\mathrm{e}^{-\eta_{2i}l} & \chi_{13i}\mathrm{e}^{-\eta_{3i}l} & \chi_{14i}\mathrm{e}^{-\eta_{4i}l} & \chi_{15i}\mathrm{e}^{-\eta_{5i}l} & \chi_{16i}\mathrm{e}^{-\eta_{6i}l} & \chi_{17i}\mathrm{e}^{-\eta_{7i}l} & \chi_{18i}\mathrm{e}^{-\eta_{8i}l} \\
\chi_{22i}\mathrm{e}^{\eta_{2i}l} & \chi_{23i}\mathrm{e}^{\eta_{3i}l} & \chi_{24i}\mathrm{e}^{\eta_{4i}l} & \chi_{25i}\mathrm{e}^{\eta_{5i}l} & \chi_{26i}\mathrm{e}^{\eta_{6i}l} & \chi_{27i}\mathrm{e}^{\eta_{7i}l} & \chi_{28i}\mathrm{e}^{\eta_{8i}l} \\
\chi_{22i}\mathrm{e}^{-\eta_{2i}l} & \chi_{23i}\mathrm{e}^{-\eta_{3i}l} & \chi_{24i}\mathrm{e}^{-\eta_{4i}l} & \chi_{25i}\mathrm{e}^{-\eta_{5i}l} & \chi_{26i}\mathrm{e}^{-\eta_{6i}l} & \chi_{27i}\mathrm{e}^{-\eta_{7i}l} & \chi_{28i}\mathrm{e}^{-\eta_{8i}l} \\
\chi_{32i}\mathrm{e}^{\eta_{2i}l} & \chi_{33i}\mathrm{e}^{\eta_{3i}l} & \chi_{34i}\mathrm{e}^{\eta_{4i}l} & \chi_{35i}\mathrm{e}^{\eta_{5i}l} & \chi_{36i}\mathrm{e}^{\eta_{6i}l} & \chi_{37i}\mathrm{e}^{\eta_{7i}l} & \chi_{38i}\mathrm{e}^{\eta_{8i}l} \\
\chi_{32i}\mathrm{e}^{-\eta_{2i}l} & \chi_{33i}\mathrm{e}^{-\eta_{3i}l} & \chi_{34i}\mathrm{e}^{-\eta_{4i}l} & \chi_{35i}\mathrm{e}^{-\eta_{5i}l} & \chi_{36i}\mathrm{e}^{-\eta_{6i}l} & \chi_{37i}\mathrm{e}^{-\eta_{7i}l} & \chi_{38i}\mathrm{e}^{-\eta_{8i}l} \\
\chi_{42i}\mathrm{e}^{\eta_{2i}l} & \chi_{43i}\mathrm{e}^{\eta_{3i}l} & \chi_{44i}\mathrm{e}^{\eta_{4i}l} & \chi_{45i}\mathrm{e}^{\eta_{5i}l} & \chi_{46i}\mathrm{e}^{\eta_{6i}l} & \chi_{47i}\mathrm{e}^{\eta_{7i}l} & \chi_{48i}\mathrm{e}^{\eta_{8i}l} \\
\chi_{42i}\mathrm{e}^{-\eta_{2i}l} & \chi_{43i}\mathrm{e}^{-\eta_{3i}l} & \chi_{44i}\mathrm{e}^{-\eta_{4i}l} & \chi_{45i}\mathrm{e}^{-\eta_{5i}l} & \chi_{46i}\mathrm{e}^{-\eta_{6i}l} & \chi_{47i}\mathrm{e}^{-\eta_{7i}l} & \chi_{48i}\mathrm{e}^{-\eta_{8i}l}
\end{bmatrix}^{-1}
\begin{Bmatrix}
\chi_{11i}\mathrm{e}^{-\eta_{1i}l} \\ \chi_{21i}\mathrm{e}^{\eta_{1i}l} \\ \chi_{21i}\mathrm{e}^{-\eta_{1i}l} \\ \chi_{31i}\mathrm{e}^{\eta_{1i}l} \\ \chi_{31i}\mathrm{e}^{-\eta_{1i}l} \\ \chi_{41i}\mathrm{e}^{\eta_{1i}l} \\ \chi_{41i}\mathrm{e}^{-\eta_{1i}l}
\end{Bmatrix}
$$

(C.51)

Appendix D. Constants in the numerical example

The constants represented in the form of $\mathcal{D}_{in}$ are

$$\begin{cases} \tilde{\mathcal{A}}_{in} = \dfrac{1}{\omega\tilde{\mathfrak{E}}\mu_n(\eta_{in}+\beta)}\left[\mu_n\nu_0 - \dfrac{(\eta_{in}+\beta)^2}{\mu_n}\right]\tilde{\mathcal{D}}_{in} \\ \tilde{\mathcal{B}}_{in} = -\dfrac{1}{\omega\tilde{\mathfrak{E}}\eta_{in}(\eta_{in}+\beta)}\left[\mu_n - \nu_0\dfrac{(\eta_{in}+\beta)^2}{\mu_n}\right]\tilde{\mathcal{D}}_{in} \\ \tilde{\mathcal{C}}_{in} = -\dfrac{\eta_{in}+\beta}{\mu_n}\tilde{\mathcal{D}}_{in} \end{cases} \tag{D.1}$$

The crucial parameters of nontrivial solutions are obtained through the eigenvalues μ_n from Eq. (65):

$$\begin{cases} \tilde{\mathcal{D}}_{1n} = \tilde{\mathfrak{E}}\mu_n \\ \tilde{\mathcal{D}}_{2n} = -\tilde{\mathfrak{E}}\mu_n \dfrac{\dfrac{(\eta_{1n}-\eta_{4n})\mathrm{e}^{\eta_{1n}l}\sinh\left[(\eta_{3n}-\eta_{4n})l\right]}{\beta+\eta_{1n}} + \dfrac{(\eta_{4n}-\eta_{3n})\mathrm{e}^{\eta_{3n}l}\sinh\left[(\eta_{1n}-\eta_{4n})l\right]}{\beta+\eta_{3n}}}{\dfrac{(\eta_{2n}-\eta_{4n})\mathrm{e}^{\eta_{2n}l}\sinh\left[(\eta_{3n}-\eta_{4n})l\right]}{\beta+\eta_{2n}} + \dfrac{(\eta_{4n}-\eta_{3n})\mathrm{e}^{\eta_{3n}l}\sinh\left[(\eta_{2n}-\eta_{4n})l\right]}{\beta+\eta_{3n}}} \\ \tilde{\mathcal{D}}_{3n} = \tilde{\mathfrak{E}}\mu_n\Xi_{1n} \\ \tilde{\mathcal{D}}_{4n} = \tilde{\mathfrak{E}}\mu_n\Xi_{2n} \end{cases} \tag{D.2}$$

where

$$\Xi_{1n} = \frac{\left(\beta+\eta_{3n}\right)\mathrm{e}^{\left(\eta_{3n}-\eta_{1n}\right)l}\left(\beta\eta_{1n}\mathrm{e}^{2\left(\eta_{1n}+\eta_{2n}\right)l}-\beta\eta_{1n}\mathrm{e}^{2\left(\eta_{1n}+\eta_{4n}\right)l}-\beta\eta_{2n}\mathrm{e}^{2\left(\eta_{1n}+\eta_{2n}\right)l}+\left(\eta_{2n}-\eta_{4n}\right)\left(\beta+\eta_{1n}\right)\mathrm{e}^{2\left(\eta_{2n}+\eta_{4n}\right)l}+\beta\eta_{4n}\mathrm{e}^{2\left(\eta_{1n}+\eta_{4n}\right)l}-\eta_{1n}\eta_{2n}\mathrm{e}^{2\left(\eta_{1n}+\eta_{4n}\right)l}+\eta_{1n}\eta_{4n}\mathrm{e}^{2\left(\eta_{1n}+\eta_{2n}\right)l}-\eta_{2n}\eta_{4n}\mathrm{e}^{2\left(\eta_{1n}+\eta_{2n}\right)l}+\eta_{2n}\eta_{4n}\mathrm{e}^{2\left(\eta_{1n}+\eta_{4n}\right)l}\right)}{\left(\beta+\eta_{1n}\right)\left(\beta\eta_{2n}\mathrm{e}^{2\left(\eta_{2n}+\eta_{3n}\right)l}-\beta\eta_{2n}\mathrm{e}^{2\left(\eta_{2n}+\eta_{4n}\right)l}-\beta\eta_{3n}\mathrm{e}^{2\left(\eta_{2n}+\eta_{3n}\right)l}+\left(\eta_{3n}-\eta_{4n}\right)\left(\beta+\eta_{2n}\right)\mathrm{e}^{2\left(\eta_{3n}+\eta_{4n}\right)l}+\beta\eta_{4n}\mathrm{e}^{2\left(\eta_{2n}+\eta_{4n}\right)l}-\eta_{2n}\eta_{3n}\mathrm{e}^{2\left(\eta_{2n}+\eta_{4n}\right)l}+\eta_{2n}\eta_{4n}\mathrm{e}^{2\left(\eta_{2n}+\eta_{3n}\right)l}-\eta_{3n}\eta_{4n}\mathrm{e}^{2\left(\eta_{2n}+\eta_{3n}\right)l}+\eta_{3n}\eta_{4n}\mathrm{e}^{2\left(\eta_{2n}+\eta_{4n}\right)l}\right)}$$

$$\Xi_{2n} = \frac{\left(\beta+\eta_{4n}\right)\mathrm{e}^{\left(\eta_{4n}-\eta_{1n}\right)l}\left(\beta\eta_{1n}\mathrm{e}^{2\left(\eta_{1n}+\eta_{3n}\right)l}-\beta\eta_{1n}\mathrm{e}^{2\left(\eta_{1n}+\eta_{2n}\right)l}+\beta\eta_{2n}\mathrm{e}^{2\left(\eta_{1n}+\eta_{2n}\right)l}-\left(\eta_{2n}-\eta_{3n}\right)\left(\beta+\eta_{1n}\right)\mathrm{e}^{2\left(\eta_{2n}+\eta_{3n}\right)l}-\beta\eta_{3n}\mathrm{e}^{2\left(\eta_{1n}+\eta_{3n}\right)l}+\eta_{1n}\eta_{2n}\mathrm{e}^{2\left(\eta_{1n}+\eta_{3n}\right)l}-\eta_{1n}\eta_{3n}\mathrm{e}^{2\left(\eta_{1n}+\eta_{2n}\right)l}+\eta_{2n}\eta_{3n}\mathrm{e}^{2\left(\eta_{1n}+\eta_{2n}\right)l}-\eta_{2n}\eta_{3n}\mathrm{e}^{2\left(\eta_{1n}+\eta_{3n}\right)l}\right)}{\left(\beta+\eta_{1n}\right)\left(\beta\eta_{2n}\mathrm{e}^{2\left(\eta_{2n}+\eta_{3n}\right)l}-\beta\eta_{2n}\mathrm{e}^{2\left(\eta_{2n}+\eta_{4n}\right)l}-\beta\eta_{3n}\mathrm{e}^{2\left(\eta_{2n}+\eta_{3n}\right)l}+\left(\eta_{3n}-\eta_{4n}\right)\left(\beta+\eta_{2n}\right)\mathrm{e}^{2\left(\eta_{3n}+\eta_{4n}\right)l}+\beta\eta_{4n}\mathrm{e}^{2\left(\eta_{2n}+\eta_{4n}\right)l}-\eta_{2n}\eta_{3n}\mathrm{e}^{2\left(\eta_{2n}+\eta_{4n}\right)l}+\eta_{2n}\eta_{4n}\mathrm{e}^{2\left(\eta_{2n}+\eta_{3n}\right)l}-\eta_{3n}\eta_{4n}\mathrm{e}^{2\left(\eta_{2n}+\eta_{3n}\right)l}+\eta_{3n}\eta_{4n}\mathrm{e}^{2\left(\eta_{2n}+\eta_{4n}\right)l}\right)}$$

References

[1] C. K. Narula, J. E. Allison, D. R. Bauer, and H. S. Gandhi, Materials chemistry issues related to advanced materials applications in the automotive industry, Chem. Mater., vol. 8, no. 5, pp. 984–1003, Jan. 1996, https://doi.org/10.1021/cm950588m.

[2] R. L. Clough. High-energy radiation and polymers: A review of commercial processes and emerging applications, Nucl. Instrum. Methods Phys. Res. B, vol. 185, no. 1–4, pp. 8–33, Dec. 2001, https://doi.org/10.1016/S0168-583X(01)00966-1.

[3] A. Ali Shah, F. Hasan, Z. Shah, N. Kanwal, and S. Zeb. Biodegradation of natural and synthetic rubbers: A review, Int. Biodeter. Biodegr., vol. 83, pp. 145–157, Sep. 2013, https://doi.org/10.1016/j.ibiod.2013.05.004.

[4] P. Colombo, G. Mera, R. Riedel, and G. D. Sorarù. polymer ‐ derived ceramics: 40 years of research and innovation in advanced ceramics. In R. Riedel and I. Chen, editors., Ceramics science and technology, 1st ed., Wiley, 2013, pp. 245–320. https://doi.org/10.1002/9783527631940.ch57.

[5] M. Menagadevi, M. Nirmala, D. Thiyagarajan, and D. Somasundram. Biomaterials and their applications. Biomed. Mater. & Devices, Jul. 2024, https://doi.org/10.1007/s44174-024-00215-y.

[6] K. E. Koumi, D. Nelias, T. Chaise, and A. Duval. Modeling of the contact between a rigid indenter and a heterogeneous viscoelastic material. Mech. Mater., vol. 77, pp. 28–42, Oct. 2014,

https://doi.org/10.1016/j.mechmat.2014.07.001.

[7] Y. K. Galadima, S. Oterkus, E. Oterkus, I. Amin, A.-H. El-Aassar, and H. Shawky. Modelling of viscoelastic materials using non-ordinary state-based peridynamics. Eng. Comput., vol. 40, no. 1, pp. 527–540, Feb. 2024, https://doi.org/10.1007/s00366-023-01808-9.

[8] K. Jaboviste, E. Sadoulet-Reboul, R. O. Teloli, and G. Chevallier. Characterizing the nonlinear behavior of viscoelastic materials: A Bayesian approach combining oberst beam experiments and digital-twin simulations. Mech. Syst. Signal Process., vol. 208, p. 110978, Feb. 2024, https://doi.org/10.1016/j.ymssp.2023.110978.

[9] S. Ding et al. Approximate contact force model for viscoelastic materials based on generalized Maxwell model. Int. J. Solids Struct., vol. 289, p. 112645, Mar. 2024, https://doi.org/10.1016/j.ijsolstr.2024.112645.

[10] C. Mandriota, N. Menga, and G. Carbone. Adhesive contact mechanics of viscoelastic materials. Int. J. Solids Struct., vol. 290, p. 112685, Mar. 2024, https://doi.org/10.1016/j.ijsolstr.2024.112685.

[11] A. V. Movahedi-Rad and T. Keller. A novel methodology of predicting temperature and rate effects on tensile properties of viscoelastic materials. Int. J. Non Linear Mech., vol. 159, p. 104613, Mar. 2024, https://doi.org/10.1016/j.ijnonlinmec.2023.104613.

[12] Y. H. Elmoghazy, B. Safaei, M. Asmael, S. Sahmani, Q. Zeeshan, and Z. Qin, Computational modelling and analysis of effect of viscoelastic

materials on damping and vibrational behaviors of composite structures—an extensive review. Arch. Comput. Methods Eng., vol. 31, no. 5, pp. 2611–2662, Jul. 2024, https://doi.org/10.1007/s11831-023-10057-4.

[13] R. Xiao, H. Sun, and W. Chen. An equivalence between generalized Maxwell model and fractional Zener model. Mech. Mater., vol. 100, pp. 148–153, Sep. 2016, https://doi.org/10.1016/j.mechmat.2016.06.016.

[14] P. L. Kinon, T. Thoma, P. Betsch, and P. Kotyczka. Generalized Maxwell viscoelasticity for geometrically exact strings: Nonlinear port-Hamiltonian formulation and structure-preserving discretization. IFAC-PapersOnLine, vol. 58, no. 6, pp. 101–106, 2024, https://doi.org/10.1016/j.ifacol.2024.08.264.

[15] X. Wang, Y. Wang, H. Qiang, J. Bai, C. Luo, and Z. Zhao. Initial stress approach-based finite element analysis for viscoelastic materials under generalized Maxwell model. AIP Adv., vol. 14, no. 6, p. 065132, Jun. 2024, https://doi.org/10.1063/5.0204292.

[16] K. Guo, A. Cornejo, and Z. Liu. Nonlinear behavior of existing pre-tensioned concrete beams: Experimental study and finite element modeling with the constitutive Serial-Parallel rule of mixtures. Structures, vol. 67, p. 106990, Sep. 2024, https://doi.org/10.1016/j.istruc.2024.106990.

[17] C. Liu, X. Wu, X. Liu, X. Li, Z. Chen, and H. Luo. Study of creep

behavior and a viscoelastic model of bamboo scrimber under short-term parallel-to-grain compression. J. Mater. Civ. Eng., vol. 36, no. 10, p. 04024295, Oct. 2024, https://doi.org/10.1061/JMCEE7.MTENG-18124.

[18] R. Yazdanparast and R. Rafiee. A 3D nonlinear viscoelastic-viscoplastic constitutive model for dynamic response of an epoxy resin. Acta. Mech., vol. 235, no. 11, pp. 6625–6639, Nov. 2024, https://doi.org/10.1007/s00707-024-04065-z.

[19] P. Patil and C. Jones. Stress relaxation and creep nanoindentation for cement paste. J. Mater. Civ. Eng., vol. 36, no. 1, p. 04023514, Jan. 2024, https://doi.org/10.1061/JMCEE7.MTENG-15725.

[20] D. Yang and X. Chu. Influence of particle shape on creep and stress relaxation behaviors of granular materials based on DEM. Comput. Geotech., vol. 166, p. 105941, Feb. 2024, https://doi.org/10.1016/j.compgeo.2023.105941.

[21] A. Feichtmayer et al. Fast low-temperature irradiation creep driven by a thermal defect dynamics. Commun. Mater., vol. 5, no. 1, p. 218, Oct. 2024, https://doi.org/10.1038/s43246-024-00655-5.

[22] Z. Zhang, Y. Chen, K. Han, G. Wei, Y. Pan, and M. Sun. Mathematical modelling for interaction between soft ground and small curvature shield tunneling considering viscoelastic characteristics influences. Appl. Math. Model., vol. 127, pp. 607–639, Mar. 2024, https://doi.org/10.1016/j.apm.2023.12.020.

[23] Y. Chen et al. Research on creep behaviour of UHPC based on experiments and viscoelastic modelling. J. Build. Eng., vol. 84, p. 108585, May 2024, https://doi.org/10.1016/j.jobe.2024.108585.

[24] Z. Shu, R. You, and Y. Xie. Viscoelastic dampers for vibration control of building structures: A state-of-art review," J. Earthq. Eng., vol. 28, no. 12, pp. 3558–3585, Sep. 2024, https://doi.org/10.1080/13632469.2024.2345180.

[25] H. Zhang, A. Li, Y. Su, G. Xu, and B. Sha. Viscoelastic dampers for civil engineering structures: A systematic review of constructions, materials, and applications. J. Build. Eng., vol. 96, p. 110597, Nov. 2024, https://doi.org/10.1016/j.jobe.2024.110597.

[26] S. N. Nguyen, J. Lee, and M. Cho. A triangular finite element using Laplace transform for viscoelastic laminated composite plates based on efficient higher-order zigzag theory. Compos. Struct., vol. 155, pp. 223–244, Nov. 2016, https://doi.org/10.1016/j.compstruct.2016.07.051.

[27] S. Chen, D. Wang, J. Yi, and D. Feng. Implement the Laplace transform to convert viscoelastic functions of asphalt mixtures. Constr. Build. Mater., vol. 203, pp. 633–641, Apr. 2019, https://doi.org/10.1016/j.conbuildmat.2019.01.116.

[28] Q. Li, X. Peng, D. Chen, and G. B. McKenna. The Laplace approach in microrheology. Soft Matter, vol. 16, no. 14, pp. 3378–3383, 2020, https://doi.org/10.1039/C9SM02242B.

[29] Sh. Kiasat, M. Filippi, A. S. Nobari, and E. Carrera. Layer-wise dynamic analysis of a beam with global and local viscoelastic contributions using an FE/Laplace transform approach. Acta. Mech., vol. 233, no. 11, pp. 4747–4761, Nov. 2022, https://doi.org/10.1007/s00707-022-03349-6.

[30] X. Li, J. Yu, H. Fang, and P. Wu. Modified state space method for bending creep and recovery behaviors of viscoelastic orthotropic laminated plate. Eur. J. Mech. A Solids, vol. 105, p. 105235, May 2024, https://doi.org/10.1016/j.euromechsol.2024.105235.

[31] E. H. Lee and J. R. M. Radok. The contact problem for viscoelastic bodies. J. Appl. Mech., vol. 27, no. 3, pp. 438–444, Sep. 1960, https://doi.org/10.1115/1.3644020.

[32] L. Cheng, X. Xia, W. Yu, L. E. Scriven, and W. W. Gerberich. Flat-punch indentation of viscoelastic material. J. Polym. Sci. B Polym. Phys., vol. 38, no. 1, pp. 10–22, Jan. 2000, https://doi.org/10.1002/(SICI)1099-0488(20000101)38:1<10::AID-POLB2>3.0.CO;2-6.

[33] M. L. Oyen. Analytical techniques for indentation of viscoelastic materials. Philos. Mag., vol. 86, no. 33–35, pp. 5625–5641, Nov. 2006, https://doi.org/10.1080/14786430600740666.

[34] Y. Y. Sun, J. Su, H. X. Song, and L. L. Ke. The size-dependent frictionless contact of piezoelectric materials. Int. J. Mech. Sci., vol. 261, p. 108685, Jan. 2024, https://doi.org/10.1016/j.ijmecsci.2023.108685.

[35] W. Yang, P. Bai, J. Fang, Y. Li, Z. Shi, and Q. Zhou. Contact responses

of transversely isotropic layered material with imperfect interface. Int. J. Mech. Sci., vol. 272, p. 109145, Jun. 2024, https://doi.org/10.1016/j.ijmecsci.2024.109145.

[36] Y. Chen, M. Zhang, and Q. J. Wang. Analysis of adhesive contact of heterogeneous elastic materials. Int. J. Mech. Sci., vol. 266, p. 108986, Mar. 2024, https://doi.org/10.1016/j.ijmecsci.2024.108986.

[37] Y.-H. Li, F. Shen, M. A. Güler, and L. L. Ke. Modeling multi-physics electrical contact on rough surfaces considering elastic-plastic deformation. Int. J. Mech. Sci., vol. 269, p. 109066, May 2024, https://doi.org/10.1016/j.ijmecsci.2024.109066.

[38] S. C. Hunter. The rolling contact of a rigid cylinder with a viscoelastic half space. J. Appl. Mech., vol. 28, no. 4, pp. 611–617, Dec. 1961, https://doi.org/10.1115/1.3641792.

[39] I. G. Goriacheva. Contact problem of rolling of a viscoelastic cylinder on a base of the same material. Z. Angew. Math. Mech., vol. 37, no. 5, pp. 877–885, Jan. 1973, https://doi.org/10.1016/0021-8928(73)90017-8.

[40] G. Fu. Theoretical study of complete contact indentations of viscoelastic materials. J. Mater. Sci., vol. 39, no. 8, pp. 2877–2878, Apr. 2004, https://doi.org/10.1023/B:JMSC.0000021469.13364.f7.

[41] J. A. Greenwood. Contact between an axisymmetric indenter and a viscoelastic half-space. Int. J. Mech. Sci., vol. 52, no. 6, pp. 829–835, Jun. 2010, https://doi.org/10.1016/j.ijmecsci.2010.01.010.

[42] I. Argatov and G. Mishuris. Frictionless elliptical contact of thin viscoelastic layers bonded to rigid substrates. Appl. Math. Model., vol. 35, no. 7, pp. 3201–3212, Jul. 2011, https://doi.org/10.1016/j.apm.2011.01.029.

[43] I. Argatov. An analytical solution of the rebound indentation problem for an isotropic linear viscoelastic layer loaded with a spherical punch. Acta. Mech., vol. 223, no. 7, pp. 1441–1453, Jul. 2012, https://doi.org/10.1007/s00707-012-0668-2.

[44] A. E. Giannakopoulos and S. Suresh. Indentation of solids with gradients in elastic properties: Part I. Point force. Int. J. Solids Struct., vol. 34, no. 19, pp. 2357–2392, Jul. 1997, https://doi.org/10.1016/S0020-7683(96)00171-0.

[45] A. E. Giannakopoulos and S. Suresh. Indentation of solids with gradients in elastic properties: Part II. axisymmetric indentors. Int. J. Solids Struct., vol. 34, no. 19, pp. 2393–2428, Jul. 1997, https://doi.org/10.1016/S0020-7683(96)00172-2.

[46] T. J. Liu and P. Li. Two-dimensional adhesion mechanics of a graded coated substrate under a rigid cylindrical punch based on a PWEML model. Appl. Math. Model., vol. 69, pp. 1–14, May 2019, https://doi.org/10.1016/j.apm.2018.12.002.

[47] M. A. Guler and F. Erdogan. Contact mechanics of graded coatings. Int. J. Solids Struct., vol. 41, no. 14, pp. 3865–3889, Jul. 2004,

https://doi.org/10.1016/j.ijsolstr.2004.02.025.

[48] M. A. Guler and F. Erdogan. Contact mechanics of two deformable elastic solids with graded coatings. Mech. Mater., vol. 38, no. 7, pp. 633–647, Jul. 2006, https://doi.org/10.1016/j.mechmat.2005.11.006.

[49] M. A. Guler and F. Erdogan. The frictional sliding contact problems of rigid parabolic and cylindrical stamps on graded coatings. Int. J. Mech. Sci., vol. 49, no. 2, pp. 161–182, Feb. 2007, https://doi.org/10.1016/j.ijmecsci.2006.08.006.

[50] A. Giannakopoulos and P. Pallot. Two-dimensional contact analysis of elastic graded materials. J. Mech. Phys. Solids, vol. 48, no. 8, pp. 1597–1631, Aug. 2000, https://doi.org/10.1016/S0022-5096(99)00068-X.

[51] S. Chen, C. Yan, P. Zhang, and H. Gao. Mechanics of adhesive contact on a power-law graded elastic half-space. J. Mech. Phys. Solids, vol. 57, no. 9, pp. 1437–1448, Sep. 2009, https://doi.org/10.1016/j.jmps.2009.06.006.

[52] X. Guo, F. Jin, and H. Gao. Mechanics of non-slipping adhesive contact on a power-law graded elastic half-space. Int. J. Solids Struct., vol. 48, no. 18, pp. 2565–2575, Sep. 2011, https://doi.org/10.1016/j.ijsolstr.2011.05.008.

[53] F. Jin and X. Guo. Mechanics of axisymmetric adhesive contact of rough surfaces involving power-law graded materials. Int. J. Solids Struct., vol. 50, no. 20–21, pp. 3375–3386, Oct. 2013,

https://doi.org/10.1016/j.ijsolstr.2013.06.007.

[54] F. Jin, X. Guo, and W. Zhang. A unified treatment of axisymmetric adhesive contact on a power-law graded elastic half-space. J. Appl. Mech., vol. 80, no. 6, p. 061024, Nov. 2013, https://doi.org/10.1115/1.4023980.

[55] S. Dag, M. A. Guler, B. Yildirim, and A. Cihan Ozatag. Sliding frictional contact between a rigid punch and a laterally graded elastic medium. Int. J. Solids Struct., vol. 46, no. 22–23, pp. 4038–4053, Nov. 2009, https://doi.org/10.1016/j.ijsolstr.2009.07.023.

[56] S. Dag, M. A. Guler, B. Yildirim, and A. C. Ozatag. Frictional Hertzian contact between a laterally graded elastic medium and a rigid circular stamp. Acta. Mech., vol. 224, no. 8, pp. 1773–1789, Aug. 2013, https://doi.org/10.1007/s00707-013-0844-z.

[57] S. Dag. Consideration of spatial variation of the friction coefficient in contact mechanics analysis of laterally graded materials: Contact mechanics analysis of laterally graded materials. Z. Angew. Math. Mech., vol. 96, no. 1, pp. 121–136, Jan. 2016, https://doi.org/10.1002/zamm.201400116.

[58] L.Z.C. Chen and W.Q. Chen. Surface Green's functions of a horizontally graded elastic half-plane. Mech. Adv. Mater. Struct., vol. 31, no. 27, pp. 9601–9610, Dec. 2024, https://doi.org/10.1080/15376494.2024.2342042.

[59] W. X. Zhong and X. Zhong. Method of separation of variables and Hamiltonian system. Numer. Methods Partial Differ. Equ., vol. 9, no. 1,

pp. 63–75, Jan. 1993, https://doi.org/10.1002/num.1690090107.

[60] W. X. Zhong. A new systematic methodology for theory of elasticity. Dalian: Dalian University of Technology Press, 1995. (in Chinese)

[61] W. X. Zhong, X. S. Xu, and H. W. Zhang. Hamiltonian system and the Saint-Venant problem in elasticity. Appl. Math. Mech., vol. 17, no. 9, pp. 827–836, Sep. 1996, https://doi.org/10.1007/BF00127182.

[62] X. S. Xu, W. X. Zhong, and H. W. Zhang. The Saint-Venant problem and principle in elasticity. Int. J. Solids Struct., vol. 34, no. 22, pp. 2815–2827, Aug. 1997, https://doi.org/10.1016/S0020-7683(96)00198-9.

[63] Q. Gu, X. S. Xu, and A. Y. T. Leung. Application of Hamiltonian system for two-dimensional transversely isotropic piezoelectric media. J. Zheijang Univ. Sci. A, vol. 6, no. 9, pp. 915–921, Sep. 2005, https://doi.org/10.1631/jzus.2005.A0915.

[64] X. S. Xu, Q. Gu, A. Y. T. Leung, and J. J. Zheng. A symplectic eigensolution method in transversely isotropic piezoelectric cylindrical media. J. Zheijang Univ. Sci. A, vol. 6, no. 9, pp. 922–927, Sep. 2005, https://doi.org/10.1631/jzus.2005.A0922.

[65] W. A. Yao and X. Li. Symplectic duality system on plane magnetoelectroelastic solids. Appl. Math. Mech., vol. 27, no. 2, pp. 195–205, Feb. 2006, https://doi.org/10.1007/s10483-006-0207-z.

[66] C. W. Lim, S. Cui, and W. A. Yao. On new symplectic elasticity approach for exact bending solutions of rectangular thin plates with two

opposite sides simply supported. Int. J. Solids Struct., vol. 44, no. 16, pp. 5396–5411, Aug. 2007, https://doi.org/10.1016/j.ijsolstr.2007.01.007.

[67] C. W. Lim, W. A. Yao, and S. Cui. Benchmark symplectic solutions for bending of corner-supported rectangular thin plates. IES J. Part A: Civ. Struct. Eng., vol. 1, no. 2, pp. 106–115, May 2008, https://doi.org/10.1080/19373260701646407.

[68] X. Xu, G. Wang, and F. Sun. Analytical and numerical methods of symplectic system for Stokes flow in two-dimensional rectangular domain. Appl. Math. Mech.-Engl. Ed., vol. 29, no. 6, pp. 705–714, Jun. 2008, https://doi.org/10.1007/s10483-008-0602-3.

[69] C. W. Lim, C. F. Lü, Y. Xiang, and W. Yao. On new symplectic elasticity approach for exact free vibration solutions of rectangular Kirchhoff plates. Int. J. Eng. Sci., vol. 47, no. 1, pp. 131–140, Jan. 2009, https://doi.org/10.1016/j.ijengsci.2008.08.003.

[70] C. F. Lü, C. Lim, and W. A. Yao. A new analytic symplectic elasticity approach for beams resting on Pasternak elastic foundations. J. Mech. Mater. Struct., vol. 4, no. 10, pp. 1741–1754, Feb. 2010, https://doi.org/10.2140/jomms.2009.4.1741.

[71] X. Xu, H. Chu, and C. W. Lim. A symplectic Hamiltonian approach for thermal buckling of cylindrical shells. Int. J. Str. Stab. Dyn., vol. 10, no. 02, pp. 273–286, Jun. 2010, https://doi.org/10.1142/S0219455410003506.

[72] W. Yao, W. Zhong, and C. W. Lim, Symplectic elasticity. New Jersey:

World Scientific, 2009.

[73] X. Xu, W. Zhang, X. Li, and G. Wang. An application of the symplectic system in two-dimensional viscoelasticity. Int. J. Eng. Sci., vol. 44, no. 13–14, pp. 897–914, Aug. 2006, https://doi.org/10.1016/j.ijengsci.2006.06.006.

[74] W. Zhang, X. Xu, and F. Yuan. The symplectic system method in the stress analysis of 2D elasto-viscoelastic fiber reinforced composites. Arch. Appl. Mech., vol. 80, no. 8, pp. 829–841, Aug. 2010, https://doi.org/10.1007/s00419-009-0343-9.

[75] W. Zhang and X. Xu. The symplectic approach for two-dimensional thermo-viscoelastic analysis. Int. J. Eng. Sci., vol. 50, no. 1, pp. 56–69, Jan. 2012, https://doi.org/10.1016/j.ijengsci.2011.09.003.

[76] L.Z.C. Chen and W.Q. Chen. Symplectic contact analysis of a finite-sized horizontally graded magneto-electro-elastic plane. Proc. Math. Phys. Eng. Sci., 2024, https://doi.org/10.1098/rspa.2024.0591.

[77] A. Y. T. Leung and J. Zheng. Closed form stress distribution in 2D elasticity for all boundary conditions. Appl. Math. Mech.-Engl. Ed., vol. 28, no. 12, pp. 1629–1642, Dec. 2007, https://doi.org/10.1007/s10483-007-1210-z.

[78] COMSOL Multiphysics® v. 6.0. cn.comsol.com. COMSOL AB, Stockholm, Sweden, 2021.

[79] L. Zhao and W.Q. Chen. Symplectic analysis of plane problems of

functionally graded piezoelectric materials. Mech. Mater., vol. 41, no. 12, pp. 1330–1339, Dec. 2009, https://doi.org/10.1016/j.mechmat.2009.09.001.

[80] L. Zhao, W.Q. Chen, and C. F. Lü. Symplectic elasticity for bi-directional functionally graded materials. Mech. Mater., vol. 54, pp. 32–42, Nov. 2012, https://doi.org/10.1016/j.mechmat.2012.06.001.